Variability in light absorption and photosynthesis within tomato canopies: a 3D model assisted analysis

Maarten van der Meer

Propositions

1. Plant morphology acclimates such that differences in light absorption and photosynthesis between north- and south-facing rows are minimal.
   (this thesis)

2. Realistic crop modelling requires incorporation of interplant variation.
   (this thesis)

3. Oceanic life cannot be protected without monitoring fish migration patterns.

4. Food policy making is useless if the human microbiome is ignored.

5. Researchers' inability to communicate science hinders rapid education of people.

6. A sustainability project for an inherently non-sustainable practice is futile.

Propositions belonging to the thesis, entitled

Variability in light absorption and photosynthesis within tomato canopies: a 3D model assisted analysis

Maarten van der Meer
Wageningen, 28 September 2022

Variability in light absorption and photosynthesis within tomato canopies: a 3D model assisted analysis

Maarten van der Meer

Thesis committee

Promotor

Prof. Dr Leo F. M. Marcelis
Professor of Horticulture and Product Physiology
Wageningen University & Research

Co-promotors

Dr Ep Heuvelink
Associate professor, Horticulture and Product Physiology
Wageningen University & Research

Dr Pieter H. B. de Visser
Researcher, Crop Physiology
Wageningen University & Research

Other members

Dr Jochem B. Evers, Wageningen University & Research
Dr Simon van Mourik, Wageningen University & Research
Prof. Dr. Katrin Kahlen, Hochschule Geisenheim University, Germany
Prof. Dr. Kathy Steppe, Ghent University, Belgium

This research was conducted under the auspices of the C.T. de Wit Graduate School of Production Ecology & Resource Conservation (PE&RC)

Variability in light absorption and photosynthesis within tomato canopies: a 3D model assisted analysis

Maarten van der Meer

Thesis

submitted in fulfilment of the requirements for the degree of doctor
at Wageningen University
by the authority of the Rector Magnificus,
Prof. Dr A.P.J. Mol,
in the presence of the
Thesis Committee appointed by the Academic Board
to be defended in public
on Wednesday 28 September 2022
at 11 a.m. in the Omnia Auditorium.

Maarten van der Meer
Variability in light absorption and photosynthesis within tomato canopies: a 3D model assisted analysis,
149 pages.

PhD thesis, Wageningen University, Wageningen, the Netherlands (2022)
With references, with summary in English

ISBN 978-94-6447-286-8
DOI https://doi.org/10.18174/572230

Contents

Chapter 1

1 General introduction

One of the wonderful things that we can do in our lives is to enjoy plants that grow next to us, simply by looking at them, preparing them into a dish and feeding them to our livestock. We can harvest what is in our backyards, greenhouses, on large scale produce in fields and these days also in buildings without any natural sunlight. We have come a long way in understanding the way plants grow and interact with their environment, including neighboring plants. We use our understanding of plant growth to make our agricultural productivity higher, more resilient to future climate change and more sustainable to feed the population across the world. This thesis is one contribution and part of a large research community that tries to understand the concepts involved in plant growth. In particular, the focus is on the variability between plants in canopy stands in controlled climatic conditions, and the way the plants are affected by this through differences in light absorption. In this thesis 3D plant modelling of plant architecture, light absorption and photosynthesis is used to explain experimental findings and explore crop growth strategies.

1.1 Crop modelling

In agricultural research process-based models (PBM) were the first developed applications to model growth in relation to the environment. These PBM consider many interacting factors and processes and simulate physiological plant processes taking into account factors and processes affecting the growth rate (e.g. temperature, water, nutrients, weeds, pests, diseases, transpiration, photosynthesis) (Marcelis et al., 1998; van Ittersum et al., 2003). Generally, processes at one integration level are used to simulate plant performance or another rate or state variable at a higher integration level. The mechanistic detail of these bottom-up models varies strongly.

1.1.1 Empirical models

Empirical models are the simplest plant productivity models used and find their use frequently in agricultural, horticultural and forestry to predict productivity in monocultures. These do not contain any physiological processes and directly relate biomass productivity to climatic or soil conditions. Although empirical models are simple and effective, they have their limitations in prediction capability and perform poorly outside the boundaries of the empirical data on which they are built (Dourado-Neto et al., 1998).

1.1.2 Light-use efficiency models

One group of mechanistic models that are extensively used rely on light use efficiency (LUE). In this type of modelling the productivity of plants is linked to light captured and the conversion of this light to assimilates. The first step is to estimate light absorption within a canopy, which is possible with the use of the classical Lambert-Beer calculation (Monsi and Saeki, 2005). Here, an extinction coefficient k is used to relate leaf area index (LAI) to the fraction of incident light intercepted to estimate the absorbance profile within a canopy (e.g. Mailhol et al., 1997). Instead of modelling photosynthesis and respiration, LUE is a lumped parameter converting absorbed light into biomass and can be adjusted with simple reduction factors when there is e.g. water or nutrient limitation, sub-optimal temperatures or other environmental factors that limit plant growth (Runyon et al., 1994; Yuan et al., 2007; Kergoat et al., 2008).

1.1.3 Photosynthesis and respiration models

A more detailed simulation than a model just based on LUE, is modelling carbon assimilation and dissimilation i.e. photosynthesis and respiration. The Farquhar-von Caemmerer-Berry (FvCB) equations are commonly used to determine photosynthesis (Lloyd and Farquhar, 1996). These equations include light, CO_2 and temperature and calculates photosynthesis based on the most limiting factor. Advances over the past decades in modelling canopy photosynthesis in PBM has gone from a one big leaf model (Thornley et al., 1992) to multi-layer models (e.g. Samson et al., 1997; Zhu et al., 2012; Boonen et al., 2002), where the model differentiates multiple layers with different light environments (Monsi and Saeki, 2005). An alternative to the multi-layer model was developed by separately integrating the sunlit and shaded leaf fractions of the canopy, resulting in an accurate and simpler single layered sun/shade model (De Pury and Farquhar, 1997). SUCROS-based models integrate both approaches (van Ittersum et al., 2003). Respiratory processes are complex to model and are usually simplified to loss functions, where coefficients for growth and maintenance respiration determine the loss of CO_2 to construct or maintain a gram of biomass.

1.1.4 Functional-structural plant models

The majority of process-based models describe the photosynthetically active vegetative plant parts according to one descriptor, usually leaf area index (LAI; leaf area m^{-2}). Simplifying the canopy by using LAI as the descriptor removes plant to plant architectural variability which is normally present within a canopy. This saves computation time and can be useful when whole canopy estimates are required, but also results in a loss of detail and inaccuracy at the individual plant level. Although at the time computationally impossible, it was early recognized (∼1960's) that a next step in plant modelling would be to combine PBM with architectural plant models to study the interaction between plant form and function and the environment. The foundation for such a model framework was the development of the Lindenmayer-systems (L-systems) by Lindenmayer (Lindenmayer, 1968a; Lindenmayer, 1968b) and later improved by (Prusinkiewicz and Hanan, 1990). L-systems were initially intended to simulate cellular automata and branching structures by reiterating production rules, and were thus ideal to describe plant form. L-systems is a language which describes both static plant structure and its dynamics (steered by functions) by intuitive rules at the organ level. The resulting combination of PBM and plant architectural modelling is known as functional-structural plant modelling (FSPM), which allows feedbacks between plant structure and functioning by simulating the 3D environment, plant architecture and plant processes (Louarn and Song 2020). FSPM make use of the Lindenmayer-systems (L-systems), thus allowing feedbacks of processes at the organ level and plant functioning at individual plant or canopy level.

Functional–structural plant models (FSPMs) explore and integrate relationships between a plant's structure and processes that underlie its growth and development (Louarn and Song 2020). These models have been developed for a wide range of crops and for many purposes (Louarn and Song 2020) including studies on effects of plant architecture on light absorption and photosynthesis in a canopy (e.g. Buck-Sorlin et al., 2011; Cieslak et al., 2010; Wiechers et al., 2011; Chen et al., 2014; Chapter 2). These models can also be used to study interplant variation by either carbon driven competition (e.g. Luquet et al., 2006; Kang et al., 2011) or signalling (which may be internal to the plant, external or an integration of both; e.g. Fournier et al., 2005; Alban et al., 2008; Evers et al., 2011) to modulate growth and development.

1.2 Light sources, and the challenges of measuring light in the crop canopy

Light, originally only from the sun and these days also from lamps, is the key to plant growth. These days high-pressure sodium (HPS) lamps are commonly used in greenhouse horticulture and these are gradually being replaced by LEDs. LEDs are more efficient than HPS lamps due to their high conversion of electrical energy into light, and due to their relatively low heat can also be placed inside the canopy closer to the plants (intra-canopy lighting). Measuring the incident light environment in a canopy has always been a time consuming task due to horizontal and vertical light heterogeneity. This resulted in many light measurement procedures and devices being used. The use of line quantum sensors and line sensors for light measurements used in this thesis will be discussed in a later section of the introduction.

1.2.1 The introduction of LEDs in agriculture and plant growth

A light-emitting diode (LED) is a semiconductor light source that emits light when current flows through it. Reasons why LEDs are interesting in agriculture are that they are energy efficient, different light spectra can be chosen to influence plant growth and development, that they have a high life expectancy and a low heat radiation which may prevent overheating the canopy (Davis and Burns 2016). By providing supplementary light within the crop reflective loss of the upper canopy reduced (Goudriaan and van Laar 1994; Marcelis et al., 1998). Furthermore, a more homogeneous vertical light distribution and therefore a higher photosynthetic use efficiency of the absorbed light could be achieved (Li et al., 2014).

Studies where supplemental intra-canopy lighting replaced top lighting showed increased fruit yield in cucumber (Hovi-Pekkanen et al., 2004; Hovi-Pekkanen and Tahvonen, 2008), an increase in sweet pepper fruit number and weight (Hovi-Pekkanen et al., 2006) and an increased net photosynthesis (P_N) and photosynthetic capacity (P_{max}; Pettersen et al., 2010). These studies show that intra-canopy lighting affect plant growth and development. Still, some studies did not find differences in whole plant biomass production between top lighting and intra-canopy lighting (Trouwborst et al., 2010; Gómez and Mitchell 2016; Yan et al., 2018). Explanations for this lack of biomass were related to a loss of total light interception due to extreme leaf curling by intra-canopy lighting (Trouwborst et al., 2010; Yan et al., 2018) and to an increased maintenance respiration of leaves lower in the canopy that acclimated to a higher light intensity (Gómez and Mitchell 2016).

Both the distribution of light absorption and the light spectrum are changed when LEDs are used in growth. With addition of for example red light at the bottom of the canopy, the red to far-red ratio (R:FR) is changed locally within the canopy. Plants compete with neighboring plants in vegetation stands and ensure survival and reproduction by showing appropriate growth responses to neighbour presence. One used cue is by perceiving and interpreting environmental signals by photo-sensory receptors. Perception of low R:FR light reflected by neighbouring vegetation (plant tissues have a high absorption of red light while largely reflecting far-red light) is a signal of neighbour presence (Casal, 2013; Ballaré and Pierik, 2017). The photo-sensory receptor phytochrome is switched to the active state when exposed to red light. Far-red light and darkness has the opposite effect, switching phytochrome to an inactive state. The balance between active and inactive phytochrome is called the phytochrome photostationary state. A lowered R:FR ratio induces shade avoidance responses (SAR) such as increased elongation of stems (Ballaré et al., 1991; Smith and Whitelam, 1997; Cole et al., 2011) and petioles (Kozuka et al., 2010), reorientation of petioles (Whitelam and Johnson 1982; Sasidharan et al., 2010; Pantazopoulou et al., 2017; Kalaitzoglou et al., 2019) and a decrease in leaf thickness resulting in more leaf area per gram of dry weight (Holmes and Smith, 1975; Smith and Whitelam, 1997), all in order for a plant to compete with its neighbours. There are plenty of reviews on the way SAR are thought to operate and their functionality (Casal, 2013; de Wit et al., 2016; Fraser et al., 2016; Ballaré and Pierik, 2017; Viczián et al., 2017; Iglesias et al., 2018).

By placing LEDs lower in the canopy however, parts of the plant are now exposed to a higher red to far-red ratio again. The link between a plants site of light perception and the sites where morphological adaptations take place is a field of study with recent advancements but is still not fully understood (Küpers et al., 2018; Iglesias et al., 2018). Plants are modular organisms and they are built-up of individual organs connected to one big network through the xylem and phloem (Kroon et al., 2005). Organs perceive their own light microclimate (light intensity, light spectrum; Chelle, 2005). Changes in morphology resulting from an individual organ's perceived light microclimate can be at the level of the organ itself (local) and at the plant level where it also affects other plant organs (long-distance). Local and long-distance morphological responses to local light spectrum can be studied in relation to phytochrome by lowering the R:FR ratio through application of FR radiation.

1.2.2 Quantum sensors usage for measuring light distribution

Point or line quantum sensors are commonly used devices for measuring light. Fixed height intervals can be used for measurements to gain an estimate of the vertical light gradient through the canopy (Särkkä et al., 2017; Paponov et al., 2020), which is often combined with measurements at fixed horizontal intervals (Hovi-Pekkanen et al., 2006; Hovi-Pekkanen and Tahvonen, 2008; Pettersen et al., 2010; Pepin et al., 2014). With the introduction of intra-canopy lighting the quantum sensors are turned horizontally towards the LED lamps to gain an estimate of the side-way directed light profile in the canopy (Pettersen et al., 2010; Pepin et al., 2014; Särkkä et al., 2017; Kaiser et al., 2019; Paponov et al., 2020).

1.2.3 Modelling light interception

For process-based models the classical Lambert-Beer calculation is often used to model light extinction of light in the canopy. Instead of using classical Lambert-Beer calculation, it is possible with FSPM to use estimations of light scattering which requires the radiance equation (e.g. Chelle and Andrieu, 1998). As this equation is set at one point, integration over all surfaces is required. Two approaches enable this integration: the Monte Carlo method (e.g. Henke and Buck-Sorlin 2017) and a deterministic method derived from the finite elements: the radiosity method (Chelle and Andrieu, 1998). Interesting scientific questions as well as practical questions for greenhouse horticulture can now be approached through simulations. For instance, understanding the consequences of different light distributions in canopies for leaf and crop photosynthesis (Sarlikioti et al., 2011b), which is being applied in the development of light diffusing materials and LED lighting systems. The distribution of light within and absorption by a canopy has a direct impact on plant growth and development.

Various FSPM studies have been performed on greenhouse cultivated crops, such as cut-rose (Buck-Sorlin et al., 2011; Zhang et al., 2021), grapevine (Prieto et al., 2019) and tomato (de Visser et al., 2010; Kang et al., 2011; Sarlikioti et al., 2011a; de Visser et al., 2014; Shin et al., 2021). Those studies aim to either optimize lighting strategies, plant architecture or plant densities to increase interception of light. Light distribution in canopies is important for crop photosynthesis as suggested by the modelling study of (Sarlikioti et al., 2011b) and as evidenced by the increased crop photosynthesis and growth of greenhouse grown tomato when the light is made more diffuse (Li et al., 2014).

1.3 Architectural parameter variability

Plant to plant variation (interplant variation) may play an important role in determining individual plant and whole canopy performance (Westerband et al., 2021), where interplant variation in architecture and photosynthesis traits have direct effects on light absorption and photosynthesis (Sarlikioti et al., 2011a). Interplant variation has been studied for a longer time in ecology, greenhouse horticulture and field crops, where in greenhouse horticulture and field crops uniformity is of importance. Fruits of greenhouse cucumber (Marcelis 1992), as well as other reproductive and indeterminate crops such as bell pepper (Wubs et al., 2009b) and tomato (Heuvelink, 1996) show a changing demand in assimilates over time and abortion of individual fruits. Differences in fruit growth have been linked to environmental factors such as light intensity, photoperiod, CO_2 concentration, temperature, relative air humidity, water and nutrient supply (Marcelis 1993; Wubs et al., 2009a; Pettersen et al., 2010) and canopy architecture (Chen et al., 2014).

1.3.1 Quantifying plant phenotype and assess the impacts of architectural trait variation

Nowadays high-throughput plant phenotyping systems allow to quickly acquire architectural data, for example from pictures taken assisted by deep learning (Li et al., 2020). This greatly reduces measurement times, allowing for more elaborate and detailed data sets. Additional time can be saved if data analysis and plant phenotype is processed at the whole plant level. It is possible to extract a mesh point cloud of the plants, implement this directly into a structural model and then estimate light absorption (Zhu et al., 2020). Despite an increase in methods for data gathering and analyzing, quite some still have heavy computational costs, limited performance of machinery by e.g. occlusion and/or a need to have the used machinery moved around, thus reducing space-time coverage (Li et al., 2020). Measuring plant architecture by ruler and protractor is still an often used technique even though it is very cumbersome.

Approaches to determine the influence of realism or parameter assumptions on light absorption and photosynthesis in model simulations performance include e.g. changes in cucumber leaf shapes and positions (Schmidt and Kahlen, 2018), comparing simplified leaves to structurally-accurate leaves in both sweet pepper (Kim et al., 2020) and tomato (Vermeiren et al., 2020), investigating the golden angle (Strauss et al., 2020), alternate branching in trees which induces variation in geometrical and topological traits (Da Silva et al., 2014), increasing internode lengths of tomato plants which was found to change light absorption and photosynthesis by 6-10% (Sarlikioti et al., 2011a), as well as in a dynamic FSPM simulation where leaf angles affected shoot dry mass production up to 20% (Chen et al., 2014).

In the last years there has been considerable improvement in model predictions of carbon-driven growth, and several models have been developed that can simulate plant architectural variation such as Greenlab (latest review; de Reffye et al., 2021) and Ecomeristem (Larue et al., 2019). In these two models main functions related to influencing variation in growth are branching, tillering time and senescence. The importance of including interplant variation in architectural and photosynthesis traits for modelling light absorption and photosynthesis can be structurally assessed by model simulations but has yet received minimal attention. Zhu et al. (2015) investigated this topic in a maize and soybean mixture, and showed that inclusion of interplant variation in maize and soybean plants can result in complementary crop light capture.

1.4 Tomato plants

In this thesis the model plant tomato *(Solanum lycopersicum)* was used as model plant for fruit-bearing crops. Tomato is the most produced vegetable in the world. The origin of tomato is found in western South America, after which it has been domesticated in Central America (Kimura and Sinha, 2008). Breeding has focused on improving the overall productivity, the resistance of the plants to (a)biotic stresses and the quality of fruits (Kimura and Sinha, 2008). Tomato is a model plant for research due to the fact that it has simple diploid genetics, a short generation time, routine transformation technology and is easy to maintain (Ranjan et al., 2012). Research studies on tomato brings knowledge that can be applied to other plants in the Solanaceae family, such as eggplant and peppers. Tomato

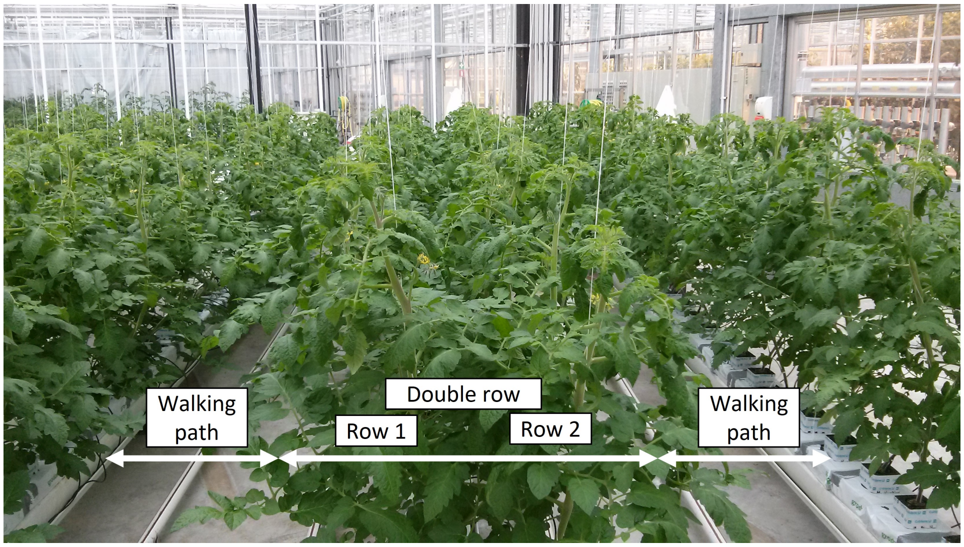

Figure 1: Double-row tomato canopy in an early growth stage showing the two rows as well as the walking path for crop maintenance and harvesting.

plants are generally cultivated in high-wire double row systems when grown in high-tech greenhouses (Fig. 1). For greenhouses the cultivars chosen have an indeterminate growth habit allowing almost year-round cultivation in the Netherlands. When the plants reach several meters high, they are lowered weekly along the path.

1.5 Knowledge gaps and hypotheses

In canopies a large variation exists between and within plants with respect to architecture and the distribution of light (both intensity and spectrum). The main hypothesis in this thesis is that including this variation gives a much more realistic simulation of the crop canopy.

Within-row variability has not been investigated thoroughly by both experimentation as well as model simulations combined. So far either some experimentation or modelling, but a clean combination of both has not been found. We hypothesize is that plants in north- and south-facing rows in the the east-west row orientation double row system will have a much larger variation in light absorption and photosynthesis and hence fruit production than plants in east- and west-facing rows in the north-south row orientation.

With the introduction of intra-canopy lighting leaves, stems and fruits are now exposed to a change in light spectrum. It is currently unknown if this could induce long-distance signalling in plant that would alter plant morphology. Extrapolation of results from studies on local lighting on de-etiolated seedlings, rosette plants or very young plants to tall plants (e.g. longer than 1 m) is difficult if not impossible. We hypothesize that mature plant parts can still induce morphological changes in young growing plant parts.

Total light absorption can be estimated by quantum sensor measurements above and below the crop, pointing, respectively, upward and downward which measures the light that is not absorbed by the canopy. However, the spatial heterogeneity of incident and absorbed light is hard to measure in detail. The spatial variability of absorbed light is important when physiological processes such as photosynthesis are compared between light treatments. By use of an FSPM an investigation can be performed comparing spatial heterogeneity of incident and absorbed light between intra-canopy lighting and top lighting systems. We hypothesize that using intra-canopy lighting increases overall crop uniformity in light absorption.

Inclusion of interplant variation in architectural and photosynthesis traits for modelling light absorption and photosynthesis has yet received minimal attention, while this could be of great importance for accurately modelling variability in a canopy. We hypothesize that including measured interplant variation in architectural and photosynthesis traits results in more accurate model simulations of light absorption and photosynthesis than a model which does not include spatial variation.

1.6 Thesis outline

The aim of this thesis was to study the variability in light absorption and photosynthesis within tomato canopies, where a combination of experimentation and 3D modelling was used. A comprehensive overview of the different components (Fig. 2) and a summary of the key objectives of each chapter are given below:

Chapter 2 Considering the importance of a uniform light distribution within a canopy, this chapter aimed to quantify the influence of row orientation on the inter- and within-row variation of light absorption and photosynthesis in a hedgerow crop. An experiment with two different row orientations of a tomato crop was conducted, which was then also used to adapt and calibrate a tomato FSPM to compare row orientations, explain experimental findings and quantify differences between rows at varying latitudes and seasons.

Chapter 3 With the introduction of intra-canopy assimilation lighting and LED lights without far-red, the natural ratios in red:far-red light absorption are changed throughout the canopy. The red:far-red light ratio has a strong effect on plant architecture. This chapter aimed to investigate whether and to which extent local supplementation of far-red light resulted in local or long-distance architectural and growth responses in full-grown tomato plants. An experiment was performed where tomato plants were horizontally separated in a lower and a upper half by use white plastic and supplementing local FR light to either of the two halves, where the lower half was full-grown.

Chapter 4 The introduction of intra-canopy lighting instead of toplighting seemed to increase crop productivity. The aim of this chapter was to identify the impact of intra-canopy versus top lighting systems on 3D light distributions in the canopy on leaflet level. Architectural data was collected from an experiment and used to parameterize a modified functional-structural plant model. This was then validated with light measurement data.

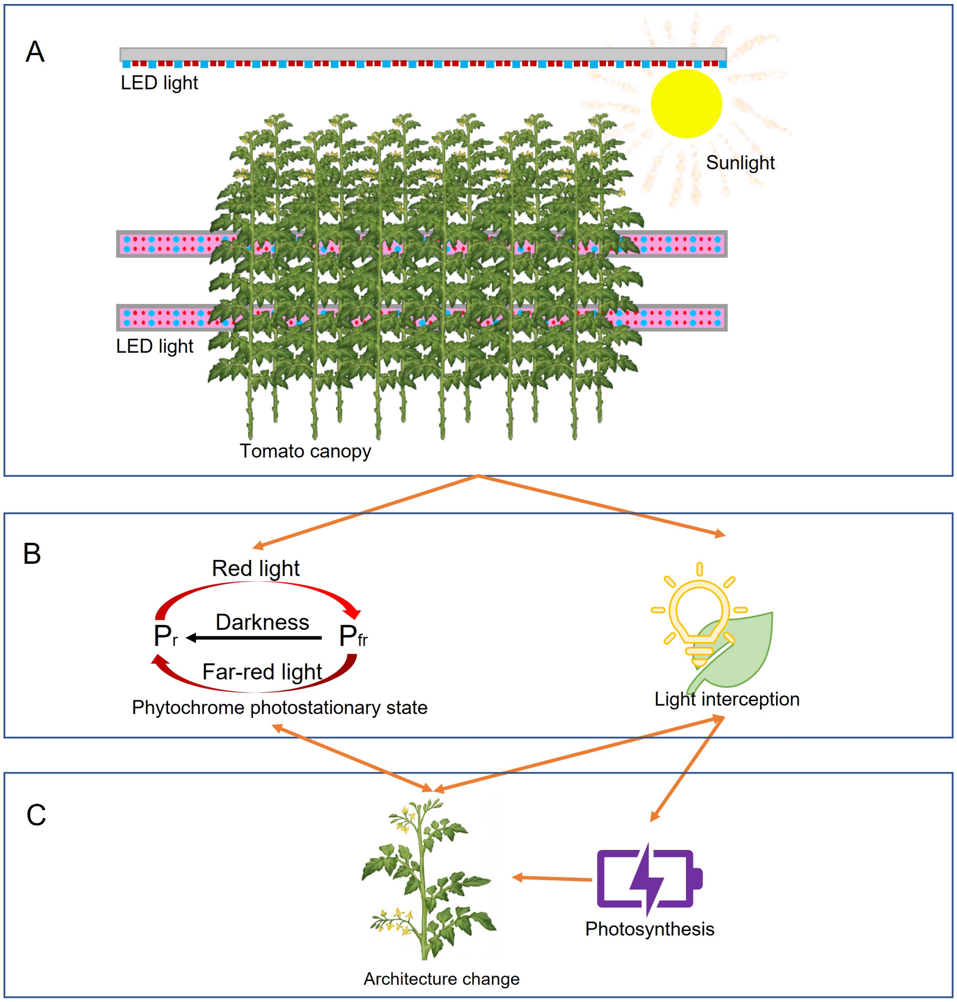

Figure 2: (A) Schematic representation of a double-row tomato crop canopy that is exposed to varying climatic conditions from sunlight, top- and intra-canopy LED lighting, resulting in (B) unequal light intensities and red:far-red ratios through the canopy affecting the phytochrome photostationary state as well as the light interception profile, which affect (C) the architecture of the plant and canopy photosynthesis. The change in architecture then visa versa affects light distribution and phytochrome photostationary state.

The model was then used to visualize heterogeneity of canopy light absorption and discussed in three directions according to voxel maps; parallel and perpendicular to the double rows, as well as in the vertical direction. The findings were then discussed in relation to experiments conducted with intra-canopy lighting.

Chapter 5 Plant to plant variation (interplant variation) may play an important role in determining individual plant and whole canopy performance, where interplant variation in architecture and photosynthesis traits have direct effects on light absorption and photosynthesis. The aim of this study was to determine the importance of observed interplant variation in architectural and photosynthetic traits on average light absorption and net photosynthesis and coefficient of variation in plant light absorption and net photosynthesis. For this we used measured interplant variation in greenhouse grown tomato canopies and used that as input in a functional-structural plant model to simulate consequences of interplant variation.

Chapter 6 The results of this thesis are summarized and put into a more general context. The advantages and the shortcomings of the methods used as well as the further steps in this research are discussed.

Chapter 2

2 Row orientation affects the uniformity of light absorption, but hardly affects crop photosynthesis in hedgerow tomato crops

[1]van der Meer, M., [2]de Visser, P. H. B., [1]Heuvelink, E., [1]Marcelis, L. F. M.

[1]Horticulture and Product Physiology, Wageningen University, Droevendaalsesteeg 1, 6708PB Wageningen, The Netherlands

[2]Business Unit Greenhouse Horticulture, Wageningen Research, Droevendaalsesteeg 1, 6708PB Wageningen, The Netherlands

An adapted version of this chapter has been published as van der Meer et al., 2021 in the journal *"in silico Plants"*.

Abstract

Light distribution within canopies is important for plant growth. We aimed to quantify the influence of row orientation on inter- and within-row variation of light absorption and photosynthesis in a hedgerow crop. An experiment with two row orientations of a tomato crop was conducted which was then used to calibrate a functional–structural plant model (FSPM). The FSPM was used to analyse light absorption and photosynthesis for each of the row facing directions in the double-row trellis system (e.g. north- and south-facing rows for the east–west row orientation). The measured leaf area decreased by 18 % and specific leaf area by 10 %, while fruit dry weight increased by 7 % for south-facing compared to north-facing rows, but total plant dry weight did not significantly differ. Model simulations showed a 7 % higher light absorption for the south-facing rows than north-facing rows, while net photosynthesis was surprisingly -4 % lower, due to local light saturation. When in the model leaf area was kept equal between the rows, light absorption for the south-facing rows was 19 % and net photosynthesis 8 % higher than for north-facing rows. We conclude that although south-facing rows would be expected to have a higher photosynthesis than north-facing rows, plants can adapt their morphology such that differences in light absorption and photosynthesis between north- and south-facing rows are minimal. Rows oriented north–south were more uniform in light absorption and photosynthesis than east–west rows, but the overall crop light absorption and photosynthesis were minimally affected (both 3 % lower compared to east–west orientation).

2.1 Introduction

Plant positioning in rows causes inter- and intra-row shading, which affects the light distribution and pattern throughout the whole day (Trentacoste et al., 2016; Campos et al., 2017). Inter- and intra-row shading have been experimentally studied in relation to weed control (Borger et al., 2010; Johnson and Davis 2015; Borger et al., 2016) and hedgerow productivity and fruit quality (review by Trentacoste et al., 2015). For weed control, row orientation is manipulated such that the crop will cast shadow on the weeds, which can reduce weed growth due to lack of sunlight (Borger et al., 2010; Johnson and Davis 2015; Borger et al., 2016). For hedgerow productivity and product quality, a north–south row orientation is often favourable as reviewed by Trentacoste et al. (2015). These authors argued that this is the result of a more equal distribution of light to the most important leaves and fruits between both east- and west-facing parts of the rows during a day in a north–south row orientation. A south-facing side can be light-saturated, while the north-facing side of a tree is still limited by light, resulting in unequal fruit set (Khemira et al., 1993), fruit abortion or fruit rot (Lombard and Westwood, 1977). Model simulations revealed that a certain canopy porosity could be required to support proper fruit growth in olives (Connor et al., 2009). Process-based models (PBMs) have been used to simulate row orientation effects on light absorption and crop production of hedgerows. Studies using PBMs revealed that the effect of row orientation on light absorption and productivity depends on architecture, season and latitude (Mutsaers, 1980; Gijzen and Goudriaan, 1989). A north– south row orientation results in increased light absorption in summer at lower latitudes of 15–55°(Mutsaers, 1980). The ratios between path width, row width and row height have major consequences for row orientation effects. Differences in light absorption and photosynthesis between row orientations diminish as the ratio between path width and row height decreases. When this ratio drops below 0.3 differences between row orientations become very small (Gijzen and Goudriaan, 1989). Functional–structural plant models (FSPMs) explore and integrate relationships between a plant's structure and processes that underlie its growth and development (Louarn and Song 2020). These models have been developed for several crops and for many purposes (Louarn and Song 2020) also for the study of plant architecture effects on light interception and distribution in a canopy (e.g. Buck-Sorlin et al., 2011; Cieslak et al., 2010; Wiechers et al., 2011; Chen et al., 2014). Sarlikioti et al. (2011b) developed a 3D static FSPM for tomato to study the responses of light absorption and photosynthesis in relation to plant architecture at the leaf level for inter- and intra-canopy shading. Their preliminary study suggested that in both summer (June) and winter (December) at a latitude of 52°light absorption in a north–south row orientation is higher than in an east–west row orientation. Light distribution in canopies is important for crop photosynthesis as suggested by the modelling study of Sarlikioti et al. (2011b) and as evidenced by the increased crop photosynthesis and growth of greenhouse grown tomato when the light is made more diffuse (Li et al., 2014). Considering the importance of a uniform light distribution within a canopy, the aim of this study is to quantify the influence of row orientation on the inter- and within-row variation of light absorption and photosynthesis in a hedgerow crop. Therefore, an experiment with two different row orientations of a tomato crop was conducted, which was then also used to adapt and calibrate a tomato FSPM. By doing so it was possible to (i) compare the growth and architecture of both rows in the north–south and east–west row orientations, (ii) explain the findings with the tomato FSPM by quantifying the light absorption and photosynthesis at leaf level for each of the rows and (iii) use the tomato FSPM to quantify light absorption and photosynthesis differences between rows at varying latitudes and seasons.

2.2 Material and methods

2.2.1 Growth conditions

Tomato plants (Solanum lycopersicum cv. Capriccia) were grown in two adjacent glasshouse compartments at Wageningen University (52°N, 5.7°E). In one compartment the plant rows were oriented from north to south, and in the other from east to west. On 8 March 2016, 5 weeks after sowing, the plants were transplanted onto gutters on rockwool slabs. The plants were grown until 20 July 2016. The crop was managed according to grower practice. Nutrient solution (EC: 2.8 and pH: 5.5; see Supporting Information-Table S1) was provided daily in a frequency matching solar radiation. Side stems were removed weekly, and from 13 April onward the bottom three leaves were removed every week. From 25 April the plants reached the high wire at a height of 3.3 m, after which they were lowered weekly. The plants were grown in double rows, with distance of 50 cm between the single rows. Distance between the mids of two adjacent double rows was 160 cm, resulting in a path of 62 cm (distance between outer leaves of each row). The distance between plants in a each single row was 50 cm. Stem density was 2.5 stems per m^2 until 7 April, when a secondary shoot was allowed to develop in the leaf axil directly below the fourth truss, thus raising the stem density to 5.0 stems per m^2. On 20 May a number of plants were removed for destructive harvests (and some additional plants) from each row to achieve the targeted 4.4 stems per m^2. Trusses were pruned to 6 fruits per truss. The CO$_2$ concentration was targeted at 600 ppm when the windows were closed and 400 ppm when the windows were open. Inside each compartment, a Hoogendoorn Box (Hoogendoorn, The Netherlands) was installed monitoring the climatic conditions at a 5-min interval. Averaged daily temperature, relative humidity and CO$_2$

(±standard deviation) over the whole growth period were 20.1 (±3.6) and 20.0 (±3.4) , 74.6 (±10.5) and 74.1 (±10.1) % relative humidity and 509 (±97) and 518 (±94) ppm CO_2 for each compartment with, respectively, north– south and east–west row orientation. The two glasshouse compartments were oriented -24°North–South. On the east, west and north side they were surrounded by other compartments, while there was a corridor on the south side. There was no artificial lighting present in surrounding compartments. Height of the greenhouse was 5 m and the rockwool slabs were 0.3 m above the floor. A picture of the plants in the greenhouse is shown in Supporting Information-Fig. S1).

2.2.2 Plant measurements

Architecture and dry weight. Dry weight of ripe fruits was recorded of twelve plants of each of the north, south, east and west facing rows during the whole experiment by weekly removal and weighing of trusses with fruits in stage 3 (‘turning’) up to stage 6 (‘red’) (Camelo Gómez 2004). For each facing row, three main stems were randomly selected from 4 center rows for destructive measurements on 20-22 April, 17-20 May and 19-20 July. At each measurement day plant architecture was measured and dry weight was determined for these three plants. On the measurements of 17-20 May and 19-20 July also three secondary stems were measured. Architectural measurements consisted of leaf area, as measured by a leaf area meter (LI-3100C, LI-COR, USA), leaf length, which was measured from the base of the petiole to the tip of the terminal leaflet using a ruler, and internode length. Plant material was dried in a ventilated oven at increasing temperature steps from 45 to 70 to 105°C, each for 24h.

Additional measurements were performed for model development during the final harvest. One plant of each row facing orientation was measured to get an estimate of parameters that were necessary for building the model architecture, but were considered non-significantly different for both row orientations. These parameters were petiole angle, petiolule angle, leaflet angle and curvature, leaf area ratio between small and big leaflets, rachis to petiolule length, the ratio between petiolule length to leaf area, leaflet length-to-width ratio and the rachis bend at the first and second big leaflet pairs, counted from the petiole to the tip of the leaf. These measurements were performed on leaves on ranks 1 to 3, 5 to 7, 10, 14, 18 and 22, counted from above.

Gas exchange. The response of net photosynthesis rate (A; μmol m^{-2} s^{-1}) to light intensity and leaf internal CO$_2$ partial pressure (C$_i$) was determined on three different heights in the canopy: 50, 80 and 150 cm from the top, which refer to leaves 7, 10 and 16, respectively. Measurements dates for this were, respectively, 10–11, 16–17 and 25–26 June, with each height taking 2 days. At each height, gas exchange was measured with the LI-6400 photosynthesis system (LI-COR), equipped with the LI-6400 fluorescence cuvette (2 cm^2 leaf area) on two leaves for each row facing side. For each measured leaf, the leaf was enclosed in the cuvette at 1400 μmol m^{-2} s^{-1} photosynthetically active radiation (PAR) (90 % red, 10 % blue), 600 μbar CO$_2$ partial pressure, temperature of 28 ± 3% fixed according to ambient temperature at start of measurements, relative humidity at 70 ±10% and a flow rate of 400 μmol m^{-2} s^{-1}. After A stabilized (≈15 min), CO$_2$ partial pressure was decreased in steps to 400, 300, 200, 100, 50 and 0 μbar. Then, CO$_2$ partial pressure was increased to 600 μbar, and after A stabilized (≈10 min) the CO$_2$ partial pressure was further increased to 800, 1200 and 1600 μbar. Then, CO$_2$ partial pressure was decreased to 700 μbar and light intensity was raised to 1800 μmol m^{-2} s^{-1}. After A stabilized (≈15 min), the light intensity was decreased in steps to 1450, 1100, 750, 450, 225, 100, and 0 μmol m^{-2} s^{-1}. At each CO$_2$ and light intensity step, the sample cell was calibrated against the reference cell, and A and C$_i$ were recorded after this.

2.2.3 Model description

An adapted version of the static greenhouse tomato FSPM of de Visser et al. (2014) was used. The adaptation consisted of a modified leaf reconstruction by replacing each single parallelogram that represented a leaflet by 6–8 parallelograms that together represent the leaflet geometry more precisely [see Supporting Information-Fig. S8]; a larger number of parallelograms did not improve the simulated light absorption [see Supporting Information-Table S3]. This model was developed on the GroIMP platform (Kniemeyer, 2008) and consists of an architectural, photosynthesis and light module.

Architectural module. The architectural parameter values for leaf area, stem length and leaf length were taken from data at the phytomer level acquired from the final destructive measurement on 20 July (Table 2). Leaf area differed significantly between north- and south-facing rows and was implemented as such. All other variables were non-significantly different ($P < 0.05$) and were averaged within each row orientation; e.g. stem length for north- and south-facing rows was averaged together and the averaged value was taken for both north- and south-facing rows in the simulations. For additional required model parameters that were not in the scope of this study a limited number of replicate measurements were taken and averaged, namely petiole angle, first and second rachis bend [see Supporting Information- Table S2]. Leaf curvature was assumed 60° and the number of leaflets were considered 11 (three bigger pairs, two smaller pairs and one terminal leaflet; see Supporting Information-Fig. S8). The leaf area was then distributed across the 11 leaflets on each leaf according to an empirical allometric relationship. The area of the composite leaf was distributed over the five leaflet pairs and the terminal leaflet for each leaf in the same manner, using the following fractions (from proximal to distal leaflet pair): 0.1296, 0.0188, 0.1516, 0.0281, 0.0948 and the terminal leaflet with 0.1541. The length of the petiole was 35 % of the total leaf length, and at that point the first leaflet pair was attached [see Supporting Information-Fig. S8]. The actual leaf area depended on the observed relationship with leaf rank. No collision avoidance of leaves was computed, since leaves of neighbouring plants do in reality not show distinct avoidance mechanisms and extremely intertwine. Then, each plant was constructed in the simulation with a random phyllotaxis initiation [see Supporting Information-Fig. S9] oriented randomly after randomly deciding the first phyllotaxis angle. We assumed that the absence of collision avoidance in modelling leaf orientation was reasonable since leaves strongly intertwine when touching another at lower parts in the crop, and so leaflets may well be oriented rather randomly. The spaces between the leaflets of the leaf allow easy penetration of the leaf environment of the neighbouring plant. Moreover, during plant management operations (leaf cutting, fruit harvesting, shifting plant position in the row weekly) the leaves of neighbouring plants are often reshuffled and become slightly mixed in a random way. Above all, this mechanical process is appearing in both row treatments equally and will not affect treatment effects. Vermeiren et al. (2020) used a similar light model as we did and concluded that a simplification of the leaflet shape in a tomato crop can lead to small deviations in simulations of light absorption and gross photosynthesis. At the canopy level, this effect is mitigated somewhat by the canopy closure in dense canopies.

Photosynthesis module. An adapted Farquhar–von Caemmerer– Berry model (FvCB model) was used to simulate photosynthesis (Farquhar et al., 1980; Qian et al., 2012). All photosynthesis parameter values were kept the same as Qian et al. (2012), with exception of J_{max28} (μmol m^{-2} s^{-1}; maximum electron transport rate at 28°C) and V_{cmax28} (μmol m^{-2} s^{-1}; the maximum carboxylation capacity if Rubisco is fully activated at 28°C). Values for J_{max28} and V_{cmax28} were estimated from gas exchange measurements. Comparison of light response curves between leaves 7 and 10 showed such small differences in Amax (<4 %) that these were considered equal for leaves 7 and 10. J_{max28} and V_{cmax28} were assumed to decrease exponentially from the 10^{th} leaf to the oldest leaf, as a result of age. This most basic assumption was taken since there was no support for any other relationship. Besides this, model simulations have shown that overestimation of photosynthesis when acclimation of photosynthetic parameters with height in the canopy is not considered is minimal when the only light source is the sun (van Ieperen and Trouwborst, 2008). Values for J_{max28} and V_{cmax28} were estimated at 235.6 and 136.0, respectively, for the 10 youngest leaves, and exponentially decreased to 145.8 and 67.7, respectively, for the oldest leaf (R2 > 0.99) by use of least-squares regression on light response curve data. This was done using the evolutionary solver in Excel, version 2016. α and θ were assumed constant throughout the whole canopy. The ratio between C_i and C_a was assumed constant at 0.7, as suggested by (Sinclair et al., 1984) for C3 species. This is valid if C_a values are larger than 300 ppm. In the experiment C_a varied between 350 and 550, resulting from CO_2 enrichment. Supporting Information-Figure S6 shows the fit of modelled and measured data of the response of net photosynthesis rate to light intensity and leaf internal partial pressure.

Light module. The light in the 3D scene was simulated in hourly time steps with a ray tracer, called Flux Light Model, provided by GroIMP. The Flux Light Model was described in detail by (Henke and Buck-Sorlin 2017). This ray tracer was based on an inversed path tracer with a Monte Carlo pseudo-random number generator as in (Veach, 1997). So, this light model differed from the light model used by Sarlikioti et al. (2011b) that was based on radiosity. However, we expect not much differences between the two models. If applied with our currently used ray numbers, the ray tracer casts enough rays to illuminate each object in the scene and will thus be comparable to the radiosity model that simulates all rays from light source to objects within a specified bounding box; for details on the models we refer to Chelle and Andrieu (1998), Sarlikioti et al. (2011b) and Henke and Buck-Sorlin (2017). The number of rays were 750 million and recursion depth was 10; these numbers were chosen such that a further increase would not improve simulation results [see Supporting Information-Table S3]. For diffuse radiation, the assumption was made of an overcast sky, where light sources were located according to azimuth at every 7.5° and zenith at every 15°. The fraction diffuse light depended on the atmospheric transmission as estimated from hourly measured global radiation outside the greenhouse (Spitters et al., 1986). The remainder fraction of light was direct light, and modelled as a point source of directional light, arriving from the hourly solar position (model from Goudriaan and van Laar 1994). The leaf reflectance and transmittance for 5 nm wavebands from 400 to 700 nm were measured with a Lambda 1050 spectrophotometer (Perkin-Elmer Inc.) coupled to a snap-in light integrating sphere. Stem optical properties were assumed to be similar to leaf properties, while fruits were assumed to absorb all light colours except for green (unripe fruits) and red (ripe fruits) wavelengths that were reflected for 100 %. A schematic representation of azimuth and solar angle in relation to row orientation is presented in (Supporting Information-Fig. S2). A comparison of simulated light extinction in a canopy with measured data and a Lambert–Beer extinction can be found in (Supporting Information-Fig. S10).

2.2.4 Model scenarios

Row orientation light absorption and net photosynthesis. Model simulations were run to study light absorption and photosynthesis for the full-grown canopy (last 2 months of the experiment; 20 May to 20 July). Hourly climatic data on CO_2, temperature and radiation were used as input and the model was run with hourly time steps. The relation between fraction direct solar light and total radiation can be seen in Supporting Information-Fig. S4. Calculations were performed for the centre 12 plants in the centre two double rows. For row orientation comparison, four model simulations were performed: $EW_{N4.6,S3.8}$ (east–west row orientation, with a differing leaf area index of 4.6 for north-facing rows and 3.8 for south-facing rows according to measurements), $EW_{N3.8,S3.8}$ (east–west row orientation, with an equal leaf area index of 3.8 for both north- and south-facing rows), $EW_{N4.0,S4.0}$ (east–west row orientation, with an equal leaf area index of 4.0 for both north- and south-facing rows; leaf area index was equal to that of the plants in the north–south row orientation according to measurements) and $\mathrm{NS}_{\mathrm{E4.0,W4.0}}$ (north–south row orientation, with leaf area equal for east- and west-facing rows according to measurements). In order to determine the sensitivity of the model to important assumptions, three additional model simulations were performed for $\mathrm{EW}_{\mathrm{N4.6,S3.8}}$: $\mathrm{EW}_{\mathrm{N4.6,S3.8,Pn}}$ (equal photosynthetic parameters through the whole canopy), $\mathrm{EW}_{\mathrm{N4.6,S3.8,Fl}}$ (flat leaves) and $\mathrm{EW}_{\mathrm{N4.6,S3.8,Rc}}$ (random leaflet curvatures between 0 and 120°).

Inter- and intra-row shading at different latitudes and seasons. For inter-row shading in an E-W row orientation, a simulation study was run for three latitudes (0°, 26°N and 52°N) for different seasons of the year (21 March, 21 June, 21 December) where north- and south-facing rows were compared in an E-W row orientation. In this simulation, CO_2 was fixed at 600 ppm, temperature at 23 °C and direct light at 77 %. The chosen days of the year (80, 171 and 356) represent the spring equinox (21 March) and the summer and winter solstices (21 June, 21 December). For these simulations the architecture of plants for north- and south-facing rows was the same with equal leaf area and a leaf area index (LAI) of 3.8. Distance between mid of the double rows was 160 cm and path width 62 cm (distance between outer leaves of two rows). In order to determine the sensitivity of the model to important assumptions, three additional model simulations were performed, where either the row distance was lowered to 130 cm, row distance was increased to 190 cm or where the photosynthetic parameters were equal through the whole canopy.

2.2.5 Statistical analysis of experimental data

Final harvest dry weight data of stem and leaves, as well as architectural data on stem length, leaf area, leaf length and specific leaf area were compared between rows within each row orientation in each compartment using an F-test (general linear model with main/secondary stem as covariate; $P = 0.05$; $n = 6$). Cumulative plant dry weight over the growth period was estimated from fruit mass of 12 plants (12 main + secondary stems) for north-, south-, east- and west-facing rows (including the weekly harvested fruits). As the recorded stem and leaf weight of three main and three secondary stems at final harvest were non-significantly different between rows within the row orientations (Table 1), the average stem and leaf weight for each row facing side was added to each of the 12 main and secondary stem fruit weights. Besides this, pruned leaf weight was estimated by averaging the leaf weight of the bottom 12–15 leaves at three consecutive harvests, comprising an average of 12 plants total per row facing side, and multiplying this with the total number of leaves harvested over time. Finally, effects of row facing side on cumulative plant dry weight and fruit dry weight per plant were tested within each row orientation using an F-test with row as blocking factor (general linear model with three plants for each row facing side per double row as block; P = 0.05; n = 4). Normality and equal variances were assumed.

2.3 Results

2.3.1 Experimental results

No significant differences were found for stem and leaf dry weight (g per plant) between the rows within the east–west as well as within the north–south row orientations (Table 1). Fruit dry weight (g per plant) was significantly higher (7 %) for the south-facing rows compared to the north-facing rows in the east–west row orientation. Between the east- and west-facing rows in the north–south row orientation there was no significant difference in fruit dry weight. No significant differences were found for cumulative plant dry weight between the rows within the east–west as well as within the north–south row orientations (Table 1). Leaf area was 18 % higher for north-facing rows than south-facing rows in the east–west row orientation (Table 2). Specific leaf area (SLA) seemed to be 10 % higher for the north-facing compared to south-facing rows, though this difference was not statistically significant. Leaf area was non-significantly different between east- and west-facing rows in the north–south row orientation. No significant differences were found in stem length and leaf length between the rows within the east–west as well as within the north–south row orientations (Table 2).

2.3.2 Model simulations

Within-row orientation differences in light absorption and net photosynthesis Model simulations for the full-grown crop (20 May to 20 July) showed a clear relationship between global incoming PAR (μmol m^{-2} s^{-1}) and ΔPAR absorbed (μmol m^{-2} s^{-1}) and Δnet photosynthesis (μmol m^{-2} s^{-1}) for the east–west row orientations (Fig. 1, Δ denotes differences between the facing sides of rows; in this case between south- and north-facing

Table 1: Measured values of dry weight of individual plant parts and cumulative plant biomass (g DW plant^{-1}; mean ±se). of the rows with different facing side for plants grown in E-W oriented rows and N-S oriented rows. Values marked in bold indicate significant differences between both facing rows within the same row orientation.

		E-W orientation			N-S orientation		
Parameter	Stem	N_{facing}	S_{facing}	p-value	E_{facing}	W_{facing}	p-value
Stem	Main	45.7 ±1.3	45.6 ±3.1	.476	43.5 ±1.7	44.9 ±3.1	.369
	Secondary	35.3 ±2	39.1 ±3.2		35.0 ±1.8	36.8 ±0.6	
Leaf	Main	38.5 ±1.9	35.7 ±3.4	.442	33.8 ±0.2	35.6 ±3.5	.215
	Secondary	30.6 ±2.2	29.2 ±3		27.9 ±3.4	32.2 ±2.1	
$Leaf_{removed}$	Main	141.8	135.3	-	140.7	139.4	-
	Secondary	61.8	59		61.3	60.7	
Fruit	Main	195.6 ±5.2	213.4 ±5.0	**.038**	211.4 ±9.8	211.0 ±4.6	.726
	Secondary	84 ±5.0	85.5 ±2.4		86.6 ±4.4	83.3 ±3.1	
$Stem_{base}$	-	34 ±1.1	33.8 ±1.7	.955	32.9 ±1	34.7 ±1.5	.309
Total	-	667.2 ±8.9	676.7 ±7.8	.268	673.1 ±13.7	678.6 ±5.8	.804

Table 2: Measured values of plant architectural parameters leaf area, stem length, leaf length and specific leaf area at the end of the experiment (20 July) of the rows with different facing side for plants grown in E-W oriented rows and N-S oriented rows. Values shown are the averages (±se) of the whole plant including main and secondary heads. Values marked in bold indicate significant differences between both facing rows within the same row orientation.

Facing side	Leaf area (cm^2)	p-value	Stem length (cm)	p-value	Leaf length (cm)	p-value	SLA (cm^2 g^{-1})	p-value
N	10356 ±564	**.007**	443 ±15	.926	30.6 ±0.5	.103	301 ±22	.227
S	8745 ±470		442 ±19		29.3 ±0.5		274 ±18	
E	8586 ±533	.150	423 ±7	.224	28.7 ±0.6	.724	280 ±10	.844
W	9416 ±477		433 ±18		29.1 ±0.7		285 ±21	

rows). On days with low global incoming radiation, which are cloudy days with a larger fraction diffuse radiation, the north-facing row had a higher light absorption and net photosynthesis compared to the south-facing row. For $NS_{E4.0,W4.0}$ (both east- and west-facing row having LAI of 4) very minimal differences were found between east- and west-facing rows, only 1 % for PAR absorption and 0 % for net photosynthesis (Fig. 1). For $EW_{N4.6,S3.8}$

(north-facing row higher LAI than south-facing row) the differences were clear. Over the whole period, south-facing rows absorbed 7 % more light, but this still resulted in a lower net photosynthesis of -4 %. With leaf area equal for north- and south-facing rows (simulation $\mathrm{EW}_{\mathrm{N3.8,S3.8}}$) the difference in light absorption of the south-facing rows compared to north-facing rows increased to 19 %, while net photosynthesis was 8% higher. The model sensitivity analysis for $\mathrm{EW}_{\mathrm{N4.6,S3.8}}$ showed that the assumption of photosynthetic parameters had a slight 2% change in daily net photosynthesis, while changing the leaf curvature to completely flat leaves increased daily PAR differences by 1 % [see Supporting Information- Fig. S7]. Model results were only minimally influenced by these parameters. In N-S rows the cumulative difference in PAR absorption and photosynthesis between the east- and west-faced row was less than 1 %. A comparison between $\mathrm{EW}_{\mathrm{N4.0,S4.0}}$ and $\mathrm{NS}_{\mathrm{E4.0,W4.0}}$ showed that $\mathrm{EW}_{\mathrm{N4.0,S4.0}}$ had a 3 % higher daily light absorption and net photosynthesis.

Inter-row shading in an east–west row orientation. Biggest relative differences between south- and north-facing rows in PAR absorbed and net photosynthesis were found when the maximum solar angle during solar noon was about 60° (Fig. 2). On Day 80 biggest daily differences in PAR absorption between south- and north-facing row were found at latitude 26, while at Day 171 and 356 biggest differences were found at latitude 0. In these cases, the biggest differences were always found in the middle of the canopy [see Supporting Information- Fig. S5]. This was always paired with light-saturated conditions; hence, the relative differences in daily net photosynthesis rate are close to half that of differences in daily absorbed PAR. An example of this was for Day 356, where daily PAR differences were +55 % and photosynthesis differences only +28 % for latitude 0. For latitude 26 this was +25 % and +13 %. The fact that the biggest differences were found for the middle leaf layer indicates that most shading is taking place on the middle layer of the canopy. Reducing the row distance from 1.6 to 1.3 m, thereby reducing path distance to 0.32 m, resulted in a lower maximum difference between north- and south-facing rows of 33 % instead of 61 % for latitude 26 on Day 80 [see Supporting Information-Table S4]. Differences in net photosynthesis were decreased by 10 % (from 32 to 22 %). Increasing the row distance from 1.6 to 1.9 m, thereby increasing path width to 0.92 m, resulted in a maximum difference in daily absorbed PAR between north- and south-facing rows of 73 % instead of 55 % for latitude 0 on Day

356. This resulted in an only small increase in differences of daily net photosynthesis of north versus south-facing row from 28 to 32 %. Hence, modifying the row distance had clear effects on daily light interception, although effects were limited for daily net photosynthesis since most additional light captured was during light-saturated conditions. Removal of leaf photosynthetic aging in the model increased daily net photosynthesis differences between north- and south-facing rows by a maximum of 6 % for latitude 26 on Day 80.

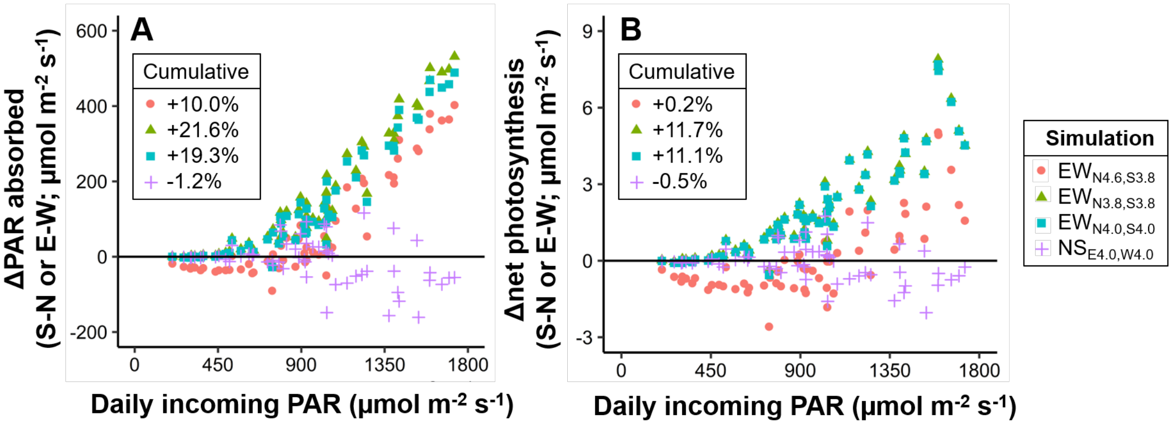

Figure 1: Simulated absolute differences in (A) PAR absorbed (μmol m^{-2} s^{-1}) and (B) net photosynthesis rate (μmol m^{-2} s^{-1}) between the two sides of a row versus incoming PAR (μmol m^{-2} s^{-1}); hence, difference between south- and north-facing rows in an E-W row orientation and between east- and west-facing rows in a N-S row orientation. '$\mathrm{EW}_{\mathrm{N4.6,S3.8}}$' denotes the model simulation where north-facing rows had a higher leaf area index than south-facing rows (leaf area index 4.6 versus 3.8 m^2 m^{-2}), whereas '$\mathrm{EW}_{\mathrm{N3.8,S3.8}}$' is the model simulation where north-facing rows and south-facing rows have equal leaf area index (3.8 m^2 m^{-2}). In '$\mathrm{NS}_{\mathrm{E4.0,W4.0}}$' both east- and west-facing rows have equal leaf area index (4.0 m^2 m^{-2}). Each data point refers to an entire plant and represents the value of 1 day (from sun rise to sun set) between 20 May and 20 July.

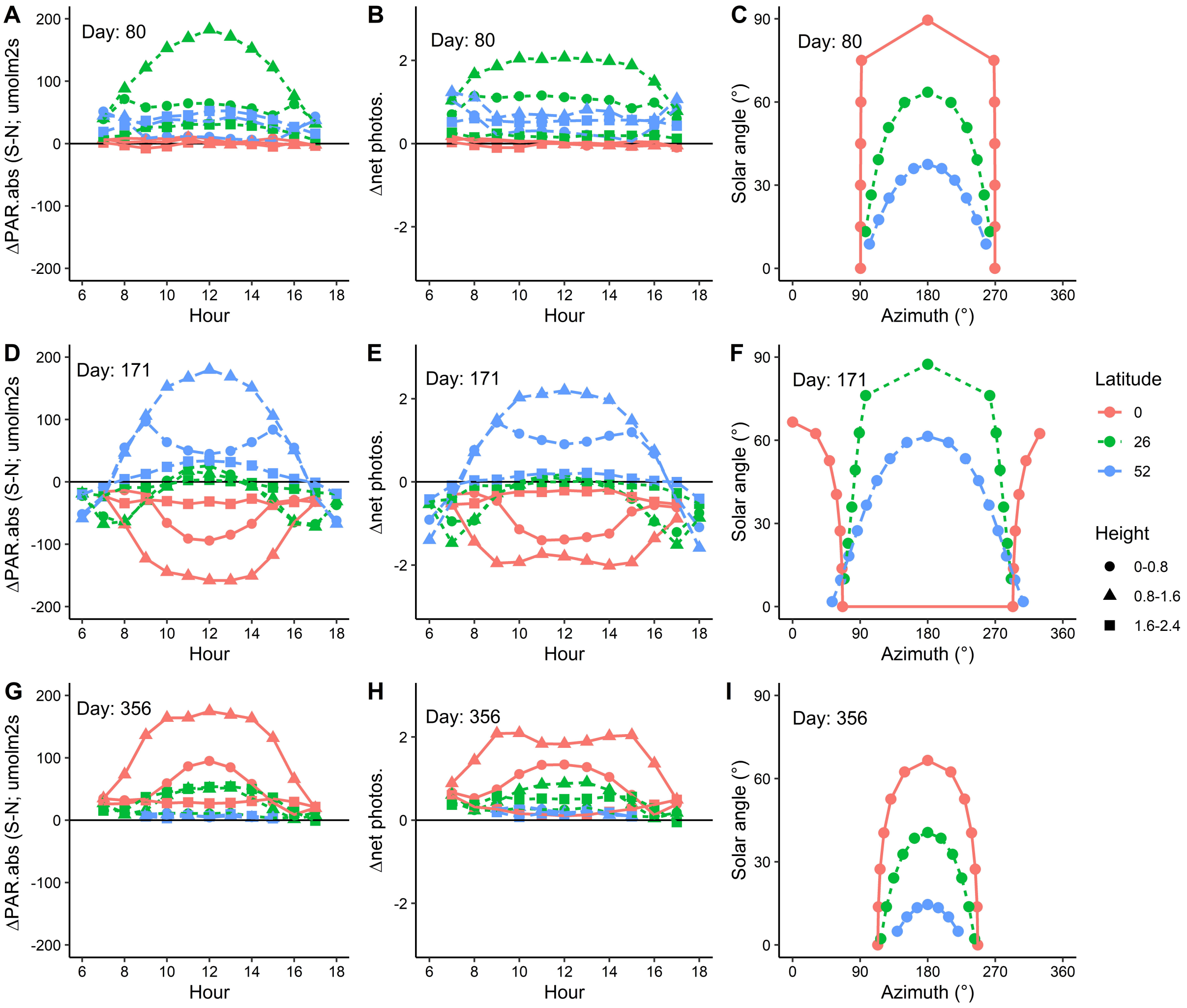

Figure 2: Hourly simulated PAR absorbed (A, D, G) and net photosynthesis (B, E, H), presented as differences (μmol m^{-2} leaf area s^{-1}) between south- and north-facing rows of east–west oriented rows for three different leaf layers from bottom to top of canopy (80 cm height interval each) at different latitudes (0, 26 and 52° Northern hemisphere) on days that represent the spring equinox (Day 80) and the summer and winter solstices (Day 171 and 356). Solar angle and azimuth are shown in C, F and I. Leaf area index of each canopy height (from bottom to top) was 1.43, 1.42 and 0.93 m^2 and was equal for the north- and south-facing rows. The numbers just above the x-axis represent cumulative differences over the whole day between the south- and north-facing rows. For schematic representation of azimuth and solar angle, we refer to Supporting Information-Fig. S2.

2.4 Discussion

2.4.1 Leaf area adaptation increased within-row net photosynthesis uniformity

Although the total plant mass was similar for north- and south-facing rows, south-facing rows produced substantially more fruit mass. Hence, dry matter partitioning differed between north- and south-facing plants. This could be due to a higher fruit temperature in the south-facing rows, when fruits were hanging below the leaves, at the stage in which they are more prone to heat maturation (Adams et al., 2001). Temperatures of tomato trusses on the outside of the canopy have been shown to be 1.9 °C higher than air temperature and 0.9 °C warmer than trusses in middle of the rows (Adams and Valdeés, 2002). With south-facing rows receiving more light the higher temperatures could have resulted in faster fruit development (Qian et al., 2015) and potentially a higher partitioning towards the fruits (Adams et al., 2001).

The increase in fruit dry weight was observed to have been compensated by a decrease in light absorption by a reduction in leaf area (Table 2). Surprisingly, north-facing plants adapted and had a larger total leaf area. This larger total leaf area partly compensated the lower light absorption per unit leaf area. An increase in leaf area is observed under shade avoidance symptoms (Kalaitzoglou et al., 2019). Another symptom, a decrease in leaf thickness (where more leaf area per gram of dry weight is required) (Holmes and Smith, 1975; Smith and Whitelam, 1997), was observed but found non-significant. Other typical shade avoidance responses were not found such as increased elongation of stems (Ballaré et al., 1991; Smith and Whitelam, 1997; Cole et al., 2011), nor a change in leaf mass.

Model simulations withincreased leaf area for plants in the north rows ($\mathrm{EW}_{\mathrm{N4.6,S3.8}}$) demonstrate that the increase in leaf area enhanced within-row uniformity in light absorption and net photosynthesis (Fig. 1). At the end of the period of 2 months, total simulated light absorption was 7 % higher for south-facing rows, while net photosynthesis rate was -4 %. To understand the difference in these relative effects on light absorption and net photosynthesis, we have to consider that during the period of the model simulations the climate consisted of days with varying light conditions. On completely cloudy days the north-facing rows had higher light absorption and higher net photosynthesis rate. On sunny days the south-facing rows absorbed more light than north-facing rows. However, during hours close to solar noon when intensity is high the effects of extra light on photosynthesis are relatively small (Fig. 2). This can also be seen in a frequency plot covering simulations of the whole 2 months [see Supporting Information- Fig. S3]. The assumptions of leaf curvature and photosynthetic aging throughout the canopy had minimal influence on model result findings [see Supporting Information-Fig. S7]. Model simulations where leaf area was equal between north- and south-facing rows ($\mathrm{EW}_{\mathrm{N3.8,S3.8}}$) show that this would have resulted in a major difference between the two rows in light absorption and net photosynthesis of 19 and 8 %, respectively.

2.4.2 Light absorption and net photosynthesis similar between row orientations

In the current modelling study a minimal difference in light absorption and net photosynthesis was found for the period of 20 May to 20 July between both row orientations, with 3 % higher light absorption and net photosynthesis for the E-W row orientation ($\mathrm{EW}_{\mathrm{N4.0,S4.0}}$) compared to the N-S row orientation ($\mathrm{NS}_{\mathrm{E4.0,W4.0}}$). This is also in accordance with model simulations of Gijzen and Goudriaan (1989), who mentioned that row orientation is less influential at higher latitudes when the path width and row height ratio was in the range of $\leq$30 %. In this study, the path width was 62 cm and row height was 2.3 m, resulting in a ratio of 27 % between both. Similarly, another study on plant spatial distribution in maize suggested that the plasticity of maize canopy results in similar daily light interception values in different inter-row distances (Maddonni et al., 2001). Furthermore, no differences were found within the N-S row orientation, in accordance with previous literature (Trentacoste et al., 2015).

2.4.3 Inter-row shading in an east–west row orientation

The model exploration showed that inter-row shading of south-facing on north-facing rows is highly season- and latitude-dependent, following similar patterns to that found in hedgerows by Trentacoste et al. (2016). The differences of 33 % between daily differences in light absorption and daily differences in net photosynthesis on Day 356 show that light saturation plays a large role in row orientations where inter-row shading occurs around solar noon. At higher angles the differences are largest when the azimuth is not following the equator. Similar to Trentacoste et al. (2016) we found that the biggest differences between north- and south-facing rows are found in the middle layer of the canopy, followed by the top and then the bottom of the canopy (Fig. 2). Different strategies could be explored to increase the uniformity in tomato production within the double rows. The sensitivity analysis showed that either reducing or increasing row distance by 30 cm had a quite large effect on light interception differences up to 28 %, although differences in photosynthesis did not exceed 11 % and thus remained similar. To reduce within-row differences between facing sides it could be worthwhile to prune leaves around the middle leaf layer of the south- or north-facing rows, as it has been shown that most light is absorbed by the middle leaf layer. This light could then penetrate to the next rows.

2.5 Conclusions

Despite the higher uniformity when rows were oriented north–south, the overall crop light absorption and photosynthesis were slightly higher for an east–west orientation (both 3 % higher). Due to plant adaptation, row orientation had a minimal influence on light absorption and net photosynthesis at 52°N, where east–west has a slightly higher light absorption and net photosynthesis. In an east–west row orientation, an increased leaf area for the north-facing rows compared to the south-facing rows enhanced the uniformity in light absorption and net photosynthesis. Here, despite inter-row shading and higher light absorption for the south-facing rows, dry weight production was unaffected due to light saturating conditions. Model explorations reveal that almost all competition for light occurs in the middle layer of the canopy, and that this is strongly dependent on season with differences in solar angle and azimuth. Model simulations for the spring equinox and the summer and winter solstices reveal that between north- and south-facing rows the differences in daily light absorption range from -37 % up to +61 %, whereas for daily net photosynthesis this range is between -23 % up to +32 %. Reducing the row distance or pruning leaves are clear strategies that minimize within double row differences in productivity.

Acknowledgements

I would like to express my gratefulness to several people during the execution of this experiment. Andre Maassen, Geurt Versteeg, Maarten Peters, Sean Geurts, Erik Schuiling, Ferdinand Diesman for taking care of plant growth, maintenance and technical assistance.

And to Nur Fauzana Mohd Kasim and Csongor Szanto for extensive help during the experiment.

2.6 Supplementary material

Figure S1: Pictures taken during the experiment at 1 (A), 6 (B), 10 (C), and 14 weeks after transplanting (D, E).

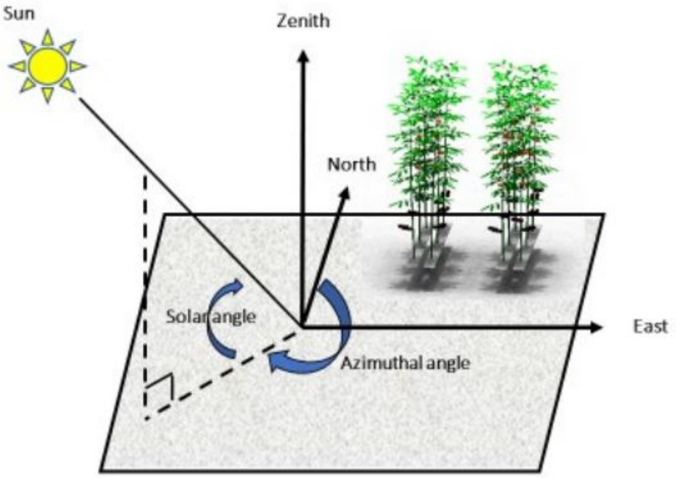

Figure S2: Schematic representation of azimuth and solar angle, in relation to plants in a row with south-north orientation.

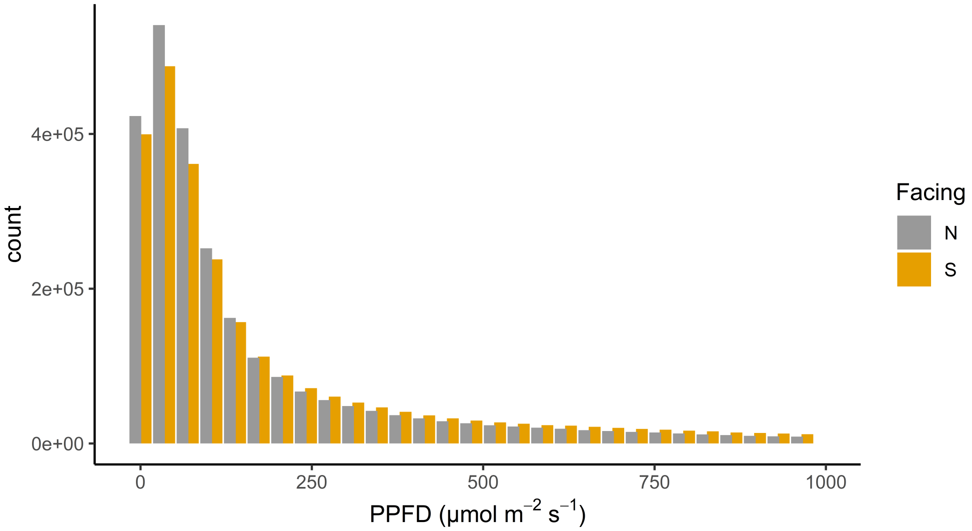

Figure S3: Frequency distribution of PPFD absorbed by each individual leaflet during the whole two month period for north and south facing rows.

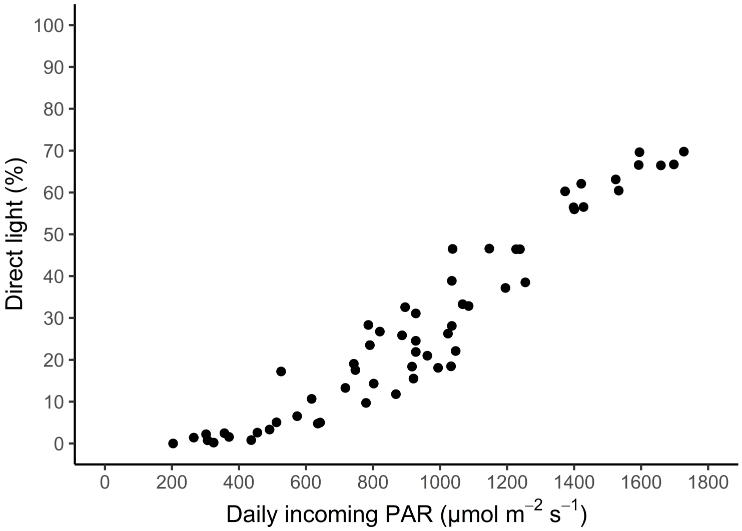

Figure S4: Simulated averaged daily direct light (%) versus daily incoming PAR (μmol m^{-2} s^{-1}) for the final two months of the experiment (20 May to 20 July).

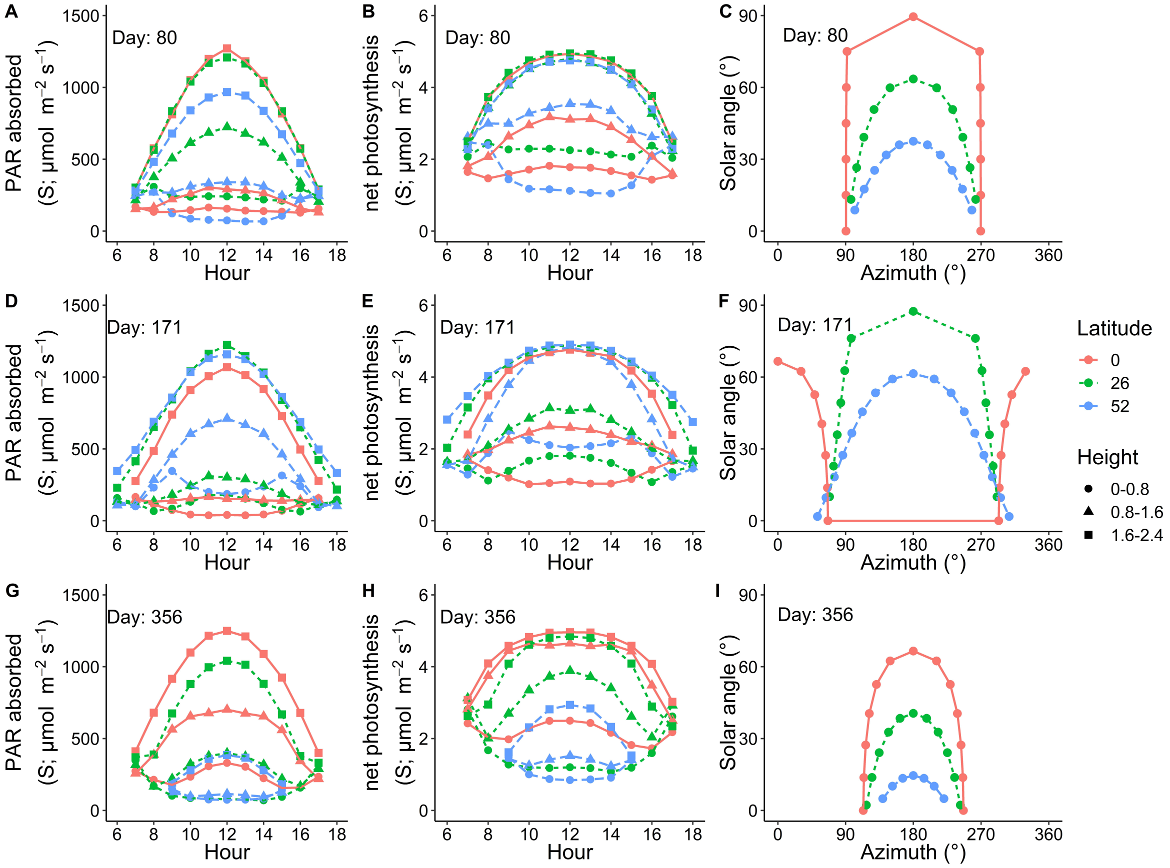

Figure S5: Hourly simulated PAR absorbed (A, D, G) and net photosynthesis (B, E, H) differences (μmol m^{-2} leaf area s^{-1}) for south-facing rows in east-west oriented rows for three different leaf layers (80 cm each) at different latitudes (0, 26 and 52° Northern hemisphere) on days that represent the spring equinox (day 80) and the summer and winter solstices (day 171 and 356). Leaf area index of each canopy height (from bottom to top) was 1.43, 1.42 and 0.93m^2.

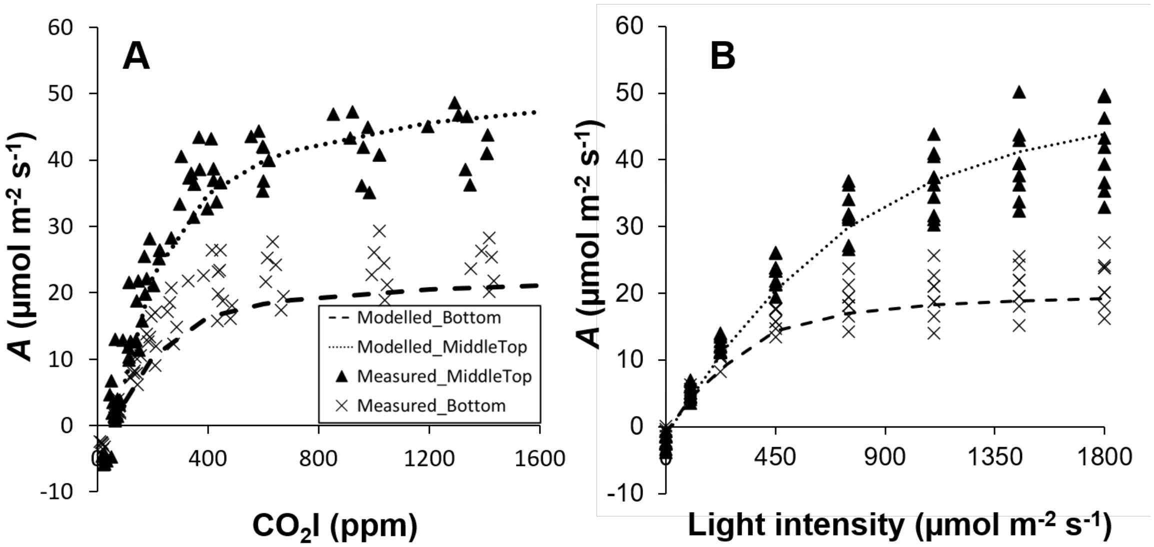

Figure S6: Measured (symbols) and modelled (lines) relation between net assimilation rate and (A) leaf internal partial pressure pressure of CO_2 and (B) incident light intensity, at the middle-top (triangles; dotted line; 50-80 cm from the top) and bottom (crosses; dashed line; 150 cm from the top) of the canopy.

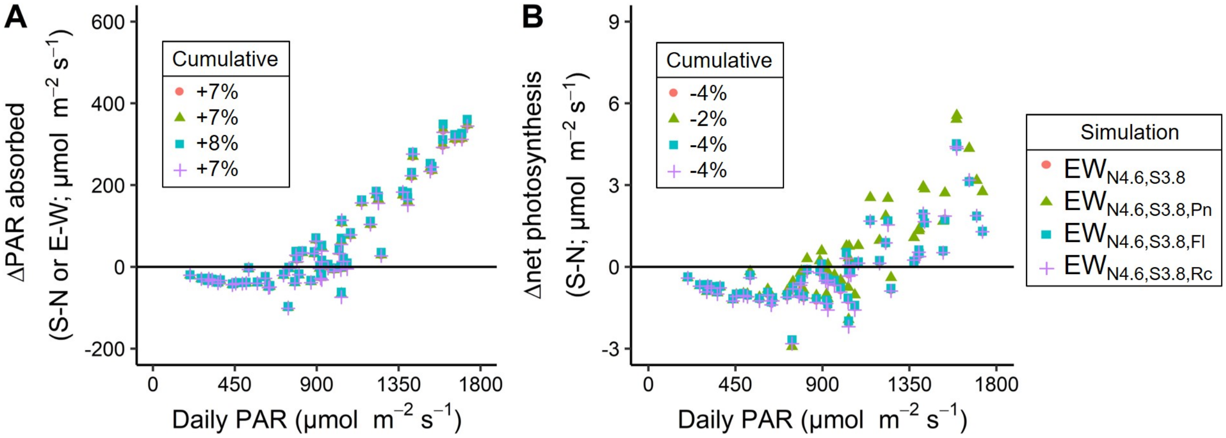

Figure S7: Sensitivity analysis EW_1. P_n stands for equal photosynthesic parameters throughout the entire canopy (no aging), F_l stands for flat leaves (0 degrees curvature in leaflets), R_c stands for random curvature (between 0 and 120 degrees), normally curvature of leaves is 60 degrees.

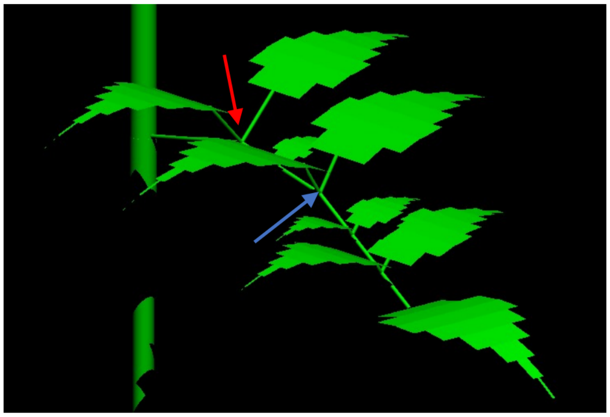

Figure S8: Simulated representation of a single leaf of a plant showing the number of leaflets and curvature. The place of the first and second bend of the rachis are depicted by respectively a red and a blue arrow.

Figure S9: Single plant showing the architecture of a plant.

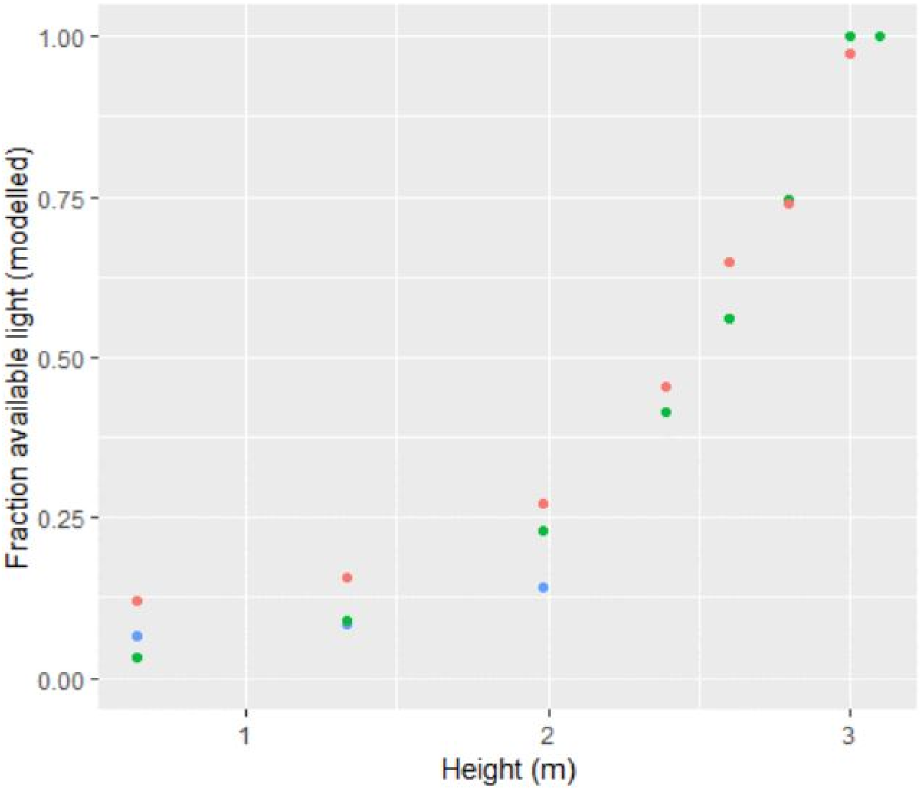

Figure S10: Comparison of simulated light extinction in the canopy compared with measurements and Lambert-Beer extinction (k=0.75).

Table S1: Composition of the nutrient solution used in the experiment. Solution EC: 2.8 and pH: 5.5.

Macronutrients	Amount	Unit	Micronutrients	Amount	Unit
NH4	1.2	mmol/l	Si	0	μmol/l
K	10.3	mmol/l	Fe	25	μmol/l
Na	0	mmol/l	Mn	10	μmol/l
Ca	5.8	mmol/l	Zn	5	μmol/l
Mg	2.59	mmol/l	B	30	μmol/l
NO3	17.2	mmol/l	Cu	0.75	μmol/l
SO4	4.76	mmol/l	Mo	0.5	μmol/l
HCO3	0	mmol/l	Cl	0	μmol/l
P	1.62	mmol/l			

Table S2: Architectural parameter values considered non-significantly different of petiole angle, rachis first bend and rachis second bend for different phytomer ranks.

Phytomer	Petiole angle	Rachis first bend	Rachis second bend
1	10.0	-22.7	-20.9
2	19.4	-25.0	-18.8
3	20.7	-15.7	-27.1
4	18.1	-22.5	-26.3
5	28.1	-25.6	-8.1
6	10.0	-20.0	-12.5
7	21.0	-22.5	-8.0
8	23.6	-20.7	-15.0
9	17.5	-15.8	-5.0
10	23.9	-17.2	3.9
11	23.9	-24.3	-3.6
12	26.4	-15.0	-10.0
13	19.6	-9.6	-5.0
14	27.5	-14.5	-3.0
15	31.2	-9.6	-6.2
16	31.3	-10.6	-10.6
17	25.0	-15.5	-1.5
18	35.5	-11.8	3.2
19	36.7	-5.8	0.0
20	40.6	-1.9	2.5
21	44.6	-7.9	-5.8
22	51.4	-7.3	-9.1
23	49.3	-11.8	-22.5
24	50.0	-23.8	-20.0
25	46.4	-16.8	-22.3
26	51.4	-21.4	-21.4
27	53.3	-6.7	-5.0

Table S3: Percentual difference of modelled crop net photosynthesis and absorption of PPFD between model runs using default or other values of input parameters such as number of parallelograms per leaflet (6 to 14, with 8 as default), ray number (50 million to 1 billion, with 750 million as default) and recursion depth (1-15, where 10 is default). Simulations were done for one light condition on day 171 with diffuse sunlight and a plant density of 4.4 m^{-2}. For the default settings simulated daily averaged photosynthesis and crop light absorption were 36.16 μmol CO_2 m^{-2} s^{-1} and 1591.85 μmol PPFD m^{-2} s^{-1}.

Parameter value	Net photosynthesis	PPFD absorbed by crop
Number of parallelograms		
6	100.10	99.86
7	100.03	99.95
10 (default)	100.00	100.00
12	100.01	100.02
14	100.02	100.03
Ray number (millions)		
50	99.94	100.08
100	99.95	99.98
250	99.98	99.98
500	99.99	99.99
750 (default)	100.00	100.00
1000	100.00	100.00
Recursion depth		
1	95.53	96.02
5	99.90	99.91
10 (default)	100.00	100.00
15	100.01	100.01

Table S4: Daily differences in PAR absorption and net photosynthesis (%) between south- and north-facing rows in an E-W row orientation at different latitudes (0, 26 and 52° Northern hemisphere) on days that represent the spring equinox (day 80) and the summer and winter solstices (day 171 and 356). Leaf area index of the canopy was 3.8. Path and row width were 62 cm and 160 cm, respectively. Distance between both rows in a double row was 0.5m.

		Daily PAR difference (S/N; %)				Daily net photosynthesis difference (S/N; %)			
Latitude	Day	Ref	Row dist (130 cm)	Row dist (190 cm)	Pn equal	Ref	Row dist (130 cm)	Row dist (190 cm)	Pn equal
0	80	1	1	1	1	0	1	0	1
0	171	-37	-23	-43	-37	-23	-15	-25	-26
0	356	55	28	73	55	28	17	32	33
26	80	61	33	75	61	32	22	32	38
26	171	-14	-9	-16	-14	-11	-8	-11	-12
26	356	25	13	36	25	13	8	17	14
52	80	35	19	46	35	20	14	24	22
52	171	25	15	30	25	9	7	8	11
52	356	14	14	16	14	11	13	12	12

Chapter 3

3 Local versus long-distance responses to far-red illumination in full-grown tomato plants

[1]van der Meer, M., [1]Gyeole, K., [2]de Visser, P. H. B., [1]Heuvelink, E., [1]Marcelis, L. F. M.

[1]Horticulture and Product Physiology, Wageningen University, Droevendaalsesteeg 1, 6708PB Wageningen, The Netherlands

[2]Business Unit Greenhouse Horticulture, Wageningen Research, Droevendaalsesteeg 1, 6708PB Wageningen, The Netherlands

An adapted version of this chapter has been submitted to the journal *"European Journal of Horticultural Science"*.

Abstract

Local and long-distance plant responses to localized light spectrum have hardly been studied in large plants. This paper aims to investigate whether local supplementation of FR results in local or long-distance architectural and growth responses in full-grown tomato plants. Tomato plants grown in a climate chamber were separated horizontally with white plastic at 85 days after sowing (lower half was 50cm and upper half 15cm long). The lower half was already full-grown and did not elongate anymore. The following 17 days both halves received 123 μmol m^{-2} red/blue light. The lower, upper, or none of the plant halves received 94 μmol m^{-2} additional far-red radiation (FR). FR supplied to the upper half increased petiole and internode elongation as well as specific leaf area (SLA) while petiole angle decreased. Moreover, dry weights of leaf stem (petiole+rachis+petiolules) and stem increased while leaf (lamina) dry weight decreased. Leaf area was unaffected. When FR was supplied to the lower half of the plant SLA, stem length, and stem dry weight of the upper half also increased, but to a lesser extent than when FR was supplied to the upper half. However, FR supplied to the lower half of the plant did not significantly affect other parameters such as petiole length, petiole angle and leaf dry weight of the upper plant half. We conclude that locally supplied FR has long-distance effects on length and dry weight of the stem and on SLA, while some other parameters (petiole elongation, petiole angle, leaf weight) are only locally affected.

3.1 Introduction

The link between a plant's site of light perception and the sites where morphological adaptations take place is a field of study with recent advancements but is still not fully understood (Küpers et al., 2018; Iglesias et al., 2018). Plants are modular organisms and are the product of build-up of individual organs connected to one big network through the xylem and phloem (Kroon et al., 2005). Each organ perceives its own light microclimate (light intensity and spectrum; Chelle, 2005). Changes in morphology resulting from an individual organ's perceived light microclimate can be at the level of the organ itself (local) and at the plant level where it also affects other plant organs (long-distance). Local and long-distance morphological responses to the local light spectrum can be studied in relation to the photoreceptor phytochrome by lowering the ratio of red (R) to far-red (FR) light, mimicking shade, through application of FR. This lowered R to FR ratio induces shade avoidance responses (SAR) such as increased elongation of stems (Ballaré et al., 1991; Smith and Whitelam, 1997; Cole et al., 2011) and petioles (Kozuka et al., 2010) and reorientation of petioles (Whitelam and Johnson 1982; Sasidharan et al., 2010; Pantazopoulou et al., 2017; Kalaitzoglou et al., 2019), in order for a plant to compete with its neighbours. There are plenty of reviews on the way SAR are thought to operate and on their functionality (Casal, 2013; de Wit et al., 2016; Fraser et al., 2016; Ballaré and Pierik, 2017; Viczián et al., 2017; Iglesias et al., 2018).

An increase in perception of FR upregulates the biosynthesis of auxin, a plant hormone strongly related to SAR (Procko et al., 2014; Tao et al., 2008). Auxin is transported from cell to cell through polar auxin transport by auxin efflux carriers PIN-FORMED3 (PIN3), PIN4 and PIN7 (Keuskamp et al., 2010; Kohnen et al., 2016). Studies with (mutant) plants where auxin was limited in biosynthesis, conjugation, transport, downstream signaling or perception showed severely weakened SAR (Keuskamp et al., 2010; Keuskamp et al., 2011; de Wit et al., 2015). The way this is thought to operate at the molecular level is that perception of FR inactivates phytochrome B, which results in a reduced phosphorylation and less degradation of the phytochrome-interacting factors (Ni et al., 2014; Shin et al., 2016). Phytochrome-interacting factors are basic helix-loop-helix transcription factors (Leivar and Quail, 2011) and promote elongation (Ni et al., 2014; Shin et al., 2016). Therefore, an increase in perceived FR increases the activity of phytochrome interacting factors, resulting in SAR.

Local versus long-distance responses to light spectrum are commonly studied in seedlings, where (de-etiolated) seedlings are used as study material, allowing for fast research (Küpers et al., 2018). These studies provide very useful information and have revealed that light spectrum perceived by an organ induces a wide range of morphological responses which can either be local or long-distance, depending on the type of organ receiving the light treatment and the morphological response looked at, as summarized by Küpers et al. (2018). Early work on cucumber (Cucumis sativus L.) (Black and Shuttleworth, 1974) and on white mustard (Sinapsis alba L.) (Casal and Smith, 1988; Casal and Smith, 1989) revealed that local illumination of the cotyledons by FR induced an increased extension growth of the first internode. This increased internode extension growth is fueled by and requires an increase in sucrose transport towards the internode (de Wit et al., 2018). Local illumination with FR on cotyledons of Brassica rapus seedlings induced hypocotyl elongation which was linked to an auxin gradient from the leaves towards the hypocotyl (Procko et al., 2014). A long-distance response was also found in Arabidopsis thaliana, where illumination with FR on the tip of a lamina induced a hyponastic response in the petiole of that particular leaf (Pantazopoulou et al., 2017; Michaud et al., 2017). Sugar content and botrytis were found to increase in both the third and fourth formed leaf, when the fourth leaf of young tomato plants was illuminated by FR, but illumination of third leaf only affected the third leaf (Courbier et al., 2020). Thus, using young plants as model plants has demonstrated that there is a variety of responses to local FR.

Extrapolation of results from studies on local lighting on de-etiolated seedlings, rosette plants or very young plants to tall plants (e.g. longer than 1 m) is difficult if not impossible, and experiments should be conducted with large adult plants (Küpers et al., 2018). That long-distance signaling is possible has been shown for root development and flowering, which are regulated by R:FR perception in the leaves (Chen et al., 2016; Endo et al., 2016; van Gelderen et al., 2018). According to the best of our knowledge there has been no research in tall full-grown plants whether FR effects on growth and morphology are local or long-distance. Therefore, this paper aimed to investigate whether and to which extent local supplementation of FR results in local or long-distance architectural and growth responses in full-grown tomato plants. A climate room experiment was performed where tomato plants were horizontally separated by opaque white plastic in a lower and a upper half and FR was locally supplemented to either of the two halves.

3.2 Material and methods

3.2.1 Plant material and growth conditions

Tomato seeds (*Solanum lycopersicum*, cv. Cappricia) were sown in a tray with stonewool (Grodan, Roermond, The Netherlands) plugs in a climate chamber, irrigated with a tomato-specific nutrient solution (EC = 2.1 dS m^{-1} and pH = 5.5; Table S1). Thirteen days since sowing, a total of 18 seedlings were transplanted onto stonewool blocks (10 cm x 10 cm x 6.5 cm) and placed onto 6 stonewool slabs (100 cm x 20 cm x 10 cm) placed in hard plastic

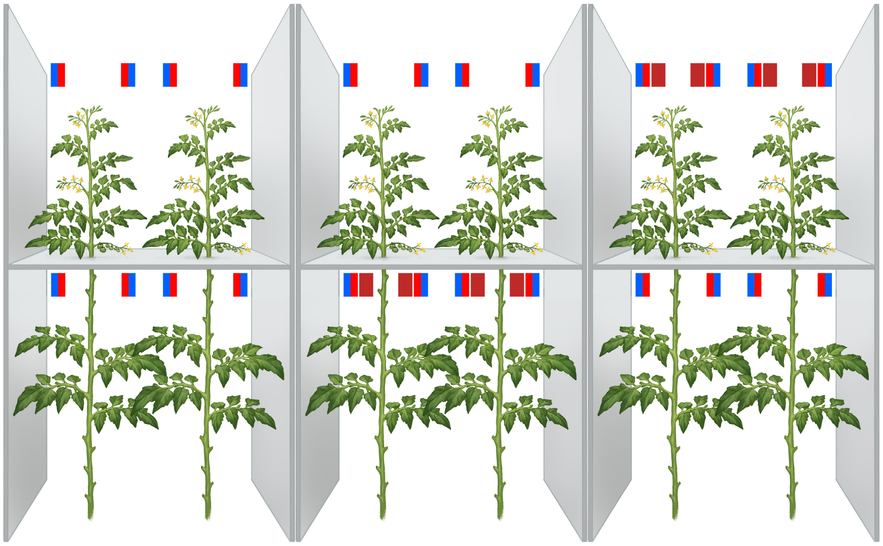

Figure 1: Tomato plants separated in lower and upper halves by use of two layers of white plastic. In each treatment both halves received R+B light by LED lighting (123 μmol m^{-2} s^{-1}) and received either no supplemental FR (left), supplemental FR (94 μmol m^{-2} s^{-1}) in the lower half of the plant (center) or supplemental FR (94 μmol m^{-2} s^{-1}) to the upper half of the plant (right).

gutters on the floor. Day length was 16 hours with a light intensity of 123 μmol m^{-2} s^{-1} at the apex. Light was provided by red and blue (RB) LEDs (ratio 76:24; GreenPower RB production modules 150 cm, Philips, the Netherlands). The distance between light source and top of the plants was kept at a maximum of 40 cm and minimum of 30 cm by raising the height of the LEDs. Setpoint for relative humidity was 70%, and setpoints for day/night temperatures were 22/20°C. Temperature and relative humidity were continuously measured in one compartment with a Hoogendoorn Box (Hoogendoorn, the Netherlands). During both repetitions, measured day and night temperatures (°C) with standard deviations were 21.8 ±0.5/ 19.9 ±0.4 and 21.8 ±0.4/ 19.8 ±0.3. Measured relative humidity (%) was 70.0 ±1.9 and 70.0 ±1.4. Combined temperature and humidity loggers were placed in each compartment during several days to compare the local climate, with average differences between treatments of at most 4.5% relative humidity and 0.1°C (ML4106 Temperature and Humidity Data Logger: Hanwell, England; Tables S2 and S3).

The plants were supported by a high wire once they reached 40 cm. The first truss (phytomere rank 12) was removed before anthesis to provide sufficient vegetative growth before the treatment began. Axillary bud outgrowths were removed at least every other day. To ensure pollination of the flowers a Vibri Vario (tomato pollinator; Royal Brinkman, the Netherlands) was used to vibrate each flowering truss 5 times a week. All trusses were pruned to 6 fruits per truss.

At 85 days since sowing the climate chamber was separated in three units by use of two layers of white/black double sided plastic (Fig. 1). Each unit contained one of 3 treatments, randomly allocated, and was 1.2 m^2 in area with 6 plants, resulting in a planting density of 5 plants m^{-2}. Within each unit the plants themselves were divided into lower (up to phytomere rank 14) and upper plant (from phytomere rank 15) halves by use of two layers of white/black double sided plastic (white sides towards both the upper and lower half of the plants); the lower half was 50 cm long and the upper stem was 15 cm at start of the treatments. In addition to the already present RB LEDs above the apex, RB LEDs were installed in an identical way at the top of the lower plant part. In this way on each level there was 123 μmol m^{-2} s^{-1} RB light. Besides the additional RB LEDs, also FR LEDs (GreenPower LED production modules FR 120 cm, Philips, the Netherlands; λ: 710-760 nm; peak at 735 nm) were installed in two of the treatments, either at the lower or upper plant half, with an intensity of 94 μmol m^{-2} s^{-1}. The R:FR ratio with standard deviation was 1.30 ±0.12. Leaves on phytomere ranks 10 to 14 were removed to make sufficient space between LEDs and the leaves. Also leaves on phytomere ranks 1 to 5 were removed due to some leaf senescence. The healthy leaves at rank 6 to 9 were kept. These were considered adult leaves since they had reached their final length and did not elongate during treatment (Table S4). Supplemental FR lasted for 17 days.

3.2.2 Plant measurements

Non-destructive plant measurements were taken on the day of treatment initiation (day 85) and at the end of the experiment (day 102). These measurements were divided in measurements on the young (phytomere ranks $\geq$15) and on the adult part (phytomere ranks 6 to 14). Measurements on the young part included internode length ($\geq$2 mm), leaf length ($\geq$5 cm) and width as measured by protractor and pictures were taken to determine the petiole angle (upper angle between petiole and stem). At the end of the experiment (day 102), destructive measurements were performed on each individual phytomere, determining leaf area (LI-3100C, LI-COR, USA) and dry weights of internode, leaf lamina, leaf stem (this term is used here for the sum of petiole, rachis and petiolules) and fruit truss. Dry weight was determined after oven drying (ventilated oven, 70°C for 24h, followed by 105°C for 24h).

3.2.3 Statistical analysis

The experiment was conducted twice. In each experiment the three treatments were randomized over 3 plots. There were 6 replicate plants per plot in each experiment. As there was no systematic difference between replicate experiments for any of the parameters tested (data not shown), data were analyzed as randomized design by ANOVA, followed by mean separation with Student's Least Significant Difference (LSD) test. Normality and equal variances were assumed. Motivated by the small number of experimental units ($n = 2$), treatment effects were tested at the 10% instead of 5% probability level to avoid that likely treatment effects would be denied (Ott and Longnecker, 2006). Data collected on the adult plant parts before and after the treatments were compared using a paired samples t-test.

3.3 Results

3.3.1 Architecture

Supplying FR to the upper half of the plant (FR_{upper}) increased stem and petiole length and specific leaf area (SLA) in the upper half of the plant, while it decreased petiole angle (upper angle between petiole and stem), hence more upright leaves (Fig. 2). Leaf area was not significantly influenced by supplemental FR. When FR was supplied to the lower plant half, stem length and SLA in the upper half of the plant also increased but to a lesser extent than when FR was supplied to the upper plant part (Fig. 2). No significant differences were found between the control (no FR) and FR_{lower} (FR supplied to lower plant half) for petiole length, petiole angle, and leaf area in the upper half of the plant.

3.3.2 Biomass

FR, whether supplied to lower or upper half of the plant, increased stem dry weight of the upper plant half, though effects of FR_{upper} were larger than that of FR_{lower} (Fig. 3). Dry weight of the leaf stem (petiole+rachis+petiolules) was significantly higher for FR_{upper} compared to the control, whereas for FR_{lower} it was in between and not significantly different from either of the other two treatments. Leaf (lamina) dry weight was the same for control and FR_{lower}, whereas this was significantly lower for FR_{upper}. Fruit dry weight seemed to increase from control to FR_{lower} to FR_{upper}, but the differences were not statistically significant due to a high variance. The treatments had no statistically significant effect on total dry weight of the upper plant half.

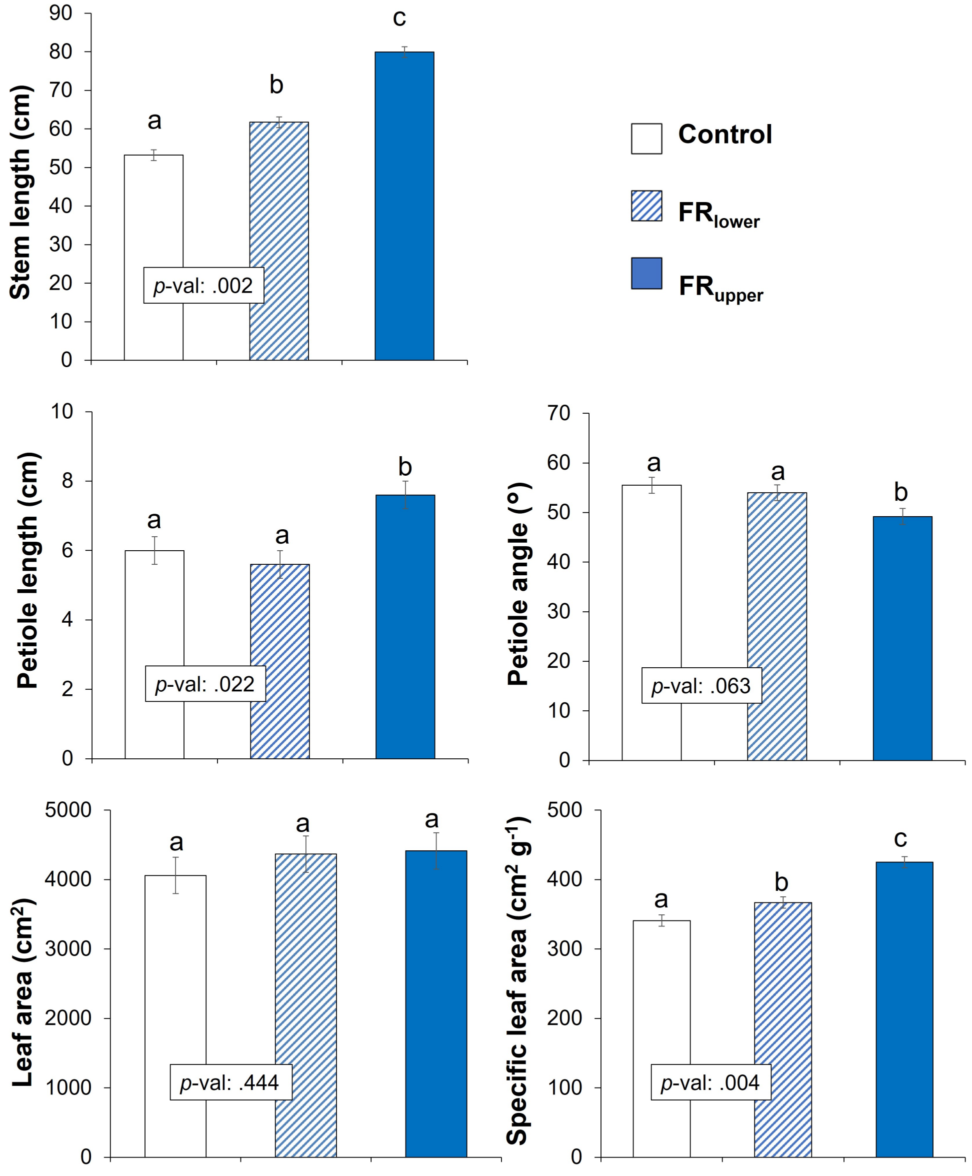

Figure 2: Architecture of the upper plant half when supplemental FR was applied to either no plant half (Control), the lower plant half (FR_{lower}) or the upper plant half (FR_{upper}). Different letters indicate significant differences (P=0.10), based on the LSD test. Standard error of the mean was based on the common variance and p-values (F-test) are given in each panel.

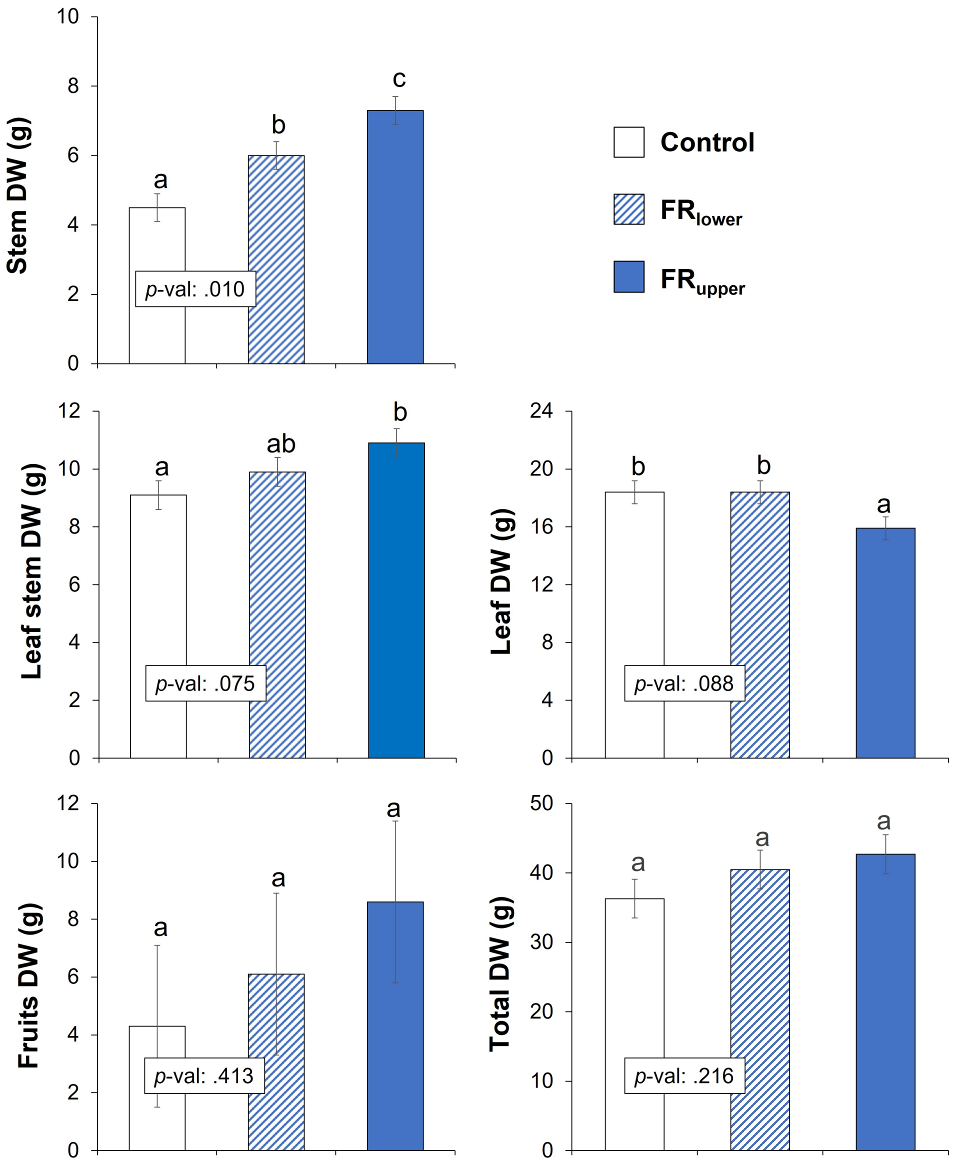

Figure 3: Dry weights of the plant organs and the total of all organs of the upper plant half when supplemental FR was applied to either no plant half (Control), the lower plant half (FR_{lower}) or the upper plant half (FR_{upper}). Leaf stem refers to sum of petiole, rachis and petiolules; leaf refers to the lamina of the leaf. Different letters indicate significant differences (P=0.10), based on the LSD test. Standard error of the mean was based on the common variance and p-values (F-test) are given in each panel.

3.4 Discussion

3.4.1 Overall response to far-red radiation supplied to the upper plant half

The observed increases in petiole and internode length due to FR illumination of the upper half of the plant is in line with findings with FR illumination of whole plants (Holmes and Smith, 1975; Ballaré et al., 1991; Smith and Whitelam, 1997; Kozuka et al., 2010; Cole et al., 2011; Kalaitzoglou et al., 2019). The decrease in petiole angle (more upright leaves) is in line with findings on small balsam (*Impatiens parviflora*) (Whitelam and Johnson 1982) and Arabidopsis thaliana (Sasidharan et al., 2010; Pantazopoulou et al., 2017), though Kalaitzoglou et al. (2019) found an increase in petiole angle when tomato plants were illuminated by additional FR.

Leaf (lamina) dry weight was significantly decreased in the upper half of the plant, while at the same time dry weights of leaf stem (petiole+rachis+petiolules) and stem increased when FR was supplied to the upper plant part (Fig. 3). The observation that there was no statistically significant increase in the upper plant half total biomass might be explained by the short duration of the F treatment. Kalaitzoglou et al. (2019) found that biomass increases with supplemental FR due to increased leaf area and hence light interception. Here, no differences were yet found for leaf area within the 17 days of treatment. The decrease in leaf dry weight while increase in dry weights of stem and leaf stem agrees with general effects of FR on dry matter partitioning (Ballaré et al., 1991; Smith and Whitelam, 1997; Cole et al., 2011; de Wit et al., 2018). Furthermore, the dry matter partitioning to fruits tended to increase (though not statistically significant), which is in line with Ji et al., (2019) when whole plants were illuminated by supplementary FR.

3.4.2 Local versus global response to far-red radiation

FR supplied to the upper half of the plant affected many variables of the upper plant half. Some of these variables such as petiole length, petiole angle and leaf weight, were not affected by FR supplied to the lower plant part. Hence, FR had a local effect but not long-distance effect on these variables. In contrast, variables like stem length, specific leaf area and dry matter partitioning to stem and leaf stem (at the expense of leaves) were affected by both supplying FR to lower or upper half of the plant. However, these effects were stronger when FR was supplied to the upper half of the plant. This indicates that in relatively tall plants

(1.3m) FR has a long distance effect on these variables, though the FR effect is smaller for organs at a distance from the FR illuminated organs. An explanation for the weaker long-distance effects compared to local effects could be that the distance itself has a limiting effect on the transport of the signal, possibly through dilution, as seen with auxin transport (Goldsmith et al., 1974) or that local synthesis of a signal molecule is more important, as proposed for auxin (Zhao, 2018).

3.4.3 Conclusions

Morphological and growth responses occurred in the upper young part of tomato plants when FR was supplied to adult leaves of the lower half of the plants. The morphological and growth responses were weaker than those resulting from locally perceived FR at the upper young plant part. Still, morphology and growth of young developing plant tissue can be influenced by light spectrum perceived by adult plant parts.

acknowledgements

We would like to express our gratefulness to several people during the execution of this experiment. Gerrit Stunnenberg, Taede Stoker and David Brink for technical assistance and support. Our colleague Nur Fauzana Mohd Kasim for extensive help during the experiment. And Anna Verhoog for the drawing of the experimental setup. This research was funded by the Wellensiek Fund, part of University Fund Wageningen.

3.5 Supplementary material

Table S1: Composition of the nutrient solution used in the experiment. Solution EC: 2.1 and pH: 5.5.

Macronutrients	Amount	Unit	Micronutrients	Amount	Unit
NH4	1,2	mmol/l	Si	0	μmol/l
K	7,2	mmol/l	Fe	35,0	μmol/l
Na	0	mmol/l	Mn	8,0	μmol/l
Ca	4,0	mmol/l	Zn	5,0	μmol/l
Mg	1,82	mmol/l	B	20,0	μmol/l
NO3	12,4	mmol/l	Cu	0,5	μmol/l
SO4	3,32	mmol/l	Mo	0,5	μmol/l
HCO3	0	mmol/l	Cl	0	μmol/l
P	1,0	mmol/l			

Table S2: Temperature (°C) and relative humidity (%) ±standard deviation measured during 4 consecutive days in each of the 3 compartments before FR treatment

Period	Treatment	Temperature	Relative humidity
Day	Control	22.5 ±0.5	67.2 ±1.5
Day	FR_{lower}	22.5 ±0.5	64.5 ±1.3
Day	FR_{upper}	22.4 ±0.5	68.7 ±1.5
Night	Control	20.8 ±0.2	66.2 ±1.0
Night	FR_{lower}	20.8 ±0.1	67.6 ±1.0
Night	FR_{upper}	20.8 ±0.1	63.1 ±0.8

Table S3: Temperature (°C) and relative humidity (%) (±standard deviation) measured during 3 consecutive days in the lower and upper halves in each compartment during FR treatment

Period	Treatment	Layer	Temperature	Relative humidity
Day	Control	Lower	21.3 ±0.6	70.4 ±2.7
Day	$\mathrm{FR_{lower}}$	Lower	21.3 ±0.6	69 ±2.4
Day	$\mathrm{FR_{upper}}$	Lower	21.3 ±0.5	69.3 ±2
Day	Control	Upper	21.4 ±0.5	67.2 ±1.9
Day	$\mathrm{FR_{lower}}$	Upper	21.4 ±0.4	67.5 ±1.4
Day	$\mathrm{FR_{upper}}$	Upper	21.3 ±0.4	66 ±0.7
Night	Control	Lower	19 ±0.5	72.4 ±4.2
Night	$\mathrm{FR_{lower}}$	Lower	19 ±0.5	71.9 ±4.6
Night	$\mathrm{FR_{upper}}$	Lower	18.9 ±0.5	71.8 ±4.5
Night	Control	Upper	19.5 ±0.3	68.1 ±1.5
Night	$\mathrm{FR_{lower}}$	Upper	19.5 ±0.2	67.8 ±1
Night	$\mathrm{FR_{upper}}$	Upper	19.4 ±0.2	66.2 ±0.8

Table S4: Paired samples *t*-tests reveal that there were no significant differences between stem length (phytomere ranks 6 to 14) and leaf length (phytomere ranks 6 to 9) at the moment the treatments started and the final day of the experiment.

Parameter	Treatment	Start of treatment	End of treatment	P-value
Stem length	Control	34.3	34.2	0.695
	FRlower	34.6	34.9	0.215
	FRupper	34.2	34.3	0.935
Leaf length	Control	36.6	36.6	1.000
	FRlower	35.4	35.2	0.357
	FRupper	35.6	35.4	0.407

Chapter 4

4 Consequences of intra-canopy and top LED lighting for uniformity of light distribution in a tomato crop

[1*]Schipper, R., [1*]van der Meer, M., [2]de Visser, P. H. B., [1]Heuvelink, E., [1]Marcelis, L. F. M.

[*]Both authors contributed equally to this manuscript and share first authorship

[1]Horticulture and Product Physiology, Wageningen University, Droevendaalsesteeg 1, 6708PB Wageningen, The Netherlands

[2]Business Unit Greenhouse Horticulture, Wageningen Research, Droevendaalsesteeg 1, 6708PB Wageningen, The Netherlands

Abstract

In the past decade, the potential of intra-canopy light-emitting diode (LED) lighting to enhance or modify crop growth and yield has been explored in greenhouse cultivation. Changes in spatial heterogeneity of light absorption that come with the introduction of intra-canopy lighting have not been thoroughly explored. We calibrated and validated an existing functional- structural plant model (FSPM), which combines plant morphology with a ray tracing model to estimate light absorption at leaflet level. This FSPM was used to visualize the light environment in a tomato crop illuminated with intra-canopy lighting, top lighting or a combination of both. Model validation of light absorption of individual leaves showed a good fit ($R^2 = 0.93$) between measured and modelled light absorption of the canopy. Canopy light distribution was then quantified and visualized in three voxel directions by means of average absorbed photosynthetic photon flux density (PPFD) and coefficient of variation (CV) within that voxel. Simulations showed that the variation coefficient within horizontal direction was higher for intra-canopy lighting than top lighting (CV=48% versus CV= 43%), while the combination of intra-canopy lighting and top lighting yielded the lowest CV (37%). Combined intra-canopy and top lighting (50/50%) had in all directions a more uniform light absorption than intra-canopy or top lighting alone. The variation was minimal when the ratio of PPFD from intra-canopy to top lighting was about 1, and increased when this ratio increased or decreased. Intra-canopy lighting resulted in 8% higher total light absorption than top lighting, while combining 50% intra-canopy lighting with 50% top lighting, increased light absorption by 4%. Variation in light distribution was further reduced when the intra-canopy LEDs were distributed over strings at four instead of of two heights. When positioning LED lamps to illuminate a canopy both total light absorption and light distribution have to be considered.

4.1 Introduction

In the past decade, the potential of intra-canopy lighting with light-emitting diodes (LED) to enhance crop growth has been explored in greenhouse cultivation, where part of the supplementary light is given from within the canopy. By providing supplementary light within the crop reflective loss of the upper canopy is reduced (Trouwborst et al., 2010). Furthermore, a more homogeneous vertical light distribution and therefore a higher photosynthetic use efficiency of the absorbed light could be achieved (Trouwborst et al., 2010). Studies with intra-canopy lighting partially replacing top lighting showed increased fruit yield in cucumber (Hovi-Pekkanen et al., 2004; Hovi-Pekkanen and Tahvonen, 2008), an increase in sweet pepper fruit number and weight (Hovi-Pekkanen et al., 2006), and an increased net photosynthesis (PN) and photosynthetic capacity (Pmax) in cucumber (Pettersen et al., 2010). In other studies no differences were found in whole plant biomass production or yield between top lighting and intra-canopy lighting (Trouwborst et al., 2010; Dueck et al., 2011; Gómez and Mitchell 2016; Yan et al., 2018). This lack of biomass gain could be related to a loss of total light interception due to extreme leaf curling by intra-canopy lighting as observed by Trouwborst et al. (2010) who used a large fraction of blue light. Gómez and Mitchell (2016) mentioned an increased maintenance respiration of leaves lower in the canopy that acclimated to a higher light intensity and an increased partitioning to non-harvestable organs as possible reasons for lack of effect on yield. All the explanations mentioned in literature about effects or absence of effects are based on differences in incident light environment which affect plant growth and morphology.

Measuring the incident light environment for individual leaves in a canopy is complex due to large horizontal and vertical light heterogeneity within a canopy. Incident light from lighting from above can be measured by quantum sensors pointing upward at different heights. Incident light from intra-canopy lighting might be measured by use of quantum sensors pointing in a sideward direction towards the intra-canopy lighting at different heights as for instance was done in Kaiser et al. (2019). Total light absorption can be estimated by measuring incident light by a quantum sensors pointing upward and measuring the non-absorbed light by quantum sensors above and below the crop, pointing, respectively, downward and upward. However, the spatial heterogeneity of incident and absorbed light is hard to measure in detail. The spatial variability of absorbed light is important when physiological processes such as photosynthesis are compared between light treatments.

A way to estimate spatial variability in light absorption is through crop modelling. Multiple process- based crop models (PBM) have been developed that include the relation between light interception and physiological processes such as photosynthesis. Many crop models use the Lambert-Beer equation (Monsi and Saeki, 2005) to estimate the light interception of a crop, based on the exponential decrease in light intensity with leaf area index (LAI) from top to bottom. With the addition of intra-canopy lighting the vertical light distribution cannot be simply represented by the Lambert-Beer calculation, while it may also have consequences for the horizontal light distribution, which is not considered in models using the Lambert-Beer equation. For simulation of intra-canopy lighting functional-structural plant models (FSPM) might be used. FSPM allow for a more detailed approach which combines 3D plant architecture and a ray tracing model to create understanding of the interaction between plant morphology, light interception, absorbance and distribution patterns at leaf level (Chelle and Bruno Andrieu, 2007; Vos et al., 2007; Chenu et al., 2008; Vos et al., 2010; Sarlikioti et al., 2011b; de Visser et al., 2014).

Various FSPM studies have been conducted for greenhouse cultivated crops, such as cut-rose (Buck-Sorlin et al., 2011; Zhang et al., 2021) and tomato (Sarlikioti et al., 2009; Sarlikioti et al., 2011b; Kang et al., 2011; de Visser et al., 2010; de Visser et al., 2014). Those studies aim to either optimize lighting strategies, plant architecture or planting densities to increase interception of light. To our knowledge however, the differences in light heterogeneity when comparing intra-canopy with top lighting have not yet been approached using an FSPM. Uniformity of spatial distribution of light over the leaves is important for maximizing crop photosynthesis. Due to the curvilinear shape of the light response curve of leaf photosynthesis the crop photosynthesis is higher when all leaves have the same intensity, compared to a situation with the same average light intensity but with variation among individual leaves. The importance of uniform light distribution was shown by Li et al. (2014) who found that a more uniform distribution of natural light in the greenhouse by diffuse greenhouse cover (a cover that converted 71% of the direct light into diffuse light) increased crop photosynthesis by 7%.

The objective of this study was to identify the impact of intra-canopy versus top lighting on 3D light distributions in the canopy. This was approached by conducting a greenhouse tomato experiment to parameterize and validate an FSPM which included simulation of light distribution by ray tracing in a 3D environment. This FSPM was then used to simulate and compare light absorption profiles between tomato canopies with intra-canopy lighting, top lighting or a combination of both intra-canopy and top lighting. The heterogeneity of light absorption was approached at the leaflet level in three directions; parallel and perpendicular to the double rows, as well as in the vertical direction.

4.2 Material and methods

4.2.1 Plant material, growth conditions and light treatments

Tomato plants (Solanum lycopersicum L. “Foundation”; Nunhems, Haelen, the Netherlands) were transplanted on the 10^{th} of February 2017 (52 days after sowing, DAS) in a glasshouse at Wageningen University, the Netherlands (52°N, 5.5°E) and grown until the 1^{st} of June 2017. The details of the experimental setup can be found in Kaiser et al. (2019), as the data acquired for this study were independently collected during the same experiment. Plants were grown on stone wool slabs (Grodan, Roermond, The Netherlands) for 111 days in a “high wire” system at 2.4 plants m^{-2}. Dimensions of the compartment were 6 by 12 meter. The plants were set up in 8 double rows with 1.5 meter double row distance. Each double row of 5m consisted of 20 plants. The glasshouse compartment was kept at 22/16°C day/night temperature, a relative humidity of 78% and 500 ppm CO_2 partial pressure was applied. This entailed removal of all side shoots, except for the axillary bud just after the sixth truss. All side walls of the greenhouse compartment were covered with a reflective screen, to prevent light pollution from neighboring compartments. In the greenhouse there was a gradient in rows receiving only red LED light to rows receiving up to 24% blue (76% red) light (see Kaiser et al., 2019). In this study rows receiving only red LED were used. Intra-canopy and top red supplemental light was provided by Greenpower PM-DR150 (Philips, Eindhoven, the Netherlands). The lamps for top lighting were pointing downward, while the lamps for intra-canopy lighting were pointing sideward to the plant rows on both sides. Lamps were on for 16 h per day, unless outside global radiation exceeded 450 W m^{-2}. Two LED strings (i.e. fixtures) of intra-canopy lighting were positioned between the plants in the double row at heights of 108 and 153 cm. Plant height during measurement period was 2m.

4.2.2 Plant architecture measurements

On 20 March (80 DAS), morphological traits of 6 plants were assessed. Stem and internode length, and leaf width and length were measured with a flexible ruler. Number of leaves and leaflets per leaf were counted. Petiole angle, first and second main rachis angles, and the insertion- and tip angle of the two biggest leaflets per leaf were measured with a protractor. Leaf length and width, and all angles were measured for rank number 4, 8, 12, 16 and 20, where rank 1 corresponded with the youngest leaf (> 2 cm) of the plant.

4.2.3 Light measurements

Vertical and horizontal light distribution was measured 0 to 2 days after the architecture measurements. A grid of photosynthetically active radiation (PAR) measurements was created (Fig. 1), using a line quantum sensor (1 m, LI-191SA, LI-COR Biosciences, Lincoln, NE, United States). The sensor was oriented upwards and positioned parallel to the gutter at regular intervals of about 50 cm in the vertical plane (at 35.5, 80, 130, 180, 230 and 280 cm from the floor). To measure the horizontal PAR distribution at each height, the sensor was oriented side-ward (towards the intra-canopy lighting) at regular intervals of 15 cm in the horizontal plane (at 0, 15, 30, 45, 60 and 75 cm from the center of the double rows). In addition, reflection from the floor was measured at 41 cm from the floor with the line sensor oriented downwards. All measurements took place in the absence of solar light, at least 2 hours after sunset. Then, either the top lighting, or the upper or lower positioned LED modules were switched on. The same light measurements were done in the greenhouse without plants.

4.2.4 Model description

An adapted version of a static greenhouse tomato functional- structural plant model (Chapter 2; de Visser et al., 2014) was used. This model was developed on the GroIMP platform (Kniemeyer, 2008) and consists of an architectural and a light module.

Plant architecture. The architectural parameter values for leaf length, leaf width, internode length, petiole angle, rachis angles and leaflet angles were taken from phytomer ranks 4, 8, 12, 16 and 20, acquired from the measurements on 20 March (80 DAS). Mean and standard deviation (SD) values for all architectural parameters for the non-measured phytomer ranks were linearly interpolated from the measured phytomer ranks [see Supporting Information-Fig. S1]. Area per leaf was estimated using a power function fit with leaf width as regressor (leaf area = 0.203*Lw 1.674, where Lw is leaf width; Schwarz and Kläring 2001).

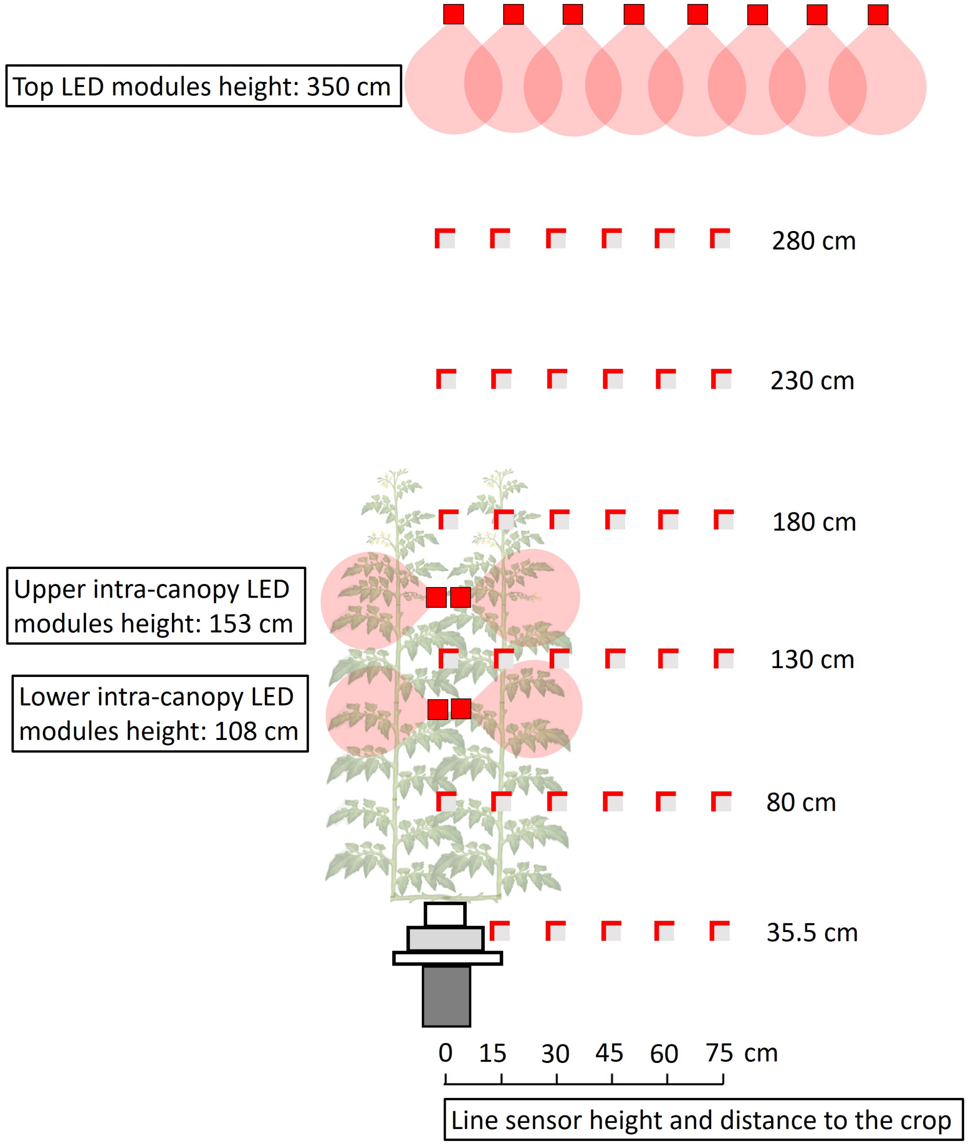

Figure 1: Side view of the light measurements in a tomato crop with LED lamps on top of the canopy and as intra-canopy lighting. Measurements were taken with a line sensor, indicated as a grey square with partly red borders. The line sensor was positioned parallel to the tomato double row at fixed distances (0, 15, 30, 45, 60 or 75 cm) from the center of the double row at fixed heights (35.5, 80, 130, 180, 230 or 280 cm). The two red borders on each grey square indicate the sides to which the line sensor was oriented in order to measure the vertical and horizontal incident light separately. Measurements for intra-canopy and top lighting were done when there was only light from one of the lighting systems at a time.

Parameter values for the equation were taken from the same paper of Schwarz and Kläring (2001). The leaf area was then distributed across the 11 leaflets (3 bigger pairs, 2 smaller pairs and one terminal leaflet) of each leaf according to an empirical allometric relationship as determined in Chapter 2. Leaflet lengths were then calculated by use of leaf area and leaflet shape according to Evers et al. (2006), after which each leaflet was constructed and represented as 10 parallelograms [see Supporting Information-Fig. S2]. Modelled architectural parameter values were acquired by drawing values from a normal distribution for each architectural trait. Internode length and leaf area were set at a minimum of 0.1 cm and 5 cm2, respectively. The apex height of the plants was set at 2 m from the floor, with the intra-canopy lighting on 1.53 and 1.28 m from the floor. The entire canopy comprised all the plants, i.e. 8 double rows of 20 plants each (Fig. 2). This simulated canopy was defined as the reference canopy.

Light module. The LEDs were reconstructed as they were in the experiment. The light distribution at a given time step was computed by the GroIMP radiation model, which is based on an inversed path tracer with a Monte Carlo pseudo-random number generator as in Veach (1998), which was upgraded to a full-spectral ray tracer by Henke and Buck-Sorlin (2018).

Greenhouse environment. The compartment was reconstructed with its major components. The white outside curtains (ILS Hortiroll Revolux w/w) were assumed to have a diffuse reflectivity of 25% for the front and left side wall (since these were behind glass) and 50% for the white curtain on the right wall (since this was inside the compartment). The white plastic that split the treatments in half was assumed to have a diffuse reflectivity of 65%, for the concrete floor this was 30% and for the plastic-covered stone wool slabs 65%. The simulations in the greenhouse were performed for moments that there was no solar radiation, nor was reflection from the greenhouse cover simulated.

Model validation. The simulated distribution of LED light inside the greenhouse compartment including plants was compared with the light measurement values performed with the line sensor during the experiment. To quantify the accuracy of the simulated light distribution, in the model virtual line sensors were placed similar to the actual measurements (Fig. 1). The light intensity at each virtual position of the line sensor was compared with the actual light measurements. The performance of the model was evaluated by the goodness of fit (R^2).

Simulation scenarios. Simulations were run with the reference canopy structure for three different lighting strategies: intra-canopy lighting, top lighting and a combination of intra-canopy and top lighting (50/50%). In each scenario the incident light of all light sources together was equal (85.5 μmol m^{-2} s^{-1}), being verified in the light model by enclosing the lamps in a black box absorbing all emitted lamp light. The top lighting modules were placed centered above each double row. Intra-canopy lighting modules were simulated at at 108 and 153 cm height similar as in the experimental setup.

Evaluation of simulated light distribution and heterogeneity. In each simulation two times six center plants were observed in each of four double rows (Fig. 2). These eight groups of six plants each were considered repetitions of each other for further calculations. Each of these sets of six simulated plants was divided into voxels to visualize the canopy light distribution. Each voxel had a width and height of 7.5 cm and a length to include all leaflets of the considered plants within that direction. The voxels were directed either (1) horizontal parallel to the row, (2) horizontal perpendicular to the row or (3) vertical. Consequently, the corresponding length of the voxels were based on either (1) the row length of the six plants in the row, (2) the width of four double plant rows (hence includes 8 plants) or (3) the height of the plants.

For each voxel, the average absorbed PPFD (μmol m^{-2} s^{-1}) and coefficient of variation (CV) within that voxel were calculated. This was done with light absorption data collected for each individual leaflet (μmol s^{-1} per leaflet; for sample sizes in each voxel see Supporting Information-Fig. S3). The average absorbed PPFD inside each voxel was calculated by dividing the cumulative absorbed light of all leaflets by the cumulative leaf area (m^2) of all leaflets inside the voxel (Fig. 3). Furthermore, the average, SD and CV of absorbed PPFD was calculated based on average values of each voxel. These SD and CV values give an indication of heterogeneity between voxels, quantifying the heterogeneity within the canopy. For calculating the CV within a voxel the four smallest leaflets on each leaf were not considered due to their small total fraction (0.09%) of the leaf area. By excluding these four smallest leaflets the calculated CV is representative for the majority of the photosynthetically active leaf area. Then, inside each voxel the absorbed PPFD was calculated for each leaflet individually and these were then used to calculate the mean absorbed PPFD with its associated standard deviation (SD) between leaflets. The CV was then calculated by dividing the SD by the mean absorbed PPFD. Furthermore, a mean CV of canopy absorbed PPFD was calculated by averaging the CV of each voxel (indicating the average CV within a canopy).

Sensitivity analysis. Besides the reference simulations there were additional model simulations that tested the sensitivity of the mean CV and SD of the absorbed PPFD to changes in height and number of the LED modules and the ratio between intra-canopy and top light. Either the height of the LED modules were increased or decreased by 30 cm, the number of LED module strings was increased from 2 to 4 (the additional 2 LED module strings were located at 131 and 86 cm from the floor, which is between and below the original two LED module strings; see Supporting Information-Fig. S4), or the ratio between intra-canopy and top light was set at 25/75% or 75/25%.

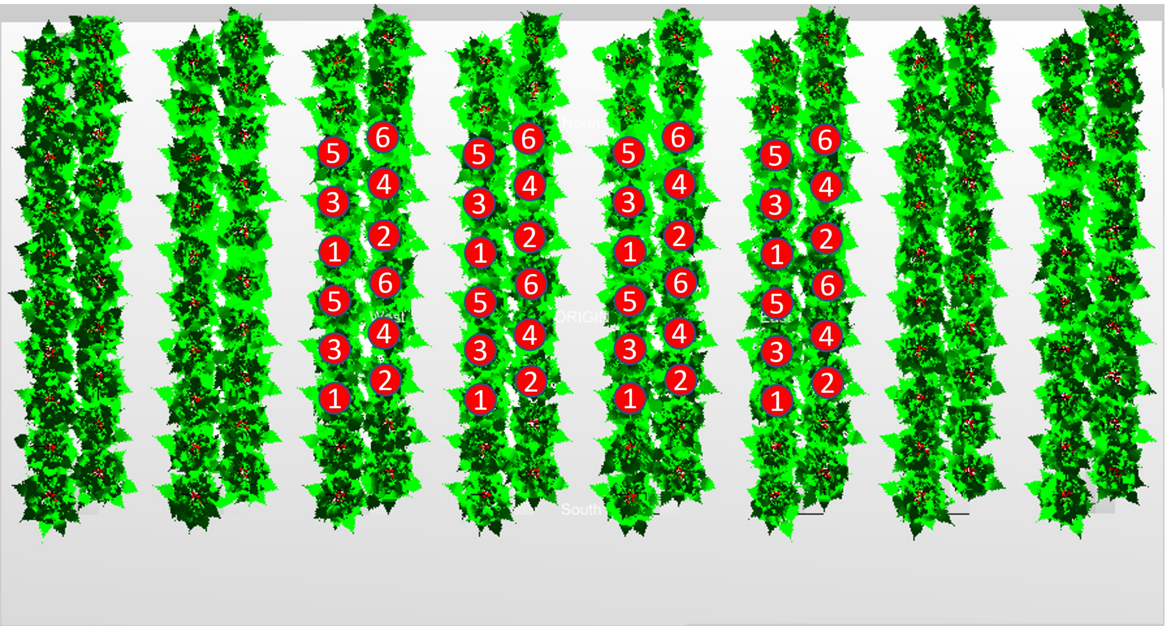

Figure 2: Top-view of the reconstructed modelled tomato canopy with architectural parameters measured on 20 March (80 DAS). In each simulation two times six center plants were observed in each of four double rows. These eight groups of six plants each were considered repetitions of each other and the absorbed light of each leaflet was used for further calculations.

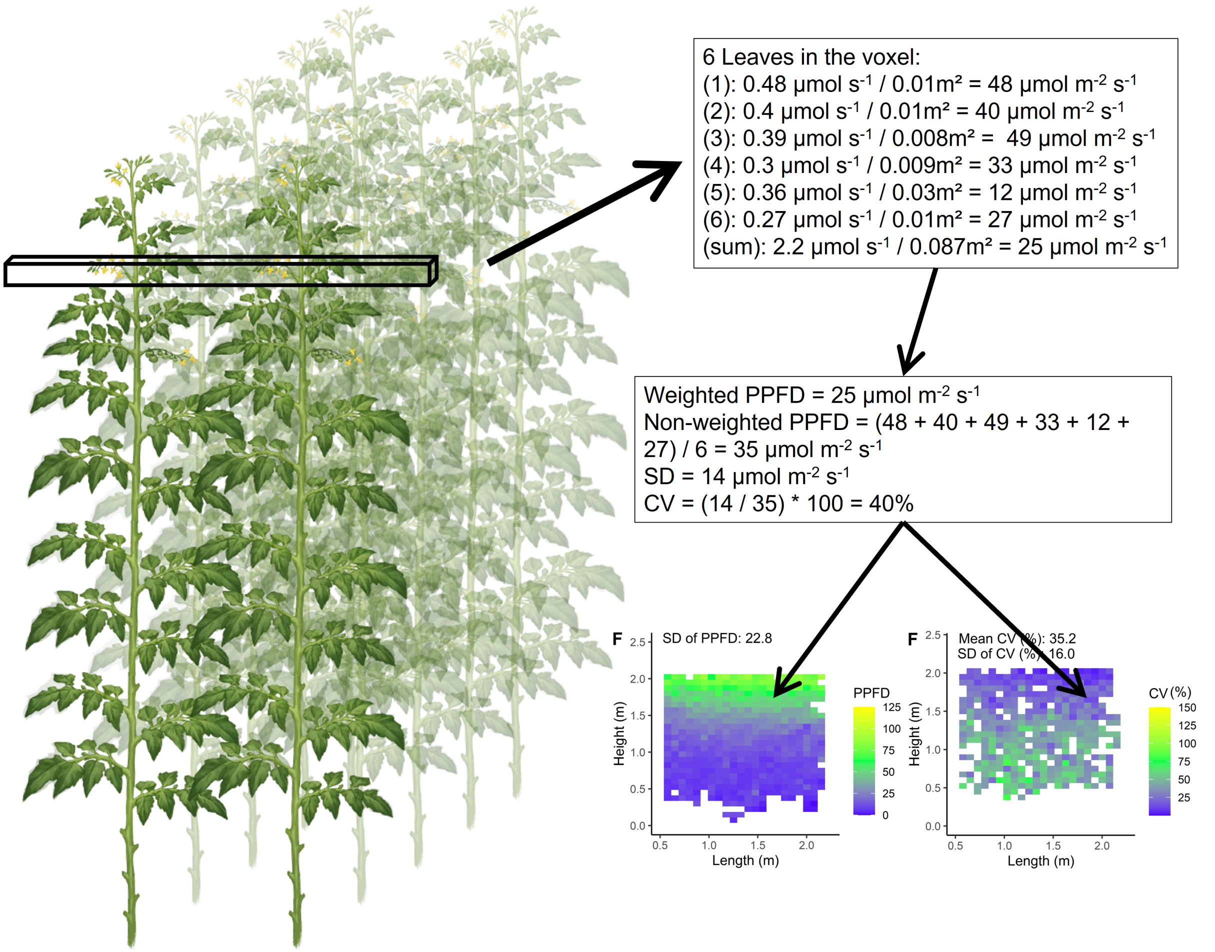

6 Leaves in the voxel:
(1): 0.48 μmol s^{-1} / $0.01m^2$ = 48 μmol m^{-2} s^{-1}
(2): 0.4 μmol s^{-1} / $0.01m^2$ = 40 μmol m^{-2} s^{-1}
(3): 0.39 μmol s^{-1} / $0.008m^2$ = 49 μmol m^{-2} s^{-1}
(4): 0.3 μmol s^{-1} / $0.009m^2$ = 33 μmol m^{-2} s^{-1}
(5): 0.36 μmol s^{-1} / $0.03m^2$ = 12 μmol m^{-2} s^{-1}
(6): 0.27 μmol s^{-1} / $0.01m^2$ = 27 μmol m^{-2} s^{-1}
(sum): 2.2 μmol s^{-1} / $0.087m^2$ = 25 μmol m^{-2} s^{-1}

Weighted PPFD = 25 μmol m^{-2} s^{-1}
Non-weighted PPFD = (48 + 40 + 49 + 33 + 12 + 27) / 6 = 35 μmol m^{-2} s^{-1}
SD = 14 μmol m^{-2} s^{-1}
CV = (14 / 35) * 100 = 40%

Figure 3: Calculation of the coefficient of variation (CV) and mean leaflet absorbed PPFD within one voxel (perpendicular to the plant row) of the tomato plant canopy. Each voxel had the dimensions of 7.5 cm width and length and a depth reaching across four double rows (8 plants). As a hypothetical example calculated values are shown. Subsequently two figures are produced to visualise the PPFD of each voxel (voxels perpendicular to the rows) in the canopy and the coefficient of variation within each voxel.

4.3 Results

4.3.1 Validation of the model

Measured and modelled incident PPFD (as observed by upward-facing sensors at different heights) showed a good correlation ($R^2 = 0.93$; Fig. 4). A sensitivity analysis showed that an increased leaf length of +25%, an increase in stem width of +50% or an increase of apex height by +30 cm had slight positive effects on the goodness of fit by up to 4% [see Supporting Information-Fig. S5]. Therefore, since all of the fits were with a high R^2 no modifications were made based on the sensitivity analysis.

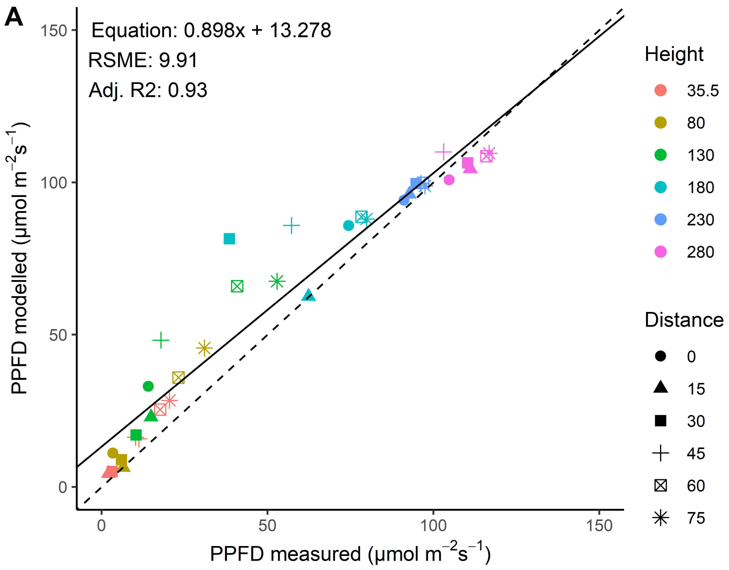

Figure 4: Relationship between measured and modelled incident PPFD (as observed by upward-facing sensors at different heights) in a greenhouse with a tomato crop illuminated by top lighting. The different symbols represent different distances to the middle of the rows in the canopy, whereas the symbol color represents height from the floor. Position of plants, lamps and sensors is shown in Figure 1.

4.3.2 Light distribution and heterogeneity with top lighting and intra-canopy lighting

The modelled light distribution for the intra-canopy lighting, top lighting and combined lighting system was visualized by 2D heat maps of absorbed PPFD per voxel (Fig. 5). Additionally, the heterogeneity was expressed as the coefficient of variation within each voxel, visualised by 2D heat maps as well (Fig. 6).

Vertical light distribution averaged parallel to row. The simulated PPFD absorbed by the leaflets was largest for leaflets close to the intra-canopy lighting modules (Fig. 5A,B,C). The absorbed PPFD values decreased with distance in a circular distribution pattern from the intra-canopy lighting modules and approached low values even within the same double row in which the intra-canopy lighting modules were located. In particular, the difference was notable in absorbed PPFD on the outsides of the double row compared to the inward row side. When top lighting was added to the intra-canopy lighting while total incident light intensity remained equal, the absorbed PPFD values showed a more homogeneous light distribution pattern through the canopy (Fig. 5B). For top lighting only, the absorbed PPFD distribution pattern in the vertical plane was much steeper with a larger SD (23.1) compared to either intra-canopy setting (SD of 19.2) or a combined lighting from top and intra-canopy lighting (SD of 15.1; Fig. 5A-C). Both the horizontal variability perpendicular to the row occurring with sole intra-canopy lighting, and the vertical variability occurring with sole top lighting, were diminished by the combination of intra-canopy and top lighting.

Vertical light distribution averaged perpendicular to row. The side view of the canopy showed the light distribution in the vertical plane and parallel to the row (Fig. 5D,E,F). With sole intra-canopy lighting (Fig. 5D), variation throughout the canopy occurred mostly in the vertical direction, when looking at the side view. Interestingly, on the height where the intra-canopy lighting was located, there were quite big differences in absorbed PPFD parallel to the row as well. With a combination of intra-canopy and top lighting the variation in absorbed PPFD slightly decreased when compared to intra-canopy lighting. For top lighting the distribution of absorbed PPFD was more homogeneous across the length of the row, but much less homogeneous with height of the canopy, resulting in larger variation of mean absorbed PPFD compared to intra-canopy lighting or a combination of intra-canopy and top lighting, when looking at the side view (SD being 22.8 versus respectively 14.4 and 13.5; Fig. 5D,E,F).

Horizontal light distribution averaged over heights. In the horizontal direction absorbed light distribution was more uniform for combined intra-canopy and top lighting (SD of 7.3) compared to intra-canopy lighting (SD of 11.9) or top lighting (SD of 11.3). In general, the horizontal light distribution (averaged over all heights) seemed more homogeneous than the vertical light distribution (averaged over horizontal layers) since (all) SD values were lower when averaging was performed over height (Fig. 5A-I).

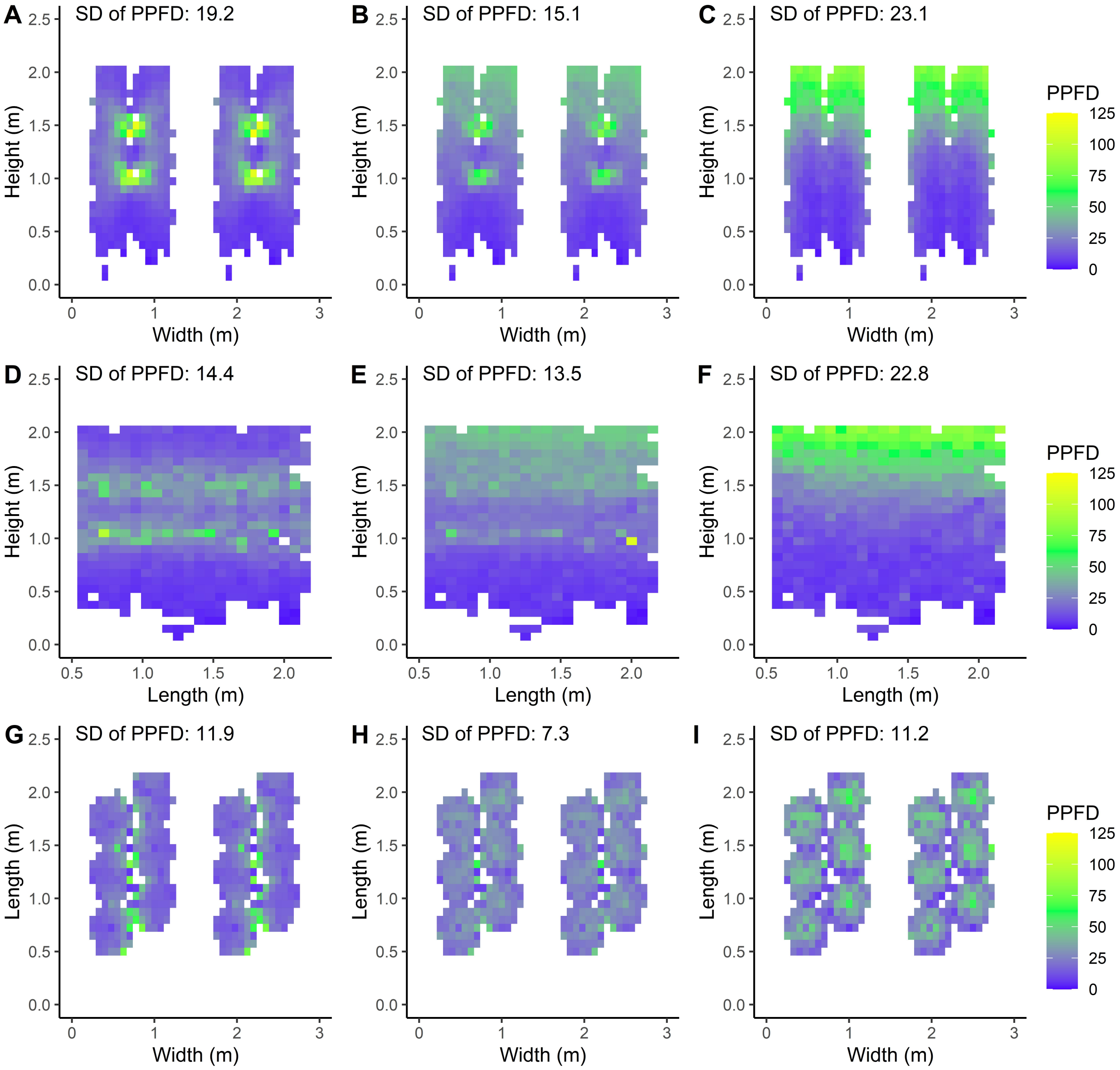

Figure 5: Front (A,B,C), side (D,E,F) and top views (G,H,I) of a double row canopy with mean absorbed PPFD (μmol m^{-2} s^{-1}) per voxel calculated as the mean taken from each leaflet's absorbed PPFD within the voxel. Three LED lamp positions are compared; (A, D, G) intra-canopy lighting, (B, E, H) combined intra-canopy and top lighting, and (C, F, I) top lighting. Each voxel had the dimensions of 7.5 cm width and length and a depth reaching 6 plants in each row (A,B,C), 8 plants across four double rows (D,E,F) or whole plant height (G,H,I). This means that the voxels are directed (A-C) parallel to the row; (D-F) perpendicular to the row and (G-I) vertically. The standard deviation (SD) is calculated over all voxels. Plants are spaced at 0.5m within each row in a double row. For visual interpretation of the distance between rows in the canopy an additional replicate double row is shown in A-C and G-I for which the same values were used as in the other row.

Variation coefficient horizontally in length direction of row. The CV of absorbed light within horizontal voxels (7.5 x 7.5 cm x 6 plants) parallel to the rows was smallest for the combined intra-canopy and top lighting; CV of 26%, compared to 36% for intra-canopy lighting and 0.31 for top lighting (Fig. 6A-C). Consequently, the light uniformity parallel to the row was best for a combined intra-canopy and top lighting setting (Fig. 6B).

Variation coefficient horizontally perpendicular to row. Within horizontal voxels (7.5 x 7.5 cm x 4 double rows) perpendicular to the rows, combined intra-canopy and top lighting showed the lowest mean CV (31%) of absorbed light, followed by top lighting (35%) and then intra-canopy lighting (44%) (Fig. 6D-F). Therefore, uniformity of absorbed PPFD is lowest for intra-canopy lighting when uniformity perpendicular to the row is considered (Fig. 6D), and is reduced by combined intra-canopy and top lighting (Fig. 6F).

Variation coefficient vertically. Within vertical voxels (7.5 x 7.5 cm x plant height), combined intra-canopy and top lighting showed the lowest mean CV (51%) of absorbed light, followed by intra-canopy lighting (65%) and top lighting (69%; Fig. 6G-I). Light heterogeneity is highest for top lighting in the vertical direction of the canopy, and is strongly reduced by combined intra-canopy and top lighting.

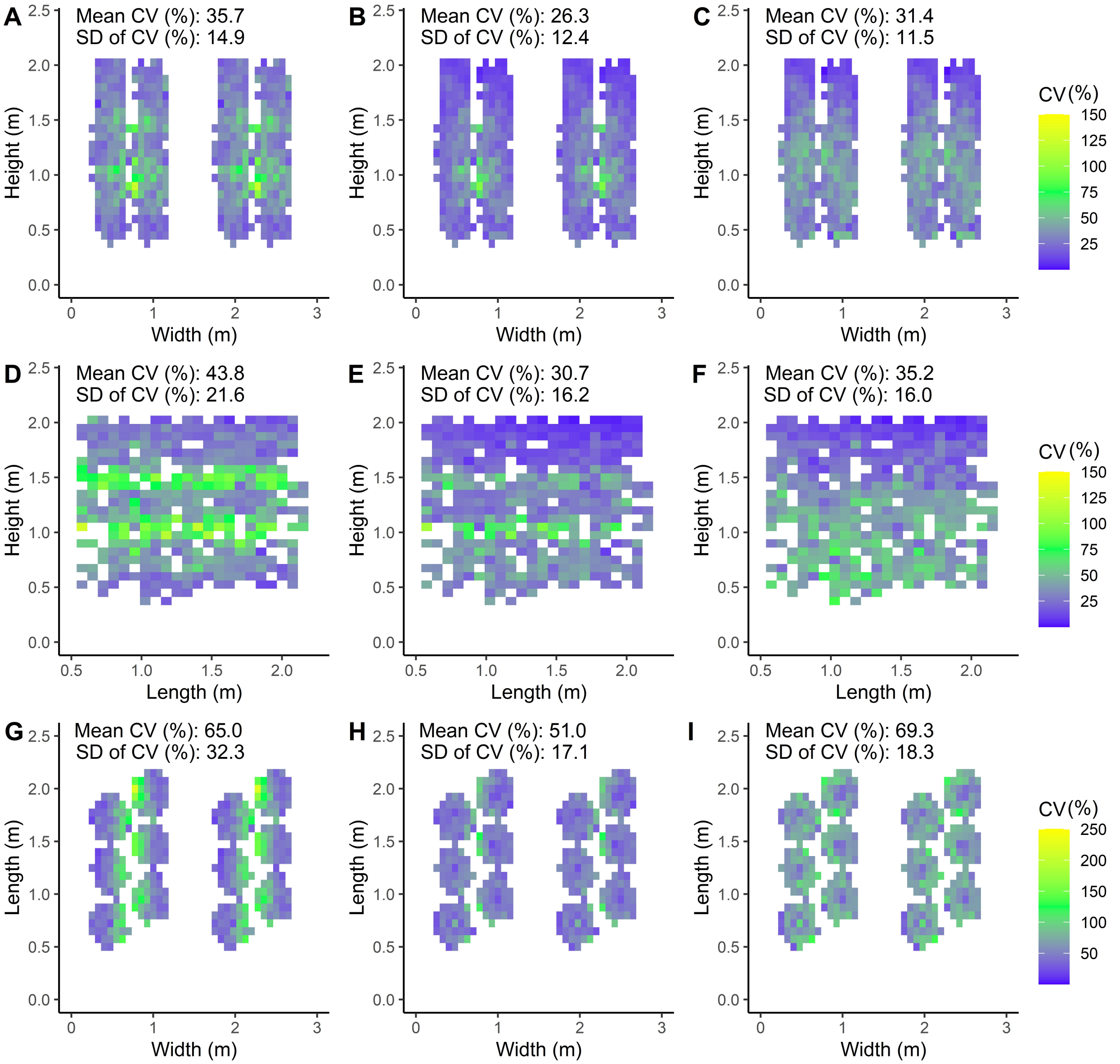

Figure 6: Front (A,B,C) , side (D,E,F) and top views (G,H,J) of the canopy with the CV (coefficient of variation) calculated as the standard deviation (SD) of the absorbed PPFD divided by the mean absorbed PPFD of the leaflets within the voxel times 100%. Three LED lamp positions are compared; (A, D, G) intra-canopy lighting, (B, E, H) combined intra-canopy and top lighting, and (C, F, I) top lighting. Each voxel had the dimensions of 7.5 cm width and length and a depth reaching 6 plants in each row (A,B,C), 8 plants across four double rows (D,E,F) or whole plant height (G,H,I). In A-C, a front view of the canopy is shown in which the CV value represents the heterogeneity of the voxel oriented parallel to the row. In D-F, a side view of the canopy is shown in which the CV value represents the heterogeneity of the voxel oriented perpendicular to the row. In G-I, a top view of the canopy is shown in which the CV value represents the heterogeneity of the voxel oriented vertical. Plants are spaced at 0.5m within each row in a double row. For visual interpretation of the distance between rows in the canopy an additional replicate double row is shown in A-C and G-I for which the same values were used as in the other row.

Average distribution in absorbed PPFD in the vertical and horizontal plane. Differences between top lighting and intra-canopy lighting occurred at the top and middle of the canopy (Fig. 7A-B). In the top of the canopy intra-canopy lighting resulted in the lowest weighted absorbed PPFD (27.3 μmol m^{-2} s^{-1} versus 48.5 for top lighting). These differences were the opposite for the middle of the canopy, where the weighted absorbed PPFD was 30.0 μmol m^{-2} s^{-1} for intra-canopy lighting versus 19.1 for top lighting. In the lower part of the canopy the differences were minor, with 11.0 μmol m^{-2} s^{-1} for intra-canopy lighting versus 9.0 for top lighting (Fig. 7C). The combination of intra-canopy and top lighting was always in between the other two treatments. The mean absorbed PPFD across all leaves in the canopy was highest for intra-canopy lighting, with a value of 24.3 μmol m^{-2} s^{-1}, compared to 23.4 for the combination of intra-canopy and top lighting and 22.5 for top lighting only. This indicates that total light absorption was 8% higher for intra-canopy lighting, and 4% for combination of intra-canopy light and top lighting compared than top lighting. The intra-canopy lighting has very high peak values for CV around the height of the LED strings (Fig. 8). The mean CV and SD over the different horizontal layers demonstrated highest values for intra-canopy lighting (48% ±22), followed by top lighting (0.43% ±18) and then the combination of intra-canopy and top lighting (37% ±18). This means that the variation within the horizontal layers is highest for intra-canopy lighting.

Sensitivity analysis of fraction and position of intra-canopy light. Changing the ratio between intra-canopy and top lighting showed that 50/50% gave the lowest CV (Fig. 9). The higher the percentage of either intra-canopy or top light, the higher the CV. Increasing or decreasing the height of the intra-canopy lighting LEDs by 30 cm largely had no effect on the variation in the horizontal plane, but variation in the vertical plane was reduced when height of the intra-canopy light was reduced by 30cm, while it increased when LED strings were raised by 30cm (Supplementary Fig. S6). Increasing the number of intra-canopy LED strings from two to four strings keeping the same total intra-canopy light output also reduced the CV [see Supporting Information-Fig. S6].

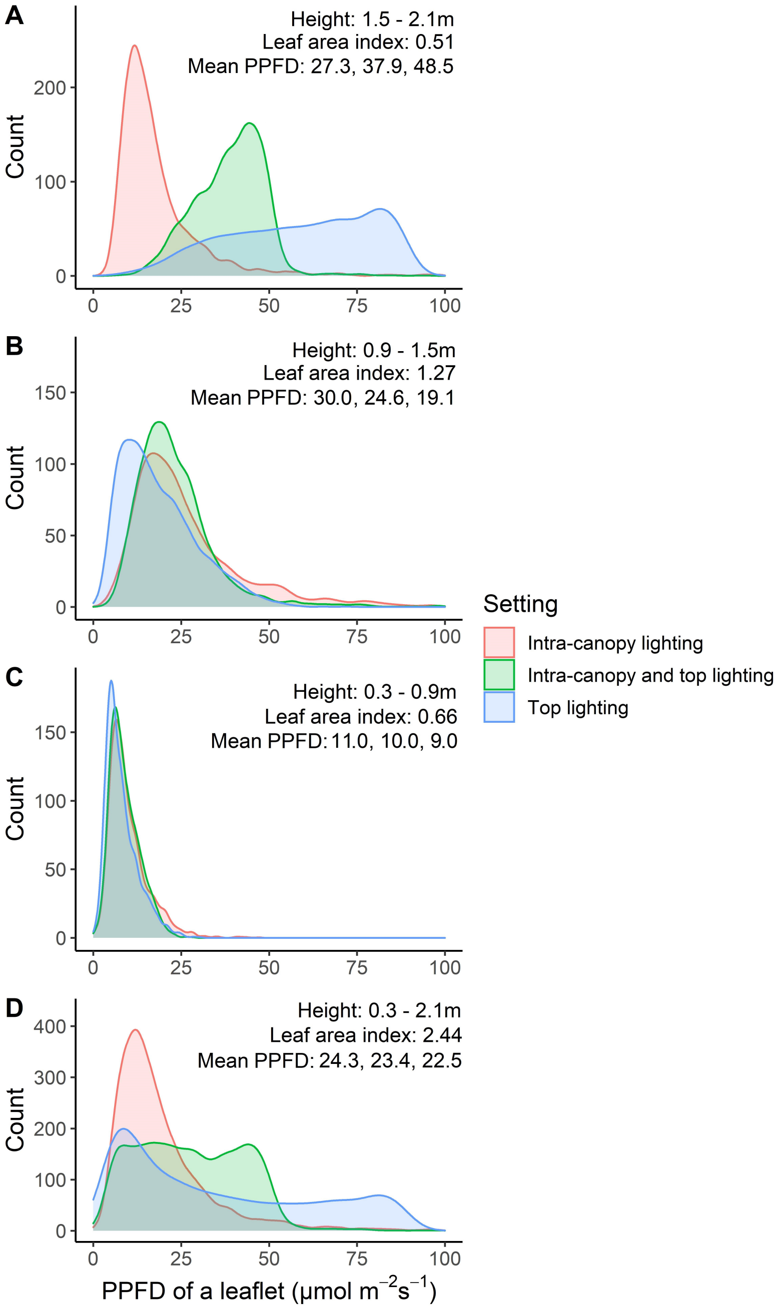

Figure 7: Frequency distribution of leaflets based on absorbed PPFD (μmol m^{-2} s^{-1}) at top (A), middle (B) bottom (C) or whole of canopy (D). Numbers in each figure indicate the height range, the leaf area index, and the mean weighted absorbed PPFD (μmol m^{-2} s^{-1}) of all leaflets for intra-canopy lighting, combination of intra-canopy and top lighting, and top lighting, respectively. From within the canopy 48 center plants were taken from four center double rows, 6 plants from each double row side.

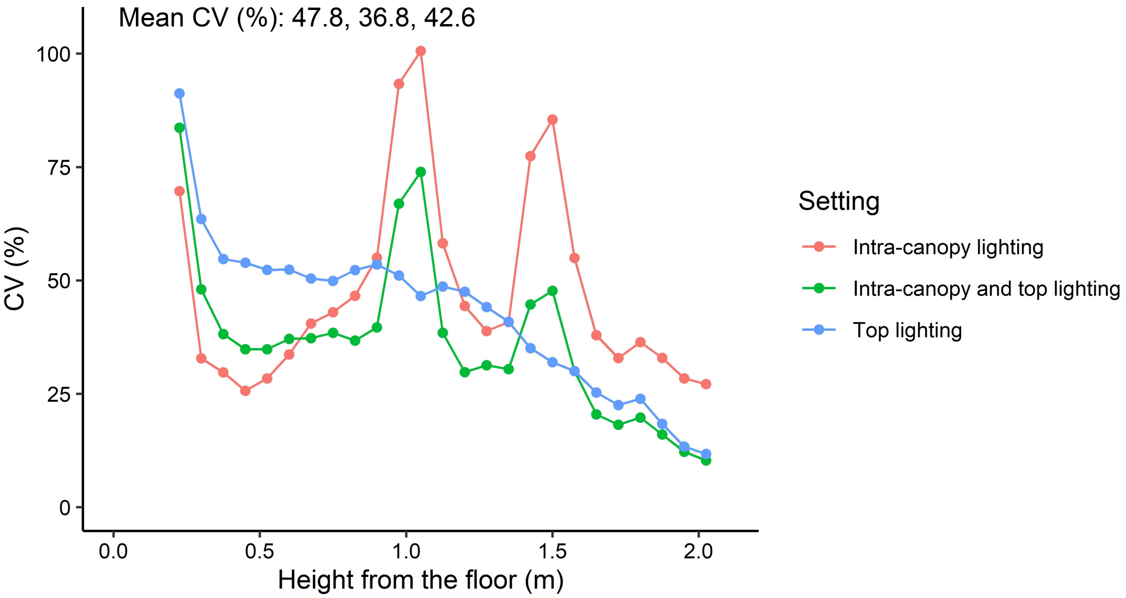

Figure 8: Coefficient of variation (CV) of absorbed PPFD in relation to height in the canopy. CV relates to the variation within horizontal layers. Each layer is represented by 7.5 cm height and takes all perpendicular and parallel leaves of 48 plants and is shown as a dot in the graph. Mean CV of all horizontal layers is provided in the top left corner for intra-canopy lighting; intra-canopy and top lighting; and top lighting, respectively.

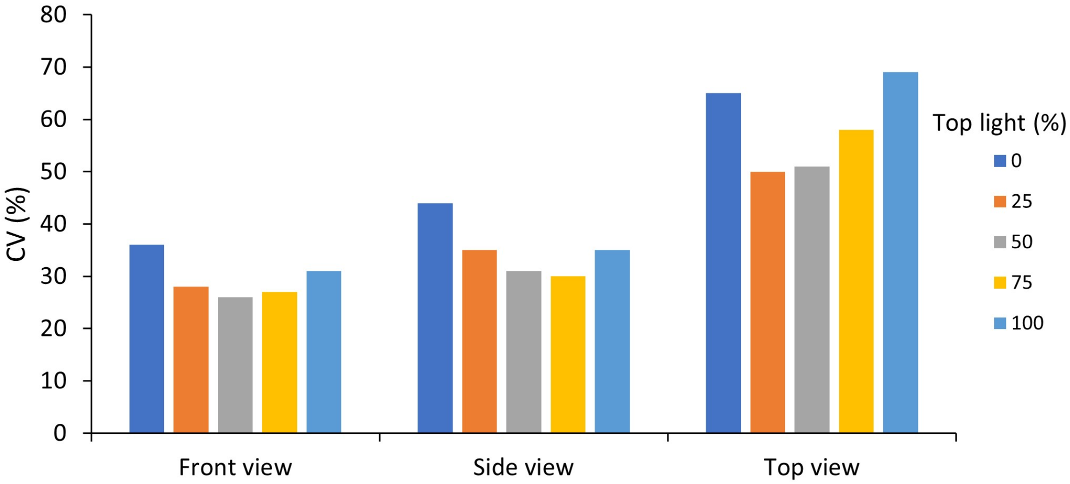

Figure 9: Effects of percentage top light (0, 25, 50, 75 or 100%) on the mean coefficient of variation (CV) within voxels of absorbed canopy PPFD for the front, side and top-view of the canopy. Top light percentage was 0, 25, 50, 75 and 100%, with respectively, 100, 75, 50, 25 and 0% intra-canopy light. Each voxel had the dimensions of 7.5 cm width and length and a depth reaching 6 plants in each row of a double row stretching across four double rows.

4.4 Discussion

4.4.1 Partial replacement of top by intra-canopy lighting increases absorbed PPFD uniformity

In our study we showed that FSPM appears to be an effective tool to visualize and quantify the distinctive extinction patterns throughout the canopy with intra-canopy lighting and/or top lighting. For intra-canopy lighting there is a strong absorption close to the LED modules and the majority of the light does not even reach the outside of the double row in which the intra-canopy lighting is located (Fig. 5A), which is a similar observation to that of de Visser et al. (2014). This may lead to local acclimation to the areas experiencing high light conditions (Joshi et al., 2019). Despite high local light intensities surrounding intra-canopy LED modules there is a lower overall variation (smaller SD) in absorbed light when compared to top lighting (Fig. 5). The combination of a higher uniformity (Fig. 5) and a higher total light absorption (Fig. 7) all favor intra-canopy lighting above top lighting. It should be realised that younger leaves are generally most photosynthetically active and are acclimated to high light conditions (e.g. Qian et al., 2012). Therefore, a more homogeneous vertical distribution does not necessarily lead to a higher photosynthesis in all cases, as a relative larger fraction of light will be absorbed by leaves with photosynthetic parameters which are less favourable for high rates of photosynthesis. On the other hand when the light profile in the canopy changes, the leaves will acclimate to the changed light profile. Our model simulations show that a combination of top lighting with intra-canopy lighting results in the most uniform light distribution in the canopy, when compared to sole intra-canopy as well as compared to sole top lighting. In addition, there is a slight increase in light absorption by 4% compared to top lighting but 4% less compared to sole top lighting. The lower light absorption of top lighting versus intra-canopy lighting, is due to some reflection of top lighting by the top layer of the canopy. So, overall a combination of top and intra-canopy lighting increases uniformity of light distribution over individual leaves and total light absorption of the canopy compared to sole top lighting. op light

Variation in light intensity along the LED string (parallel to the row) was still present despite the string having a LED at every few cm showing the effect of plant-caused variation due to irregularly oriented leaves and randomly occurring open spaces in the crop. It is possible that in reality leaves turn towards the light (as shown for cucumber by Kahlen et al., 2008) and thus reduce their irregular positioning. Research on diffusing solar light has shown that a more uniform light distribution over the laves in the canopy can increase crop photosynthesis and growth (Li et al., 2014). In **Chapter 2** it was shown that increased variation in light distribution due to different sun exposures between plant rows hardly resulted in yield reduction in a similar tomato crop, since leaves adapted in size and thickness. Moreover, effects of higher spatial light intensity variation may depend on average light intensity, being larger when light intensities are high as the relative response of leaf photosynthesis slows down at high light intensity. Consequences of changed light distribution on morphological and physiological acclimation of leaves and consequence for photosynthesis and growth request for further research.

4.4.2 Impact on crop production

A combination of intra-canopy and top lighting is recommended for reducing canopy heterogeneity in absorbed light (Figs. 5, 6, 8, 9). The simulation results also show that there is an optimum for the fraction of intra-canopy light for optimizing uniformity. This optimum was at about 50% intra-canopy light and 50% top light. When there is also solar light (coming from the above) the optimum ratio of intra-canopy lighting to top lighting is likely to increase; most likely the optimum fraction of intra-canopy light is when the intra-canopy light is similar as the total light from top light and sun. Furthermore, the position of the intra-canopy lamps is important. Too high positioning may lead to light loss to the greenhouse cover and too low positioning may lead to light loss to the floor. Distributing the intra-canopy light over different heights in the canopy also increased the light uniformity [see Supporting Information-Fig. S6].

Experimental comparison between lighting strategies by means of photosynthetic characteristics is difficult for various reasons. The most obvious is that measurements are time consuming and limited in number. Our findings demonstrate that there is a large variation in local light conditions when comparing lighting treatments. Joshi et al. (2019) found a 3-4 times higher photosynthetic capacity for bell pepper at intra-canopy lighting on the inside of the canopy close to the LEDs compared to the control without supplementary lighting. Such acclimation of photosynthesis to changed light intensity may take place within a week (Hogewoning et al., 2006). Apart from acclimation, intra-canopy lighting simulations showed an increased light absorption compared to top lighting. Further experimental studies are needed to investigate effects on light distribution, photosynthesis, growth, and yield by intra-canopy lighting. Studies with intra-canopy lighting partially replacing top lighting showed increased fruit yield in several studies (Hovi-Pekkanen et al., 2004; Hovi-Pekkanen et al., 2006; Hovi-Pekkanen and Tahvonen, 2008) but having not effects in other studies (Trouwborst et al., 2010; Dueck et al., 2011; Gómez and Mitchell 2016; Yan et al., 2018).

4.5 Conclusions

Positioning of LED lamps above or in between the canopy (intra-canopy) has large effects on total canopy light absorption and the distribution of the absorbed light over the leaves. Intra-canopy lighting resulted in 8% higher total light absorption than top lighting, while combining 50% intra-canopy lighting with 50% top lighting, increased light absorption by 4%. Combining intra-canopy and top lighting resulted in a more uniform canopy light absorption than intra-canopy or top lighting alone.

Acknowledgements

We would like to express our gratefulness to several people during the execution of this experiment. Theoharis Ouzounis, Habtamu Giday, Joke Oosterkamp, Andre Maassen, Geurt Versteeg, Maarten Peters, Sean Geurts, Erik Schuiling, Ferdinand Diesman for taking care of plant growth, maintenance and light installation in the greenhouse experiment. The work of Maarten van der Meer was in part funded by the Wellensiek fund, part of University Fund Wageningen. The work of Rachel Schipper is part of the "LED it be 50%" program and is supported by Glastuinbouw Nederland, Signify, WUR Greenhouse Horticulture, Nunhems (BASF) and the Netherlands Organization for Scientific Research (NWO), which is partly funded by the Ministry of Economic Affairs. The cultivation of the plants in the greenhouse was financially supported from the Carbon LED project (Carbonfootprint reduction via LED based production systems), funded by Climate KIC. We thank Signify for designing the light plan of the greenhouse experiment and BASF Vegetable Seeds (Nunhems) for providing the tomato seeds.

4.6 Supplementary material

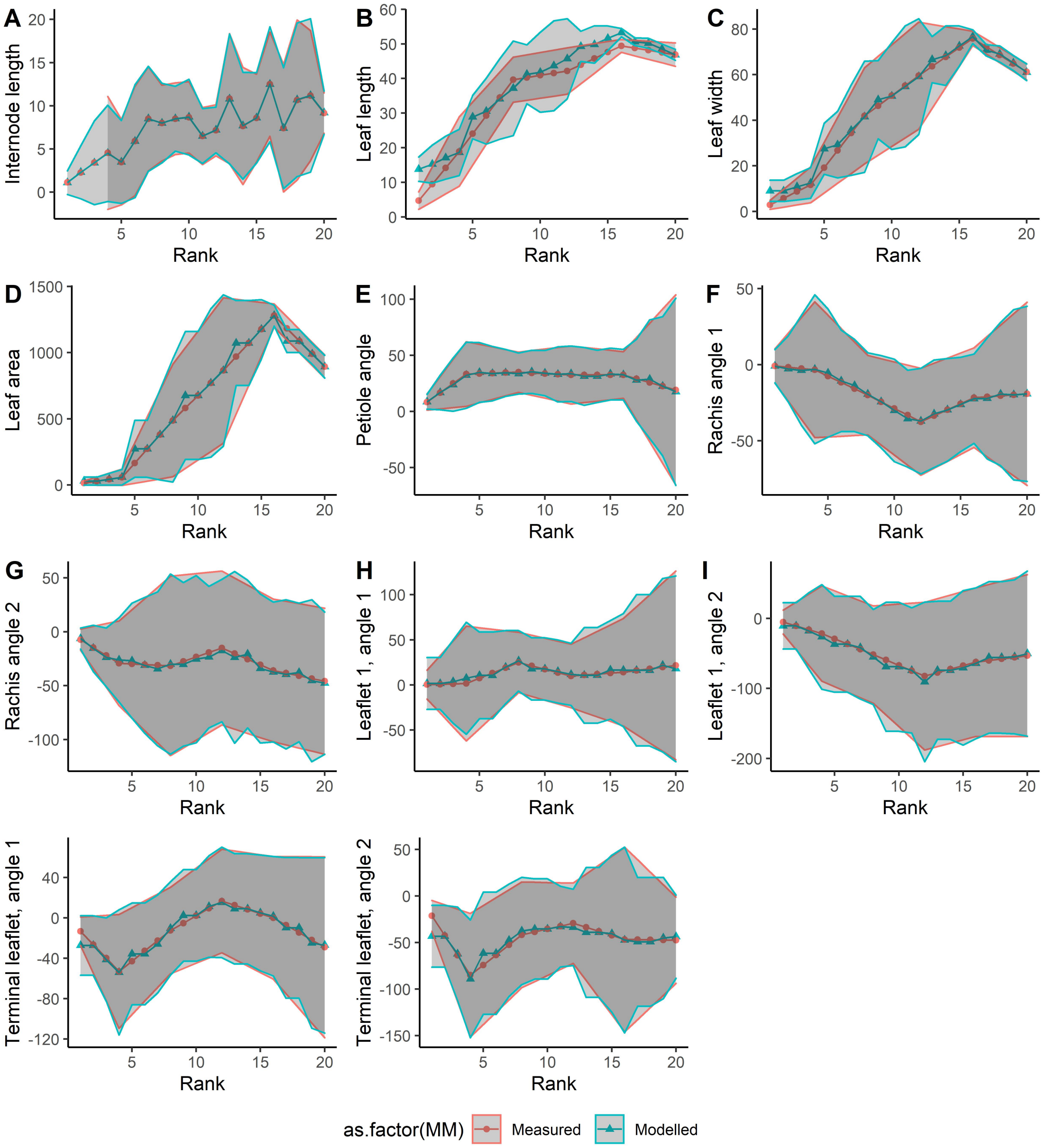

Figure S1: Measured vs modelled mean plant architecture values with confidence interval (2 times standard deviation). The architectural parameter values for leaf length, leaf width, internode length, petiole angle, rachis angles and leaflet angles were taken from phytomer ranks 4, 8, 12, 16 and 20 (counted from the top; from the first leaf 2 cm), acquired from the measurements on 20 March (81 DAT). Mean and standard deviation (SD) values for all architectural parameters of the non-measured phytomer ranks were linearly interpolated between the measured phytomer ranks.

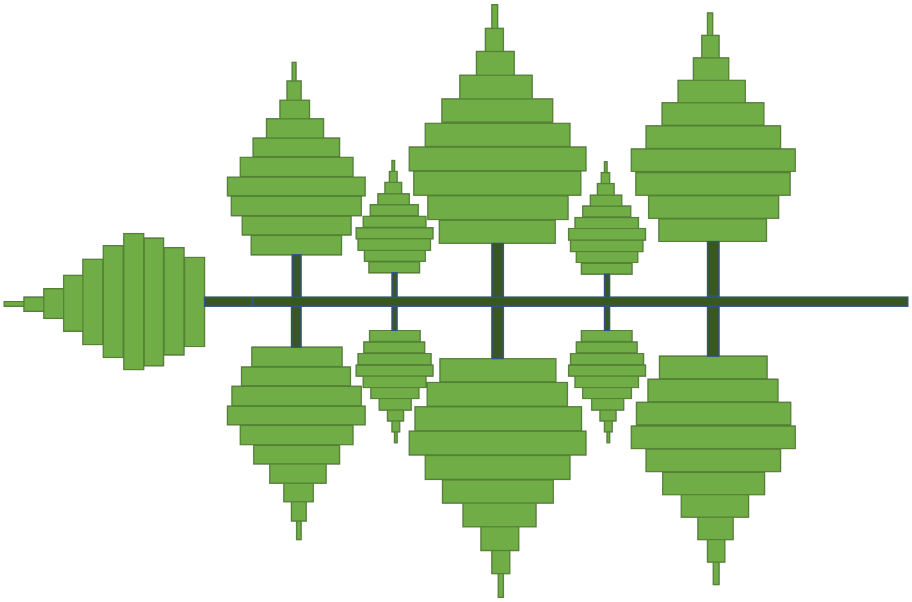

Figure S2: Representation the reconstruction of a single leaf with leaflets as used in the model. Each leaf consisted of 4 small and 7 larger leaflets.

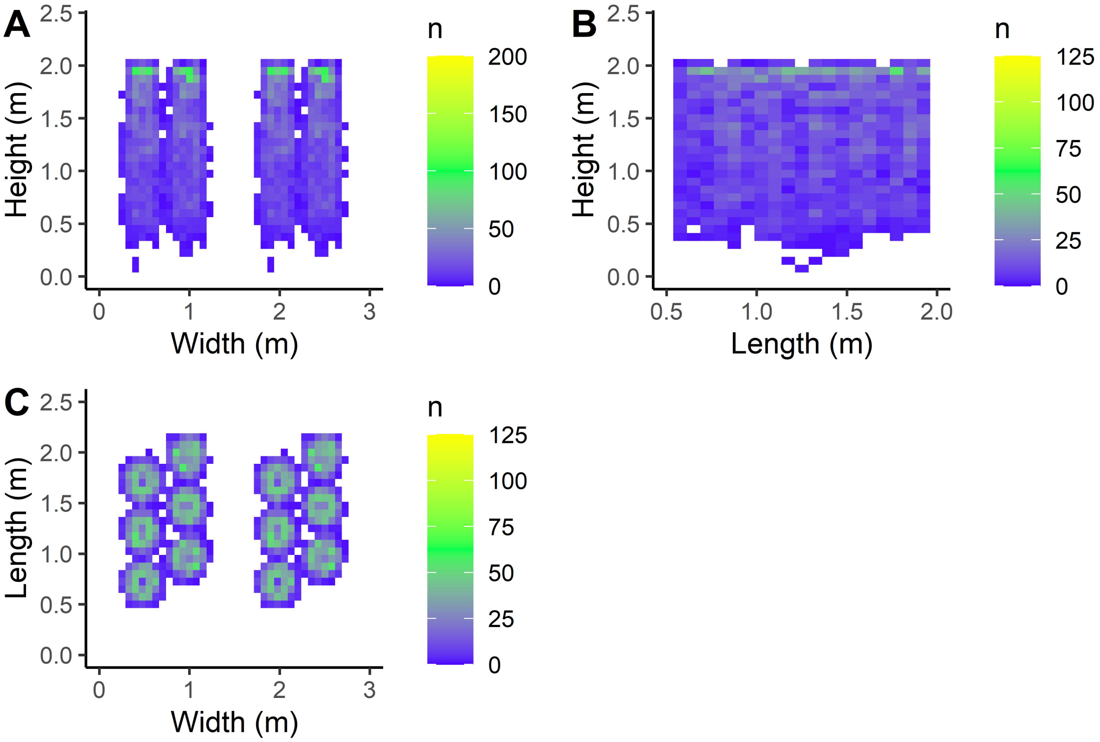

Figure S3: A front, side and top view of a double row canopy with the number of leaflets used for absorbed light calculations within each voxel. Each voxel had the dimensions of 7.5 cm width and length and a depth reaching 6 plants in each row (A), 8 plants across four double rows (B) or whole plant height (C). This means that the voxels are directed (A) parallel to the row; (B) perpendicular to the row and (C) vertically. Plants are spaced at 0.5m within each row in a double row. For visual interpretation of the distance between rows in the canopy an additional replicate double row is shown in A,C for which the same values were used as in the other row.

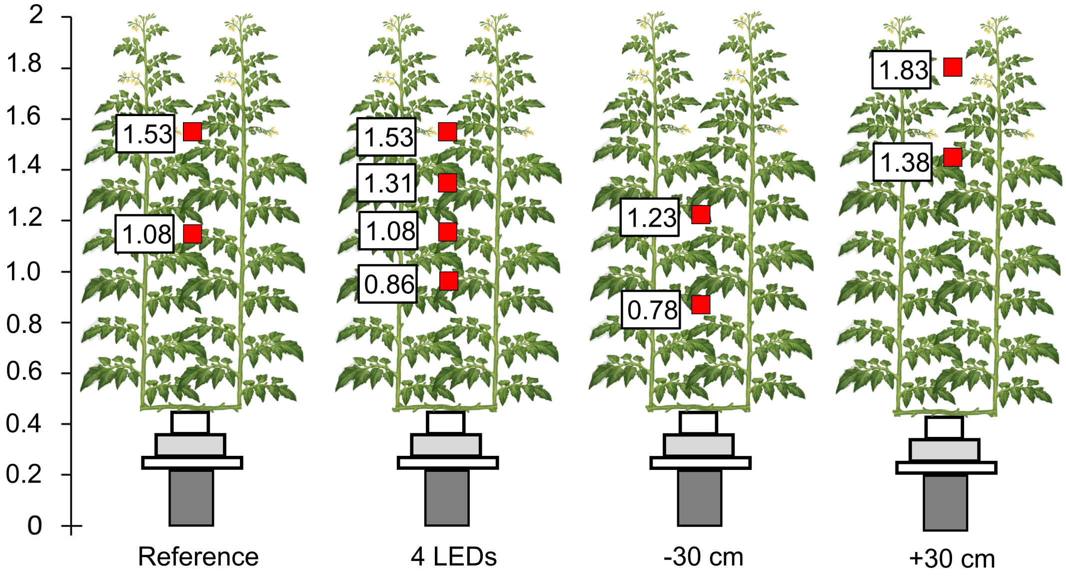

Figure S4: Relationship between measured and modelled incident PPFD (as observed by upward-facing sensors at different heights) in a greenhouse with a tomato crop illuminated by top lighting for model scenarios (A) reference simulation; (B) leaf length +25%; (C) stem width +50% (D); apex height +30 cm. The different symbols represent different distances to the middle of the row canopy, whereas the symbol color represents height from the floor. Reference apex height was 200 cm.

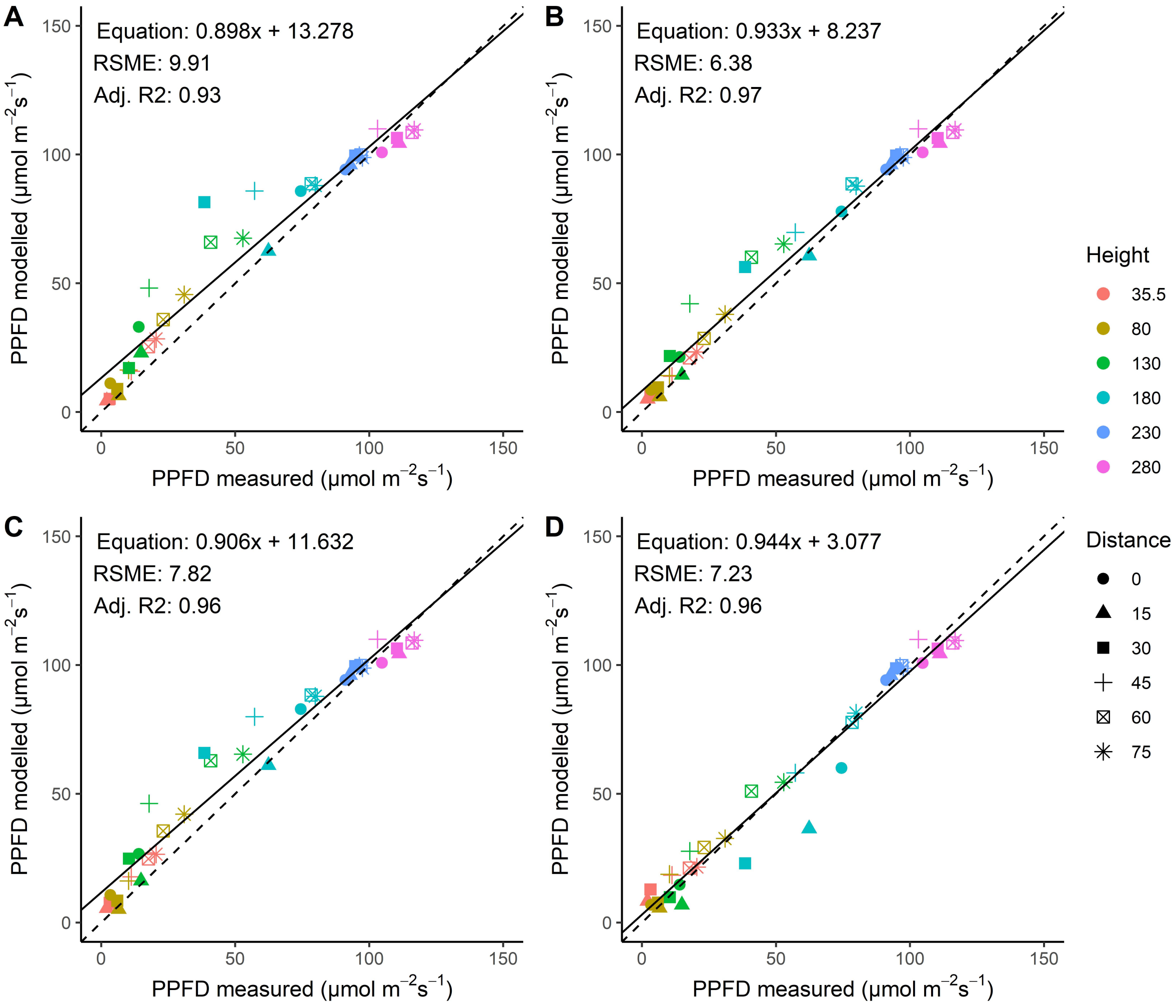

Figure S5: Relationship between measured and modelled upward-facing line sensor incident PPFD values in a greenhouse with a tomato crop illuminated by top lighting for model scenarios (A) reference simulation; (B) leaf length +25%; (C) stem width +50% (D); apex height +30 cm. The data point shape is representing the distance to the middle of the row canopy, whereas the data point color represents height from the floor. Reference apex height was 200 cm.

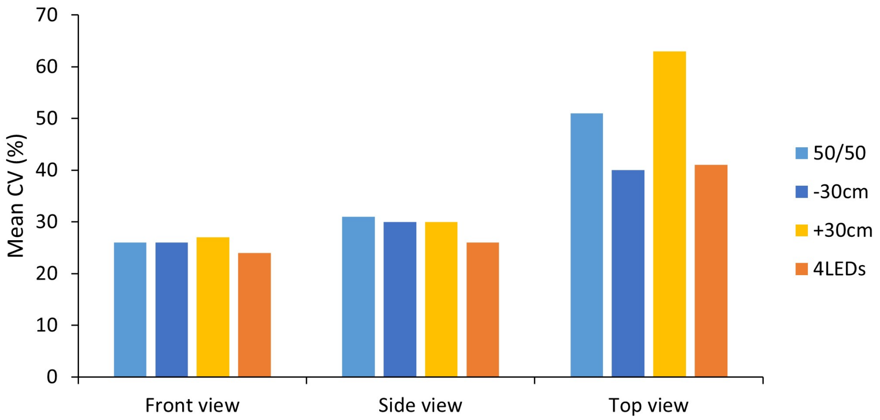

Figure S6: Sensitivity analysis of the relationship between mean coefficient of variation (CV) within voxels of absorbed canopy PPFD with differing simulation scenarios, evaluated for the front, side and top-view of the canopy. Number and position of LED modules as well as standard deviation of architecture are evaluated. Simulation scenarios are performed with 50% intra-canopy lighting and the sensitivity analysis scenarios are follows; '50/50' is the reference simulation; '-30 cm' has the intra- canopy lighting LED modules lowered from 108 and 153 cm to 78 and 123 cm; '+30 cm' has the intra-canopy lighting LED modules raised from 108 and 153 cm to 138 and 183 cm; '4 LEDs' has two additional intra- canopy lighting module locations on 81 and 131 cm. Each voxel had the dimensions of 7.5 cm width and length and a depth reaching 6 plants in each row (Front View), 8 plants across four double rows (Side View) or whole plant height (Top View).

Chapter 5

5 Consequences of interplant trait variation for canopy light absorption and photosynthesis

[1]van der Meer, M., [1]Lee, H., [2]de Visser, P. H. B., [1]Heuvelink, E., [1]Marcelis, L. F. M.

[1]Horticulture and Product Physiology, Wageningen University, Droevendaalsesteeg 1, 6708PB Wageningen, The Netherlands

[2]Business Unit Greenhouse Horticulture, Wageningen Research, Droevendaalsesteeg 1, 6708PB Wageningen, The Netherlands

Abstract

Plant to plant variation (interplant variation) may play an important role in determining individual plant and whole canopy performance, where interplant variation in architecture and photosynthesis traits have direct effects on light absorption and photosynthesis. We aimed to quantify the importance of observed interplant variation on both whole-plant and canopy light absorption and photosynthesis. Plant architecture was measured in two experiments with tomato crops (*Solanum lycopersicum*) grown in glasshouses in the Netherlands. Experiment 1 included four cultivars grown under three supplementary lighting treatments and Experiment 2 included two different row orientations. Measured interplant variation of the architectural traits internode length, leaf area, petiole angle and leaflet angle, as well as literature data on interplant variation of photosynthesis traits alpha, J_{max28} and V_{cmax28} were incorporated in a functional–structural plant model (FSPM). The FSPM was used to analyze light absorption and net photosynthesis of whole plants in response to phytomer level interplant variation in architectural and photosynthesis traits. Introducing interplant variation in architecture and photosynthesis traits in a functional-structural plant model did -depending on the trait- not or negatively affect canopy light absorption and net photosynthesis compared to the reference model without interplant variation. Introducing interplant variation of architectural and photosynthesis traits in FSPM results in more realistic simulation of variation of plants within a canopy. Furthermore, it can improve the accuracy of simulation of canopy light interception and photosynthesis, though these effects at canopy level are relatively small (<4% for light absorption and <7% for net photosynthesis).

5.1 Introduction

Plant to plant variation (interplant variation) may play an important role in determining individual plant and whole canopy performance (Westerband et al., 2021), where interplant variation in architecture and photosynthesis traits have direct effects on light absorption and photosynthesis (Sarlikioti et al., 2011a). Interplant variation has been studied for a longer time in ecology, greenhouse horticulture and field crops, where in greenhouse horticulture and field crops uniformity is of importance. Fruits of greenhouse cucumber show a changing demand in assimilates over time and abortion of individual fruits (Marcelis 1992). These characteristics result in non-uniform fruit growth and is also observed in other reproductive and indeterminate crops such as bell pepper and tomato (Heuvelink, 1996; Wubs et al., 2009b). Differences in whole plant fruit growth have been linked to environmental factors such as light intensity, photoperiod, CO_2 concentration, temperature, relative air humidity, water and nutrient supply (Marcelis 1993; Wubs et al., 2009a; Pettersen et al., 2010) and canopy architecture (Chen et al., 2014).

Functional–structural plant models (FSPMs) explore and integrate relationships between a plant's structure and processes that underlie its growth and development (Louarn and Song 2020). These models have been developed for a wide range of crops and for many purposes (Louarn and Song 2020) including studies on effects of plant architecture on light absorption and photosynthesis in a canopy (e.g. Buck-Sorlin et al., 2011; Cieslak et al., 2010; Wiechers et al., 2011; Chen et al., 2014; Chapter 2). This is also used to study interplant variation in organ growth and development by either an hypothesis of carbon driven competition (e.g. Luquet et al., 2006; Kang et al., 2011) or the integration of other forms of signalling (which may be internal to the plant, external or an integration of both; e.g. (Fournier et al., 2005; Alban et al., 2008; Evers et al., 2011).

In the last years there has been considerable improvement in carbon-driven growth through sink strength modelling, and several successfully models have been developed that can predict variability such as Greenlab (de Reffye et al., 2021) and Ecomeristem (Larue et al., 2019). Main functions for determining variability are branching, tillering time and senescence. The importance of including interplant variation in architectural and photosynthesis traits for modelling light absorption and photosynthesis can be structurally assessed by model simulations but has yet received minimal attention. Zhu et al. (2015) investigated this topic in a maize and soybean mixture, and showed that inclusion of interplant variation can result in complementary light capture.

The aim of this study was to determine the importance of observed interplant variation in architectural and photosynthetic traits on canopy light absorption and net photosynthesis and coefficient of variation in plant light absorption and net photosynthesis. For this we used measured interplant variation in greenhouse grown tomato canopies and used that as input in a functional-structural plant model to simulate consequences of interplant variation.

5.2 Material and methods

5.2.1 Architectural data acquisition

Data on plant architecture were collected in two separate experiments with tomato crops (*Solanum lycopersicum*) grown in glasshouses in Bleiswijk, the Netherlands (Exp 1) and Wageningen, the Netherlands (Exp 2; described in Chapter 2).

Experiment 1 - Cultivar x lighting. Four tomato cultivars (cv. ‘Foundation’, ‘Progression’, ’Extension’ and ’9112’) were sown on the 28^{th} of August 2015 and transplanted into the glasshouse compartments (6 Oct 2015) when the first truss emerged, having a split stem and 8-10 leaves per stem. Three treatments with supplementary lighting to natural light were applied to the four tomato cultivars: (1) HPS top lighting (110 μmol m^{-2} s^{-1}) + LED intra-canopy lighting (53 μmol m^{-2} s^{-1}) at two heights (2 and 2.5m); (2) LED top lighting (110 μmol m^{-2} s^{-1}) + LED intra-canopy lighting (53 μmol m^{-2} s^{-1}) at two heights (2 and 2.5m); (3) LED top lighting (110 μmol m^{-2} s^{-1}) + two intra-canopy lighting (53 μmol m^{-2} s^{-1}) at two heights (2.5 and 3m). Top lighting was provided using either HPS or LED lamps (Philips Greenpower, 95% red and 5% blue, Signify, Eindhoven, The Netherlands)) at a height of 4.75 m above the floor. Intra-canopy lighting was provided Philips Greenpower inter lighting LED lamps (95% red and 5% blue, Signify, Eindhoven, The Netherlands). Lower and upper leaves were on average at 1.5 and 3.5 m height above the floor respectively, whereas the rockwool slab was at 0.9m height of the floor. Lamps were turned on 14 October 2015, gradually increasing the duration of lighting to a daily maximum of 19 h (0:00 h until 1 h after sun set). When the outside solar radiation exceeded 600 W m^{-2}, the lamps were switched off.

Plant architecture was measured 16 weeks after transplanting (25 - 29 January, 2016) on five plants in each of the 12 treatments (4 cultivars x 3 light treatments), in total 60 plants. Leaf length and width, internode length, petiole angle and 1^{st} and 2^{nd} rachis bending angles were measured at every phytomer rank (Fig. 1). Leaf length was measured from the petiole to the tip of the terminal leaflet. Leaf width was measured between the tips of the two longest leaflets. The measured internode length was the distance between the insertion points of two consecutive plant organs (leaves or truss). Petiole angle and 1^{st} and 2^{nd} rachis bend angle were measured relative to the horizon. Rachis bend angles were measured at the first and second big leaflet pairs (Fig. 1). Stem density on the day of measuring was 3.1 stems m^{-2}. Leaf area was estimated from leaf length and leaf width for the second experiment according to the formula

$$Leaf\ area = A * (leaf\ length * leaf\ width)^B \tag{1}$$

where A and B are dimensionless parameters where values for each cultivar are taken from data of Exp. 2 (for values see supplementary Table S1).

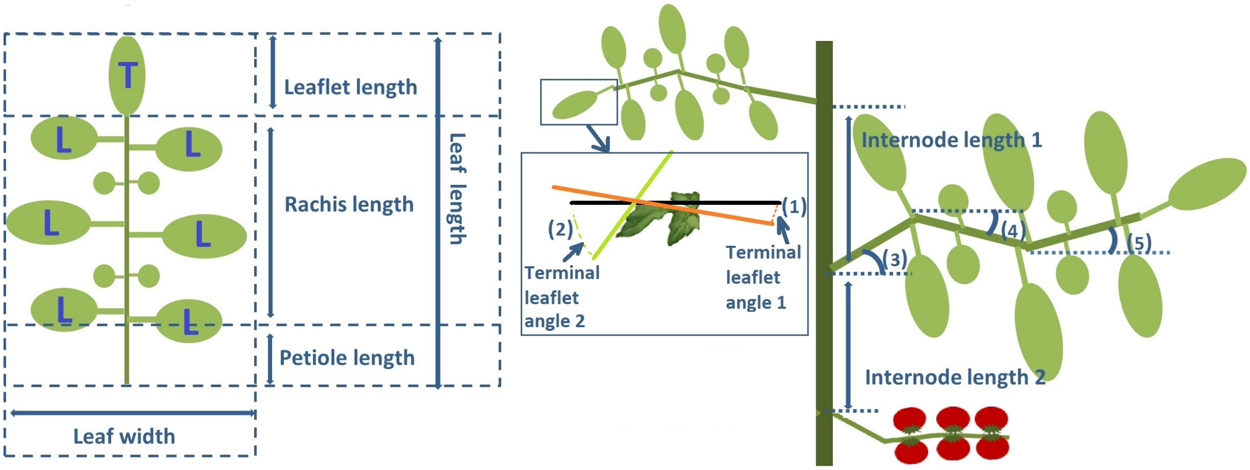

Figure 1: Diagram of measured plant architecture at phytomer level. On the left side a leaflet with a terminal leaflet (T) and six lateral leaflets (L). On the right hand side a stem section with two phytomers each containing an internode, petiole and leaflet. Indicated are (1, 2) a zoomed in terminal leaflet showing the measurement of terminal leaflet angle 1 (from the base of the leaflet to the middle point) and terminal leaflet angle 2 (from the tip of the leaflet to the middle point) relative to the horizon (3, 4, 5) petiole angle, 1^{st} rachis bend and 2^{nd} rachis bend which are all measured relative to the horizon, and internode lengths 1 and 2 of the two phytomers.

Experiment 2 - Row orientation. Five week old tomato plants (cv. "Capriccia) were transplanted into greenhouse compartments in either a north-south or east-west row orientation on the 8^{th} of March, 2016. The plants were grown until 20 July 2016. Nutrient solution (EC: 2.8 and pH: 5.5; see Supporting Information Table S2) was provided daily in a frequency matching solar radiation. Side stems were removed weekly, and from 13 April onward the bottom three leaves were removed every week. From 25 April the plants reached the high wire at a height of 3.3 m, after which they were lowered weekly. The plants were grown in double rows, with distance of 50 cm between the single rows. Trusses were pruned to 6 fruits per truss. The two glasshouse compartments were oriented -24 North–South. Architecture of 12 plants were measured in both the north-south and east-west row orientations 19 weeks after transplanting (20 July 2016), in total 24 plants. For this study, architectural measurements on each phytomere of internode length, leaf length and leaf area were used. Stem density on the day of measuring was 4.4 stems m^{-2}. For more details on this experiment see Chapter 2.

5.2.2 Modelling

The tomato functional-structural plant model used in Chapter 2 was adapted and re-parameterized. This model was developed on the GroIMP platform (Kniemeyer, 2008) and consists of an architectural, photosynthesis and light module. The essentials of each module are briefly explained, while for a more elaborate explanation we refer to Chapter 2.

Architectural module. Architecture trait reference values were estimated encompassing all measurements on the 84 plants total (60 from Exp. 1 and 24 from Exp. 2) of both experiments and were used to construct a reference plant (Fig. 2). This reference plant was copied 216 times (6 double rows with 36 plants per double row) to construct a reference canopy, where each plant was rotated (0 to 360°, drawn at random) relative to its neighbor, and these orientations were then fixed during all simulations. Taking measurement data together from two experiments and of five genotypes increased the range where trait variability was derived from. This was done as follows. Firstly, for each trait a mean and variance were calculated for each phytomer rank of each genotype for each treatment in each experiment. Afterwards, for every trait for every phytomer rank the calculated means and variances were averaged. In this way one mean value with standard deviation was calculated for each phytomer for leaf area, stem length and leaf length with measurements of both experiments; and for rachis bend and leaflet angles with data of the first experiment. The number of leaflets were 11 (six lateral and one terminal leaflet) and leaf area was then distributed across the 11 leaflets on each leaf according to an empirical allometric relationship. The area of the composite leaf was distributed over the five leaflet pairs and the terminal leaflet for each leaf in the same manner, using the following fractions (from proximal to distal leaflet pair):

0.1296, 0.0188, 0.1516, 0.0281, 0.0948 and the terminal leaflet with 0.1541 (from Exp. 2). The length of the petiole was 35% of the total leaf length, and at that point the first leaflet pair was attached.

Photosynthesis module. An adapted Farquhar-von Caemmerer-Berry model (FvCB model) was used to simulate photosynthesis (Farquhar et al., 1980; Qian et al., 2012). Mean values with variation for alpha, J_{max28} and V_{cmax28} were taken from a set of measurements at the middle and top height of the canopy as described in Qian et al., 2012. Jmax and Vcmax were assumed to decrease in an exponential way from the 10^{th} leaf from the top to the oldest leaf as a result of a decrease in light; Jmax decreased from 309 to 232 μmol m^{-2} s^{-1} and Vcmax from 117 to 97 μmol m^{-2} s^{-1}. Variation in photosynthesis parameters was introduced as a fraction of the mean. This assumption of exponential decrease was taken since there was no support for any other relationship. Besides this, model simulations have shown that overestimation of photosynthesis when acclimation of photosynthetic parameters with height in the canopy is not considered is minimal when the only light source is the sun (van Ieperen and Trouwborst, 2008).

Light module. The light in the 3D scene was simulated in hourly time steps with a ray tracer, called Flux Light Model, provided by GroIMP. The Flux Light Model was described in detail by Henke and Buck-Sorlin (2017). This ray tracer was based on an inversed path tracer with a Monte Carlo pseudo-random number generator as in (Veach, 1997). The number of rays were 750 million and recursion depth was 10; these numbers were chosen such that a further increase would not improve simulation results (see Supplementary Table S3). For diffuse radiation, the assumption was made of an overcast sky, where light sources were located according to azimuth at every 7.5^o and zenith at every 15^o. The remainder fraction of light was direct light, and modelled as a point source of directional light, arriving from the hourly solar position (model from Goudriaan and van Laar 1994).

5.2.3 Model scenarios

One reference canopy was created, which contained 216 plants. Each plant was rotated (0 to 360°, drawn at random) relative to its neighbor and for the reference canopy this was the only source of variation. The rotation of the plants relative to their neighbors was kept the same for every model simulation such that any differences in light absorption and net photosynthesis are the result of including interplant variation of architectural and/or photosynthesis traits. No collision avoidance of leaves was computed, since leaves of neighbouring plants do in reality not show distinct avoidance mechanisms and extremely intertwine. Every model simulation was run with fixed environmental variables.

Model simulations were run to study light absorption and photosynthesis for a full-grown tomato canopy under differing architectural and photosynthesis trait variations. Trait variation was introduced by drawing from the normal distribution for each trait from these measured data and was independent of other ranks in the same plant. To ensure equal leaf area and internode length between different model scenarios, for each phytomer value drawn there was a plant on the mirrored other side of the canopy with a value that deviated the opposite from the mean [see Supporting Information-Fig. S1]. 10 scenarios with or without interplant variation for specific traits were compared; (1) reference (2) internode length (3) leaf area (4) petiole angle (5) leaflet angle (6) full architecture (internode length, leaf area, petiole angle and leaflet angle combined) (7) alpha (8) Jmax and Vcmax (9) full photosynthesis (alpha, Jmax and Vcmax combined) and (10) everything combined (full architecture and full photosynthesis).

Planting densities were 1.5, 2.4 and 3.3 plants m^{-2}, with LAI 1.75, 2.80 and 3.85, respectively.The model was run with hourly time steps at a fixed CO$_2$ concentration of 600 ppm and a temperature of 23^{o}C. The model was run for summer and winter solstices (21 June, 21 December) at latitude 52^o with both days 0 and 77% direct light. Each model simulation was repeated 5 times with a different value for the random number generator, which randomizes any parameter with a random component in it, i.e. the values drawn from the normal distribution as well as the light model ray tracer. Differences between 5 repetitions were on maximum 2.2% for canopy light absorption, 6.4% for average net photosynthesis, 26.5% for the coefficient of variation of plant light absorption and 23.0% for the coefficient of variation of plant net photosynthesis. Calculations were performed for the centre 12 plants in the centre two double rows (24 plants in total).

5.3 Results

5.3.1 Architectural variation in tomato canopies

The coefficient of variation (CV) of internode length and leaf area remained fairly constant from bottom to top with a maximum of 60% for internode length and 43 % for leaf area (Fig. 2). For petiole angle the standard deviation was rather large in the bottom with a maximum of 46°, compared to a minimum of 8° in the top. For leaflet angles of the lateral and terminal leaflets the ranges were similar between a minimum of 11° found at the top leaves and a maximum of 56° at the bottom of the canopy.

5.3.2 Interplant variation reduces canopy light absorption and net photosynthesis

Introducing interplant variation of architectural and photosynthesis traits had rather small effects on canopy light absorption and net photosynthesis in all planting densities, ranging from +0.3 to -2.2% for the individual traits (Fig. 3; see Supporting Information-Fig. S4) for absolute values on light absorption and net photosynthesis for the reference scenario). When interplant variation of all architectural traits were simultaneously included in the model the canopy light absorption was 3.1% lower and net photosynthesis was 2.4% lower than for the simulation without any interplant variation. Adding interplant variation of all photosynthesis traits to interplant variation in all architecture traits further decreased canopy net photosynthesis by -1.1%; hence net photosynthesis was 3.5% lower when variation in architectural as well as photosynthesis traits were considered compared to a crop without any interplant variation. The coefficient of variation in plant light absorption and net photosynthesis increased with a higher planting density in every model scenario, for the reference this was from 2.4 to 5.5% for PAR absorption, and from 2.0 to 5.6% for net photosynthesis when planting density increased from 1.5 to 3.3 plants m^{-2} (Fig. 3). Introducing interplant variation in internode length and leaf area increased CV in light absorption and net photosynthesis by up to 4.0%.

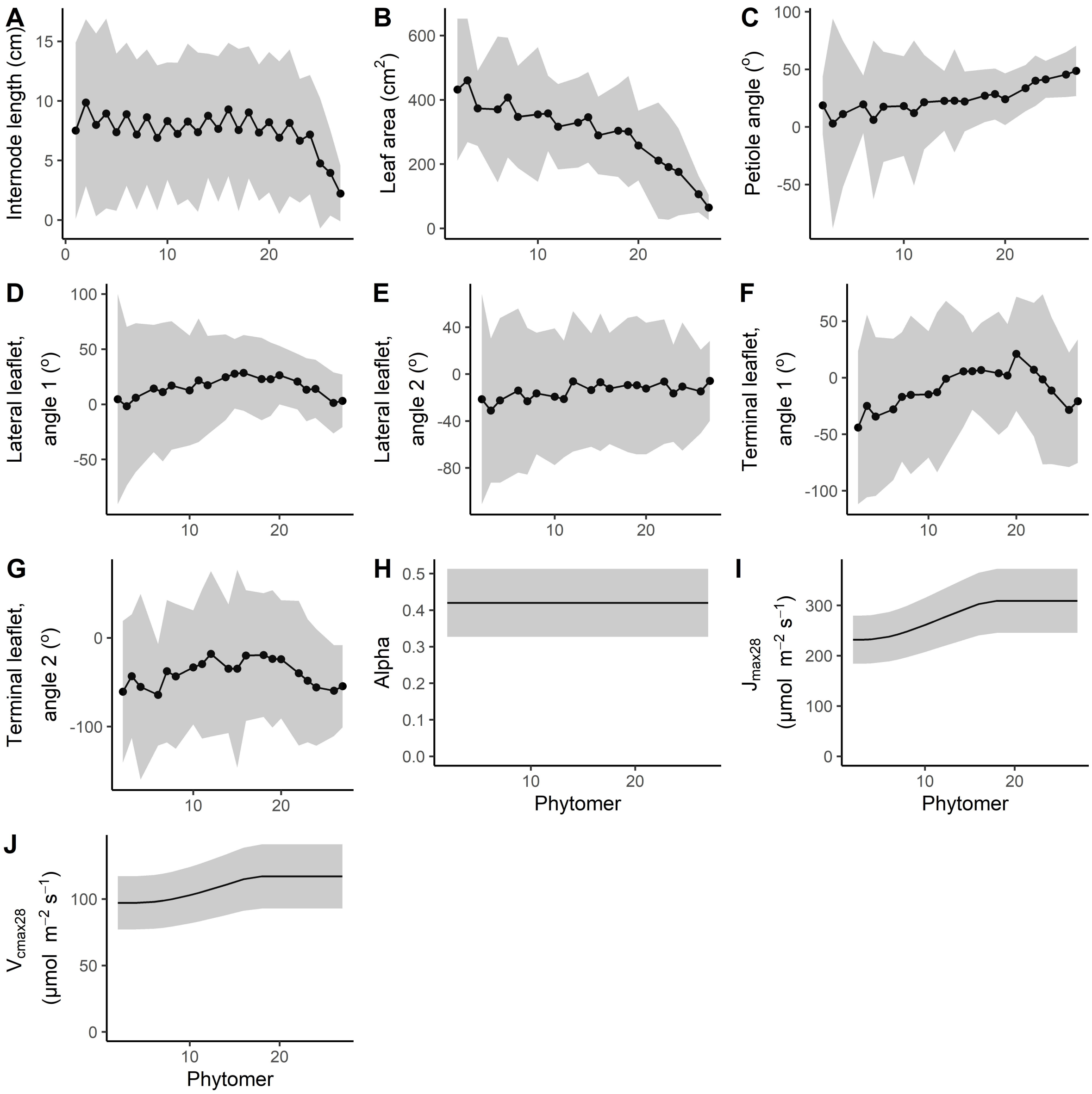

Figure 2: Measured interplant variation of (A-G) architectural traits combined from two glasshouse experiments (for details on how the architectural parameters were measured see Fig. 1), as well as (H-I) interplant variation in photosynthesis traits. Alpha, J_{max28} and V_{cmax28} mean values with variation were taken from (Qian et al., 2012) whom performed measurements on two heights. Mean values for J_{max28} and V_{cmax28} were assumed equal from the 1^{st} to 9^{th} top from the leaf and then decrease exponentially as a result of lower light levels from the 10^{th} leaf from the top to the lowest leaf of the plant. Variation in photosynthesis parameters was kept relational to the mean. Data is represented as the mean ±2 times the standard deviation. Every 4^{th} phytomer bears a truss instead of a leaf, and is therefore presented as missing data, with exception of internode length.

5.3.3 Season and fraction direct light have minor effects on canopy light absorption and photosynthesis

Introducing interplant variation in all architectural traits had a limited effect on canopy light absorption up to -3.3% on both summer and winter solstice for both 0 and 77% direct light (Fig. 4). Largest effects were observed for canopy net photosynthesis of up to -6.8% on the winter solstice on a direct light day when interplant variation was introduced for every architecture and photosynthesis trait. On this day there was an increase in canopy light absorption at the upper part of the canopy while decreased in the lower part of the canopy, resulting in a lower canopy net photosynthesis (Fig. 5). Interplant variation in light absorption and net photosynthesis was largest (12.3%) for the reference on the winter solstice with 77% direct sunlight, compared to a maximum of 2.4% on other combinations of solstice and direct sunlight.

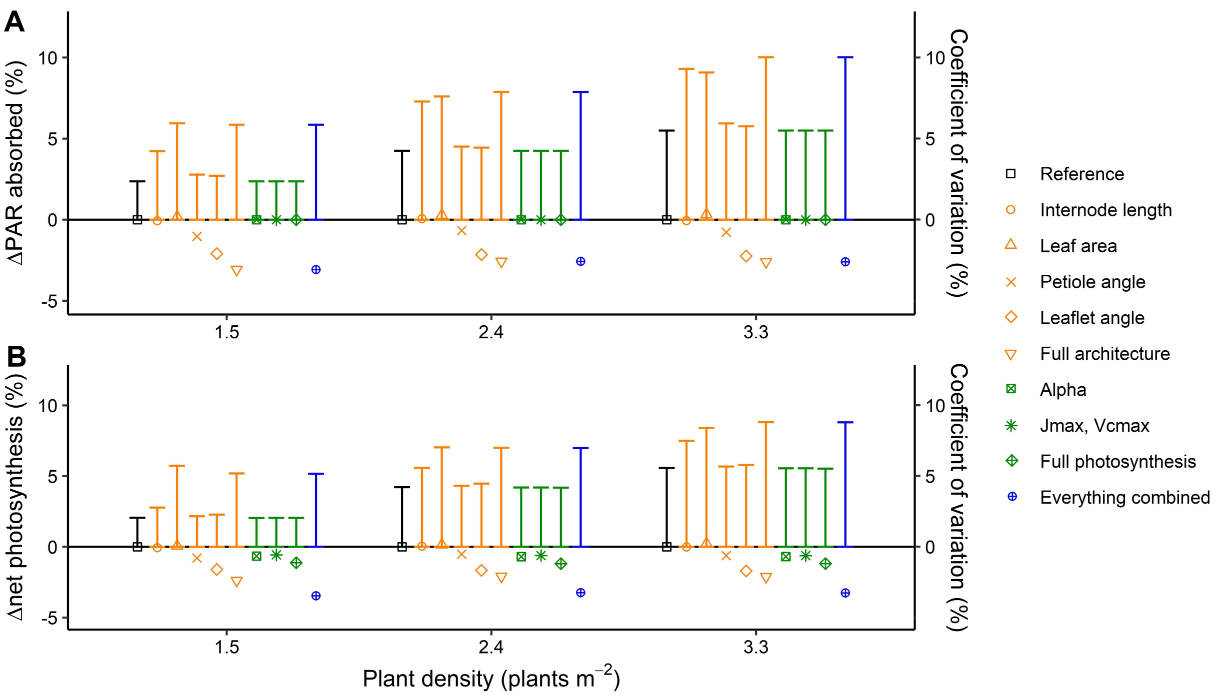

Figure 3: Simulated effects of interplant variation in architectural and photosynthesis traits on canopy light absorption (symbols) and the coefficient of variation in plant light absorption and net photosynthesis (%; vertical bars) at three planting densities. Canopy light absorption and plant net photosynthesis are presented as % change compared to the reference where the rotation of plants relative to their neighbors (0 to 360°, drawn at random) was the only source of variation. The rotation of the plants relative to their neighbors was kept the same for every model simulation such that any differences in light absorption and net photosynthesis are the result of including interplant variation of architectural and/or photosynthesis traits. Data are the averaged values of all hourly time steps in a day of 24 plants (centre 12 plants of the centre two double rows) from five repetitions (simulations with each a different random number generator for the light model and drawings from the normal distribution), at two fractions of direct light (0 and 0.77) and two solstices summer and winter (DOY 171 and 356), resulting in a total of 480 plants.

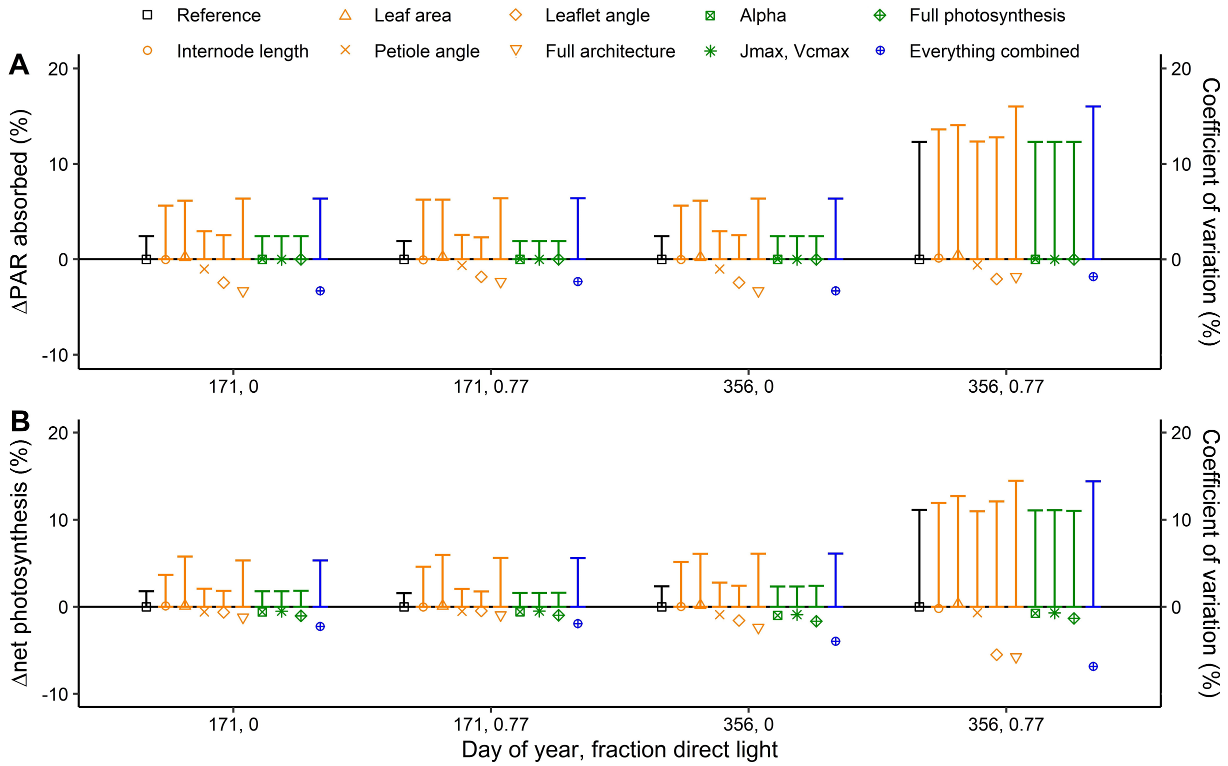

Figure 4: Simulated effects of interplant variation in architectural and photosynthesis traits on canopy light absorption (symbols) and the coefficient of variation in plant light absorption and net photosynthesis (%; vertical bars) at two fractions of direct sunlight (0 and 0.77) and at summer and winter solstices (DOY 171 and 356). Canopy light absorption and net photosynthesis are presented as % change compared to the reference where the rotation of plants relative to their neighbors (0 to 360°, drawn at random) was the only source of variation. The rotation of the plants relative to their neighbors was kept the same for every model simulation such that any differences in light absorption and net photosynthesis are the result of including interplant variation of architectural and/or photosynthesis traits. Data are the averaged values of all hourly time steps in a day of 24 plants (centre 12 plants of the centre two double rows) from five repetitions (simulations with each a different random number generator for the light model and drawings from the normal distribution) and three different planting densities (1.5, 2.4 and 3.3 plants m^{-2}, resulting in a total of 360 plants).

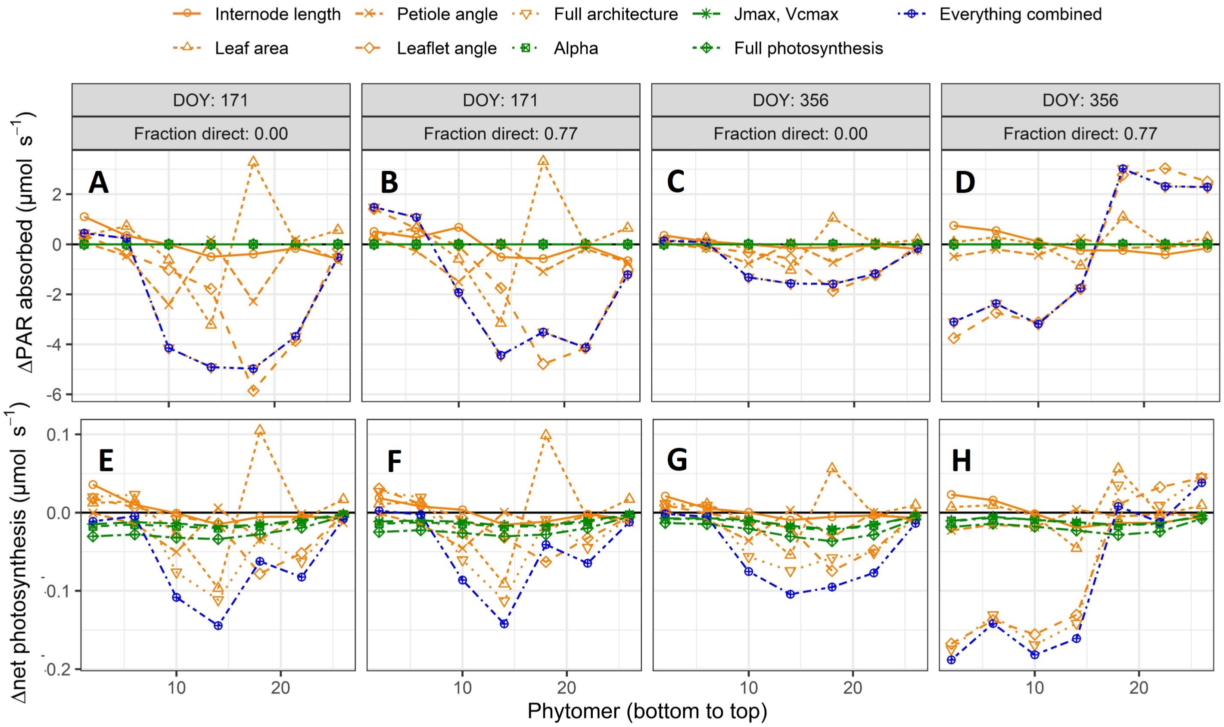

Figure 5: Simulated effects of interplant variation in architectural and photosynthesis traits on differences in leaf light absorption and net photosynthesis at two fractions of direct sunlight (0 and 0.77) and at summer and winter solstices (DOY 171 and 356). Each simulation is compared to the reference where the rotation of plants relative to their neighbors (0 to 360°, drawn at random) was the only source of variation. The rotation of the plants relative to their neighbors was kept the same for every model simulation such that any differences in light absorption and net photosynthesis are the result of including interplant variation of architectural and/or photosynthesis traits. Data represent the average of 3 adjacent phytomer ranks (i.e. phytomer rank 2 is the average of phytomer ranks 1 to 3; phytomer rank 6 the average of phytomer ranks 5 to 7) of all hourly time steps in a day from 24 plants (centre 12 plants of the centre two double rows) from five repetitions, at three different planting densities (1.5, 2.4 and 3.3 plants m^{-2}), resulting in a total of 360 observed plants.

5.4 Discussion

5.4.1 Interplant variation reduces canopy light absorption and net photosynthesis

The aim of this study was to determine the importance of observed interplant variation in architectural and photosynthetic traits on canopy light absorption and net photosynthesis and the coefficient of variation in plant light absorption and net photosynthesis. What we found is that introducing interplant variation in architecture and photosynthesis traits in a FSPM did -depending on the trait- not or negatively affect canopy light absorption and net photosynthesis compared to the reference model without interplant variation. Considering realistic variation of all architectural and photosynthesis traits reduced daily canopy light absorption by -1.8 to -3.3% and daily canopy net photosynthesis by -1.9 to -6.8%, with largest differences in winter at a lower solar angle. It has to be noted that all our model simulations were performed for a fully grown tomato crop.

By using a fully grown tomato crop in a static FSPM the traits could be individually explored at a relative ease. This was justified as tomato has a near year-round growth season where the majority of the production is in a canopy that is relatively static. This study used well established photosynthesis modelling with a plant architecture (e.g. (Zhang et al., 2021; Chapter 2) to understand the influence of certain architectures resulting from plant variability at a long-lasting growth stage. The same architectural parameters can have varying effects when actual growth is simulated (e.g. Chen et al., 2014), and would result in the observation that during a growth cycle traits may have positive or negative effects depending on the developmental stage in which the research is performed (Falster et al., 2018). By use of a static FSPM the observation was that mainly interplant variation in leaflet angles reduces canopy light absorption and photosynthesis, while interplant variation in leaf area increased the coefficient of variation the most in plant light absorption and net photosynthesis. This suggests that for the purpose of accurately determining canopy light absorption and net photosynthesis, petiole and leaflet angle should be considered, whereas leaf area should be considered for accurately determining the coefficient of variation in plant light absorption and net photosynthesis. Previous static tomato FSPM reported values of differences in canopy net photosynthesis up to 7% for simulations when leaflet angle was changed of the architecture of a full-grown crop (Sarlikioti et al., 2011a; Chapter 2). Values in this study were within the same range, although in this case interplant variation in architectural and photosynthesis parameters was introduced instead of a sensitivity analysis.

Applying interplant variation in photosynthetic traits reduced canopy net photosynthesis. The negative effects on net photosynthesis can be explained by the non-linear relationship between alpha, J_{max} and V_{cmax} with photosynthesis (Wilson et al., 1992; Sarlikioti et al., 2011b; Zhu et al., 2012; Song et al., 2013; Von Caemmerer, 2013). The observation of a negative effect on average net photosynthesis when light is re-distributed toward the top of the canopy is shown by (Vermeiren et al., 2020) and observed in this study on a winter solstice with 77% direct light (Fig. 5D, H). A higher fraction of light absorption by the top of the canopy is critical at the young stage to increase light absorption for canopy establishment (Richter et al., 2010) and can have stacking effects, as observed by (Chen et al., 2014) with increases in biomass production up to 20%.

5.4.2 Increased planting density increases coefficient of variation in plant light absorption and net photosynthesis without affecting average net photosynthesis

Higher planting density increased the coefficient of variation in plant light absorption and net photosynthesis for every scenario with interplant variation in architectural and photosynthesis traits without affecting overall canopy photosynthesis. This naturally has to do with an increase in light competition within the canopy. In experiment 2 with differing row orientations the CV in fruit productivity was on average 12.8%. In this model simulation CV values for whole plant net photosynthesis were found up to 12.3% for the highest case, although generally lower than 8%. It has to be noted that the model was not yet able to capture all interplant variability. In reality there is a lot more interplant variability which we did not consider here where productivity also depends on local (a)biotic factors which are not considered, such as temperature, humidity, pathogens, roots, biological variation and more. Of every architectural and photosynthesis parameter included in this study we have shown that introducing interplant variation in leaf area results in the highest coefficient of variation in plant light absorption and net photosynthesis.

5.4.3 Conclusions

Introducing interplant variation in architecture and photosynthesis traits in a functional-structural plant model did -depending on the trait- not or negatively affect canopy light absorption and net photosynthesis compared to the reference model without interplant variation. Introducing interplant variation of architectural and photosynthesis traits in FSPM results in more realistic simulation of variation of plants within a canopy. Furthermore, it can improve the accuracy of simulation of canopy light interception and photosynthesis, though these effects at canopy level are relatively small (<4% for light absorption and <7% for net photosynthesis).

Acknowledgements

The project was funded by the Wellensiek Fund. We thank the CarbonLED project for sharing the architectural data of one of their greenhouse experiments.

5.5 Supplementary material

Table S1: Values for the dimensionless parameters A and B of Eq. 1 for calculating leaf area of Exp. 1 according to an empirical relationship acquired from data in Exp. 1.

Cultivar	A	B
Foundation	0.2533	1.0125
Progression	0.2389	1.0164
Extension	0.2257	1.0350
9112	0.1963	1.0624

Table S2: Composition of the nutrient solution used in the experiment. Solution EC: 2.8 and pH: 5.5.

Macronutrients	Amount	Unit	Micronutrients	Amount	Unit
NH4	1.2	mmol/l	Si	0	μmol/l
K	10.3	mmol/l	Fe	25	μmol/l
Na	0	mmol/l	Mn	10	μmol/l
Ca	5.8	mmol/l	Zn	5	μmol/l
Mg	2.59	mmol/l	B	30	μmol/l
NO3	17.2	mmol/l	Cu	0.75	μmol/l
SO4	4.76	mmol/l	Mo	0.5	μmol/l
HCO3	0	mmol/l	Cl	0	μmol/l
P	1.62	mmol/l			

Table S3: Testing assumptions made in ray number and GroIMP's setseed (random number generator) on canopy light absorption and net photosynthesis on two simulated days of the year (DOY).

DOY	milRays	setSeed	Light absorbed (μmol m^{-2} s^{-1})	Net photosynthesis (μmol m^{-2} s^{-1})
171	750	5	1307.8 ±24.8	7.91 ±0.07
171	1250	5	1307.7 ±24.8	7.91 ±0.07
171	750	6	1307.7 ±24.6	7.91 ±0.07
171	1250	6	1307.5 ±24.8	7.91 ±0.07
356	750	5	601.8 ±61.7	5.70 ±0.37
356	1250	5	601.8 ±61.7	5.70 ±0.37
356	750	6	601.8 ±61.6	5.71 ±0.37
356	1250	6	601.8 ±61.6	5.71 ±0.37

Table S4: Absolute values and standard deviation of light absorbed and net photosynthesis per m^2 floor area for model simulations with the reference scenario on different days of the year (171, 356), planting densities (1.5, 2.4 and 3.3) and fractions of direct sunlight (0 and 0.77). Simulation results were averaged over planting density for the first four rows, and averaged over the combination of day of year (DOY) and fraction direct light for the last three rows. This was done as no clear interaction effects were observed was observed from the individual plots differing these individually.

DOY	Plant density (plants m^{-2})	Fraction direct light	Light absorbed (μmol m^{-2} s^{-1})	Net photosynthesis (μmol m^{-2} s^{-1})
171	1.5, 2.4, 3.3	0	1132.1 ±27.5	40.85 ±0.73
171	1.5, 2.4, 3.3	0.77	1098.4 ±21.2	36.80 ±0.58
356	1.5, 2.4, 3.3	0	361.4 ±8.8	19.93 ±0.47
356	1.5, 2.4, 3.3	0.77	461.8 ±56.9	22.80 ±2.54
171, 356	1.5	0, 0.77	697.4 ±16.5	24.97 ±0.51
171, 356	2.4	0, 0.77	771.3 ±32.8	30.90 ±1.30
171, 356	3.3	0, 0.77	821.5 ±45.2	34.41 ±1.92

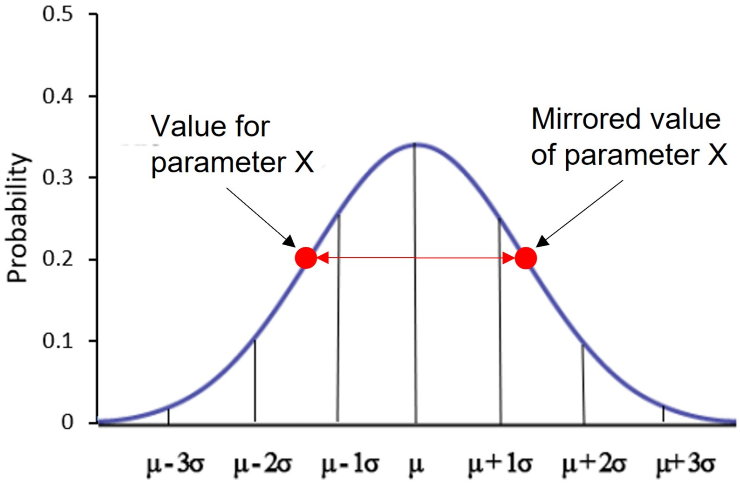

Figure S1: Example of implementing interplant variation for trait X. To keep the total trait value equal across the canopy as a whole a value is taken from the normal distribution and a mirrored value is taken for another plant in the canopy.

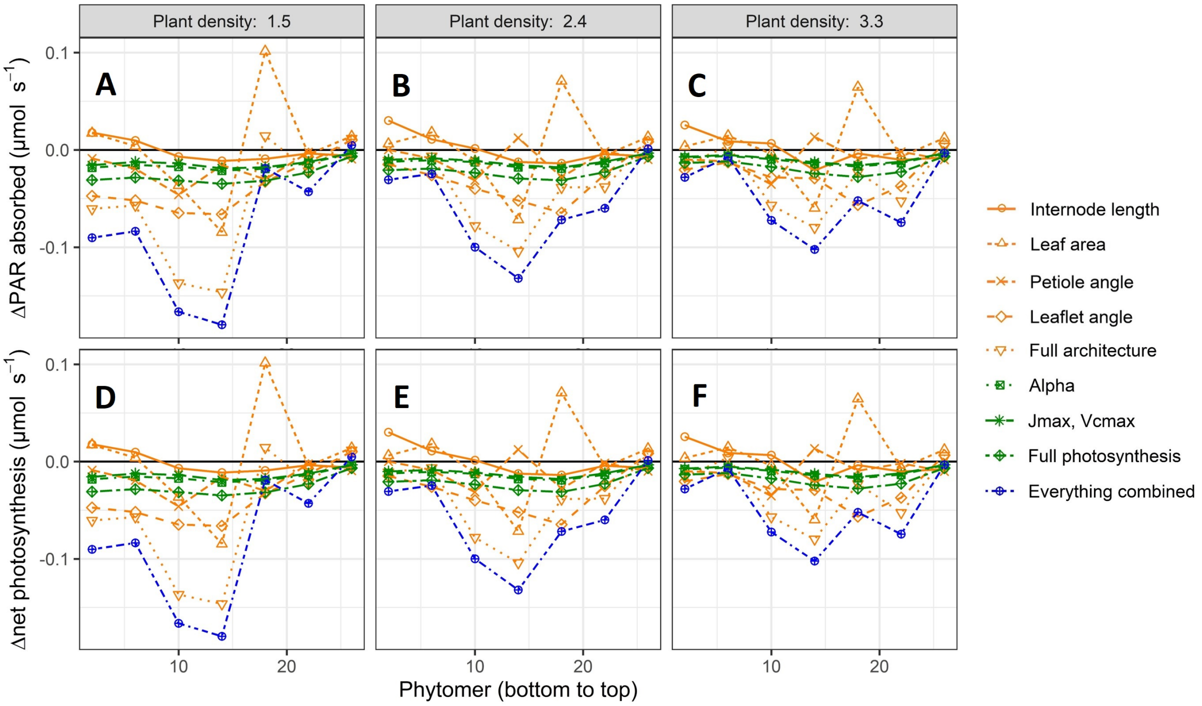

Figure S2: Simulated effects of interplant variation in architectural and photosynthesis traits on absolute differences in leaf light absorption and net photosynthesis (in μmol s^{-1}) at three planting densities (1.5, 2.4 and 3.3 plants m^{-2}). Each simulation is compared to the reference where the rotation of plants relative to their neighbors (0 to 360°, drawn at random) was the only source of variation. The rotation of the plants relative to their neighbors was kept the same for every model simulation such that any differences in light absorption and net photosynthesis are the result of including interplant variation of architectural and/or photosynthesis traits. Data represent the average of 3 adjacent phytomer ranks (i.e. phytomer rank 2 is the average of phytomer ranks 1 to 3; phytomer rank 6 the average of phytomer ranks 5 to 7) of all hourly time steps in a day from 24 plants (centre 12 plants of the centre two double rows) from five repetitions, at two fractions of direct light (0 and 0.77) and two solstices summer and winter (DOY 171 and 356), resulting in a total of 480 observed plants.

Chapter 6

6 General discussion

In this thesis variability in light absorption and photosynthesis within tomato canopies was explored with a 3D model assisted analysis. Light distribution in canopies is important for crop photosynthesis as suggested by several modelling studies (e.g. Buck-Sorlin et al., 2011; Cieslak et al., 2010; Sarlikioti et al., 2011b; Wiechers et al., 2011; Chen et al., 2014; Chapters 2 and 5) and as evidenced by the increased crop photosynthesis, growth and yield of greenhouse tomato when light is made more diffuse (Li et al., 2014). Photosynthesis follows a curvilinear pattern with light intensity which results in a higher overall crop photosynthesis when light is more uniformly distributed (Wilson et al., 1992; Sarlikioti et al., 2011b; Zhu et al., 2012; Song et al., 2013; Von Caemmerer, 2013). Besides this, exposing leaves lower in the canopy to a higher light intensity results in maintaining a higher photosynthetic capacity for these leaves (Trouwborst et al., 2011). Therefore, distributing light more homogeneously throughout the crop is desired.

6.1 Variability in light interception and photosynthesis in a canopy

6.1.1 Variability due to row orientation

A clear source of variability in canopy light distribution is the arrangement of plants, where in a cultivation system row orientations can play a big role. Row orientation affects inter- and intra-row shading and hence daily light distribution (Trentacoste et al., 2016; Campos et al., 2017). For hedgerow productivity and product quality, a north–south row orientation is often favourable as reviewed by (Trentacoste et al., 2015). These authors argued that this is the result of a more equal light distribution to the most important leaves and fruits between both east- and west-facing parts of the rows during a day in a north–south row orientation. A south-facing side can be light-saturated, while the north-facing side of a tree is still limited by light, resulting in unequal fruit set (Khemira et al., 1993), fruit abortion or fruit rot (Lombard and Westwood, 1977).

In this thesis I quantified the influence of row orientation on the inter- and within-row variation of light absorption and photosynthesis in a hedgerow crop by combining experimentation and modelling (Chapter 2), which had not been done so far. What I hypothesized is that plants in north- and south-facing rows in an east-west row orientation double row system would have a much larger variation in light absorption and photosynthesis and hence fruit production than plants in east- and west-facing rows in the north-south row orientation.

Against my own expectation, I showed that due to plant acclimation, row orientation had a minimal influence on canopy light absorption and net photosynthesis. A larger total leaf area by plants in north-facing rows partly compensated the lower light absorption per unit leaf area. An increase in leaf area is observed as one of the shade avoidance symptoms (Kalaitzoglou et al., 2019). Other typical shade avoidance responses were not found in my experiment (Chapter 2) such as a decrease in leaf thickness (leaf area per gram of dry weight) (Holmes and Smith, 1975; Smith and Whitelam, 1997), increased elongation of stems (Ballaré et al., 1991; Smith and Whitelam, 1997; Cole et al., 2011), nor a change in leaf mass. So despite a higher uniformity in light distribution when rows are oriented north–south, the overall crop light absorption and photosynthesis was slightly higher for an east–west orientation (both 3 % higher). Despite an overall equal canopy light absorption and photosynthesis there were still significant differences in fruit production at the row level between the north- and south-facing rows due to a higher partitioning to fruits in the south-facing rows.

In a production system where product quality is of high importance variation in fruit growth is not desired. The hypothesis that plants in north- and south-facing rows in an east-west row orientation double row system would have a much larger variation in light absorption and photosynthesis and hence fruit production than plants in east- and west-facing rows in the north-south row orientation is supported by my measurements (Chapter 2). Acclimation of the plants was the result of differences between facing rows in light absorption, and fruit production was different between the rows. Still, the acclimation of the plants was unexpected and shows an interesting opportunity. Model simulations by Connor et al. (2009) revealed that a certain canopy porosity could be required to support proper fruit growth in olives by having sufficient sunlight on the fruits during the month before harvest. Pruning of the leaves in the upper part of the canopy could result in a more equal light distribution to the most important leaves and fruits between both north- and south-facing parts of the rows during a day in an east-west row orientation. In this way, an enhanced total canopy light absorption and photosynthesis could be maintained while balancing the light distribution in the canopy between the rows.

6.1.2 Variability due to intra-canopy lighting

An increase in leaf area for the north-facing row in the row orientation experiment was a surprise. With the introduction of LEDs and in particular intra-canopy lighting however, changes in morphology can be expected as the light intensity and spectrum are changed in the canopy. The spatial heterogeneity of light absorption that come with the introduction of intra-canopy lighting had not been thoroughly explored compared to top lighting. A reason for this is that the commonly used method to estimate light absorption based on the Lambert-Beer law for light extinction cannot be applied when intra-canopy lighting is used (Monsi and Saeki, 2005).

Model simulations of de Visser et al. (2014) and this thesis (Chapter 4) showed that most of the light from intra-canopy lighting is absorbed by leaves close to the lamps, suggesting that leaf acclimation will take place close to the lamps. Joshi et al. (2019) found a 3-4 times higher photosynthetic capacity in leaves on the inside of the canopy when intra-canopy lighting LEDs were introduced in a canopy with natural background radiation compared to the control. Besides local leaf acclimation, the link between a plant's site of light perception and the sites where morphological acclimation takes place is a field of study with recent advancements but is still not fully understood (Küpers et al., 2018; Iglesias et al., 2018).

With the introduction of LEDs the lower half of plants experience a different light spectrum compared to top lighting. Hence I investigated whether and to which extent local supplementation of FR results in local or long-distance architectural and growth responses in full-grown tomato plants (Chapter 3). I hypothesized that mature plant parts can still induce morphological changes in young growing plant parts. What I found is that locally supplied FR has long-distance effects on length, dry weight of the stem and on SLA, confirming the hypothesis. Some other parameters (petiole elongation, petiole angle and leaf weight) are only affected by the local light environment. The morphological and growth responses from far-red light applied at the bottom of the plants were weaker than those resulting from locally perceived FR at the upper young plant part. The confirmation of the hypothesis is a clear indicator that future studies on light spectrum should look into the integration of light spectrum perceived on different heights of the plant.

Besides inducing long-distance morphological acclimation, the horizontal and vertical variability in light absorption is directly affected by intra-canopy lighting (Chapter 4). Studies where supplemental intra-canopy lighting replaced top lighting showed increased fruit yield in cucumber (Hovi-Pekkanen et al., 2004; Hovi-Pekkanen and Tahvonen, 2008), an increase in sweet pepper fruit number and weight (Hovi-Pekkanen et al., 2006) and an increased net photosynthesis (Pn) and photosynthetic capacity (Pmax; Pettersen et al., 2010). Still, some studies did not find differences in whole plant biomass production between top lighting and intra-canopy lighting (Trouwborst et al., 2010; Dueck et al., 2011; Gómez and Mitchell 2016; Yan et al., 2018). This lack of biomass gain could be related to a loss of total light interception due to extreme leaf curling such as observed by Trouwborst et al. (2010) when intra-canopy lighting was applied with a large fraction of blue light. Gómez and Mitchell (2016) mentioned an increased maintenance respiration of leaves lower in the canopy that acclimated to a higher light intensity and an increased partitioning to non-harvestable organs as possible reasons for lack of effect on yield. All the explanations mentioned in literature about effects or absence of effects are based on differences in incident light environment which affect plant growth and morphology.

Incident light from lighting from above can be measured by quantum sensors pointing upward at different heights. Incident light from intra-canopy lighting might be measured by use of quantum sensors pointing in a side-ward direction towards the intra-canopy lighting at different heights as for instance done in Kaiser et al. (2019). However, spatial heterogeneity of incident and absorbed light is hard to measure in detail. The spatial variability of absorbed light is important when physiological processes such as photosynthesis are studied (Joshi et al., 2019). I hypothesized that using intra-canopy lighting increases overall crop uniformity in light absorption (Chapter 4). By use of an FSPM an investigation was performed comparing spatial heterogeneity of incident and absorbed light between intra-canopy lighting and top lighting systems. I showed with model simulations that the leaflets in intra-canopy lighting generally have a more uniform overall light absorption. The hypothesis is therefore supported by my model simulations. The variation coefficient however is roughly the same in both the horizontal and vertical direction for intra-canopy lighting as compared to top lighting. This means that the relative variation between leaves is the same for intra-canopy and top lighting. A combination of intra-canopy and top lighting always has a more uniform canopy light absorption than intra-canopy or top lighting alone. Besides this, there was an 8% higher total light absorption with the use of intra-canopy lighting compared to top lighting.

Special attention should be given to the way how intra-canopy and top lighting studies are compared to each other. It is difficult to make a fair comparison between intra-canopy and top lighting in an experimental situation. Light is lost due to structural parts of the greenhouse, management equipment such as wires and reflection through the sides of small compartments. Besides this, top lighting modules also block sunlight whereas intra-canopy lighting hardly blocks natural sunlight. Most of intra-canopy lighting is directly absorbed by the surrounding. Still, light can be lost on the sides of a compartment where intra-canopy lighting is pointed side-ward. In literature there has been no mention of how a fair comparison can be made. Having the same number of lamps does not mean that incident light is equal between treatments. The height at which incident light should be measured for top lighting when this is to be compared to intra-canopy lighting remains difficult. An over- or underestimation would result in an inherently unfair comparison between treatments. Model simulations in this thesis did not explicitly model the full greenhouse structure, apart from the reflection of walls, the floor, heating pipes and gutter. In most FSPM the greenhouse structure is not explicitly modelled. Due to this a fair comparison could be made between intra-canopy lighting and top lighting (Chapter 4).

In the absence of sunlight a rough idea can be given on how to make a fair comparison between intra-canopy and top lighting. For top lighting the light intensity could be measured just above the top of the canopy. By comparing this to calculations on how much light there would be without any light loss to structural components of the greenhouse, an estimation of light loss can be acquired. Lamps in the intra-canopy lighting can then be adjusted in intensity based on this. I still don't have a suggestion on how and at which distance intra-canopy lighting should be measured with a line sensor. Still, the efficiency of intra-canopy lighting could be largely underestimated if the incident light is estimated higher than it would be in reality.

6.1.3 Including interplant variation; is more realistic also better?

As has been shown in Chapters 2 and 3, the plants acclimated to their growing conditions. This also resulted in architectural variability. It has been shown in several studies that increased light absorption and photosynthesis can be achieved by looking for advantageous crop architectures (Sarlikioti et al., 2011a; Da Silva et al., 2014; Perez et al., 2017). The desired architecture depends on the stage of crop development, where traits related to leaf area are of importance particularly in the early stage (Perez et al., 2017), as a rapid establishment of leaf area is critical at the young stage to increase light absorption (Richter et al., 2010). When LAI is high and the canopy intercepts most incident light, other attributes related to leaf and leaflet arrangement within the crown have a greater influence on light capture by changing light distribution within the crown.

Inclusion of interplant variation in architectural and photosynthesis traits for modelling light absorption and photosynthesis has yet received minimal attention, while this could be of importance for accurately modelling variability in a canopy. I studied the importance of observed interplant variation in architectural and photosynthetic traits on canopy light absorption and net photosynthesis and determind the coefficient of variation in plant light absorption and net photosynthesis (Chapter 5). Here I hypothesize that including measured interplant variation in architectural and photosynthesis traits results in more accurate model simulations of light absorption and photosynthesis than a model which does not include spatial variation. For this I used measured interplant variation in greenhouse grown tomato canopies and implemented this in a FSPM. What I found with model simulations is that introducing interplant variation in architecture and photosynthesis traits in a functional-structural plant model did -depending on the trait- not or negatively affect canopy light absorption and net photosynthesis compared to the reference model without interplant variation. A theory that has to do with acclimation of plants in relation to crop growth efficiency is the tragedy of the commons, where plant communities are invaded by other species that invest more in capturing light, at the expense of other plants and energy cost (Anten and Vermeulen, 2016). In the end all plants end up using more energy for competition which is not good for the community as a whole. In agriculture and horticulture we aim for a higher productivity while using less resources. Here I showed that a uniform average crop would have been better than having a crop with variability included. Despite being capable of improving the accuracy of simulation of canopy light interception and photosynthesis the effects at canopy level were relatively small (<4% for light absorption and <7% for net photosynthesis).

Therefore the hypothesis that including measured interplant variation in architectural and photosynthesis traits results in more accurate model simulations of light absorption and photosynthesis than a model which does not include spatial variation was rejected as the impact on modelling light absorption and photosynthesis was only small. For quite some parameters there was no influence of including interplant variation on canopy light absorption and photosynthesis, while for other parameters there was no influence on the CV of plant light absorption and photosynthesis. This gives an indication that including interplant variation in architectural and photosynthesis parameters is a cumbersome effort which does not have a large impact on simulated averages of a canopy. Still, for a crop where the harvestable product is the crop itself, such as for lettuce, predicting individual variability is of greater importance. It should also be taken into account that the finding of limited importance of including interplant variation is for a dense tomato canopy (a monoculture) with a relative high leaf area index. For canopy mixtures it has been shown that interplant variation can explain complementary light capture (Zhu et al., 2015). Besides, the findings of Chapter 5 should not be translated to early stages of plant development. Dynamic functional-structural plant models such as Greenlab (de Reffye et al., 2021) or EcoMeristem (Larue et al., 2019) could be used to assess the importance of variability in a dynamic growth setting. This would answer the need to include parameter variability in different developmental stages.

6.2 The added value and limitations of using a 3D assisted modelling approach

6.2.1 Benefits to the approach assisted by 3D modelling

Functional-structural plant models (FSPMs) explore and integrate relationships between a plant's structure and processes that underlie its growth and development (Louarn and Song 2020). In this thesis growth and development itself was not simulated. Instead the tomato crop was considered static as the majority of growth happens in a stage where it remains relatively constant over time. According to Louarn and Song (2020) the use of FSPM in this research is on the integration of plant architecture and primary production. Researchers with similar intentions that used a static FSPM have for example quantified the effects of shoot-bending on cut rose production under greenhouse conditions (Zhang et al., 2021). Prieto et al. (2019) used a similar approach in grapevine to compare the gains in photosynthesis enabled by different training systems.

At a latitude of 52°N the daily light integral increases until the 24^{th} of June and then decreases again. Leaf area and leaf thickness acclimate to the light intensity a crop receives (Oguchi et al., 2003). By assuming that leaf acclimation was minimal during the final two months of the row orientation experiment, it was possible to quantify differences in productivity between north-south and east-west row orientations. Findings of the row orientation experiment (Chapter 2) with the use of 3D modelling could not so easily have been explained by standard light distribution measurements. It was now possible to take the climate data of the past months, incorporate this and calculate the effects. Then a sensitivity analysis was performed where leaf area was modified which revealed the importance of acclimation for the uniformity. An explanation of observed differences in light absorption and photosynthesis could be given as well with model simulations, where on completely cloudy days the north-facing rows had higher light absorption and higher net photosynthesis rate. On days with roughly 25% direct sunlight and higher the south-facing rows absorbed more light than north-facing rows, where photosynthesis was higher for south-facing rows with roughly 60% direct sunlight and higher.

In Chapter 4 FSPM was a useful tool to accurately visualize and quantify the distinctive extinction patterns throughout the canopy with intra-canopy lighting and/or top lighting. Doing the same kind of work with physical measurements would have been very time consuming and not have resulted in the same level of detail. Here I made use of the large amount of data that can be produced on an organ level, where leaflet light absorption was taken as the level of detail. In addition to this, future model simulations could be performed where the number and type of intra-canopy LEDs could be varied and placed on different heights to determine the effect on variability in light absorption. FSPM would be of perfect use for this, as predictions can be made to determine the best strategies to be tested in real experimental setups.

Reducing variation among plants can also be obtained by optimizing plant spacing strategies in plant factories (Nicole et al., 2016). In the study of Nicole et al. (2016) I simulated lettuce plants that were re-spaced further apart during growth when the ground cover reached a certain threshold to reduce competition between plants. In that study I used FSPM for it's predictive power to beforehand determine the optimal moment for re-spacing, where a large set of combinations was tested virtually. With the acquired information interesting follow-up experimentation can more easily be determined.

6.2.2 Limitations to the approach assisted by 3D modelling

Obvious limitations in my research on a 3D assisted modelling approach were the requirement of data to calibrate models and the limited availability of data to validate these models. Light measurements performed in experiments were useful in determining the overall accuracy of simulated light absorption. Still, there were plenty of architectural and photosynthesis parameter values and assumptions made based on limited data availability. The number of leaflets, the distribution of leaf area between leaflets as well as the ratio between rachis length of a leaf and its leaflets are three of such examples, where literature has shown that impacts of simplifying leaf structure are small but unpredictable (Vermeiren et al., 2020). For the row orientation experiment there was a number of 6 plants per facing direction measured for architecture, which was rather limited. With this amount no parameter variability could be included with precision. This was however also not the intent of the study, and required accuracy comes and goes with specific research questions.

A more extensive data set for the intra-canopy lighting made it possible to study the interplant variation in architectural traits on light absorption and photosynthesis. An obvious limitation for that study was the fact that photosynthesis was not measured in the experiment and that parameter values were taken from literature of (Qian et al., 2012). Measuring photosynthesis requires a lot of time and expensive machinery and it is therefore generally financially not feasible to measure on every height to determine variability for every phytomer if this is just a part of the scope of a study. Due to the large plant size used in my model studies, automatic phenotyping was not readily available either. This might be something for the future, although this will more readily be available for smaller plants (Li et al., 2020). Phenotyping large plants on a high-throughput system is available only to a limited extent, though progress is made in this field (Li et al., 2020).

Because FSPMs deal with a lot of entities, parameters, spatial scales and heterogeneity, they are usually more complex and less easy to use than process-based crop models. In the same way as other types of complex models (Grimm and Railsback, 2005), complexity generally results in more time-consuming model development and maintenance. The availability of dedicated modelling platforms has significantly improved model re-usability and accessibility in the past years (Kniemeyer et al., 2007; Barczi et al., 2008; Pradal et al., 2008; Marshall-Colon et al., 2017). Still, the number of parameters and data required for parameterizing an FSPM remains cumbersome.

6.3 Advise for growers

Ultimately, for growers there is the potential to increase uniformity in fruit production. One way is by having either a favorable row orientation, i.e. a north-south row orientation at a latitude of 52°, or reducing the differences in light absorption between rows in the crop by for example pruning leaves on the row side which receives more light (i.e. the south-facing row in an east-west row orientation) (Chapter 2). Another suggestion would be to utilize the potential of intra-canopy lighting in increasing the homogeneity of light distribution in a canopy. This would also result in a higher total light absorption since there would be limited reflective losses (Chapter 4). Besides increasing light capture, the spectrum of the intra-canopy lighting can be chosen to induce desired plant architectural acclimation (Chapter 3). When a dense canopy is formed later in the growing season the interplant variation in architecture has a limited influence on light absorption (Chapter 5), and hence the location of intra-canopy lighting is then less relevant.

6.4 Possibilities for further research

I studied the effects of far-red light on long-distance signalling in the plant (Chapter 3). No distinction was made between different types of tissue. The study of e.g. Pantazopoulou et al. (2017) demonstrates that the location where far-red is applied matters for the response. I have shown that mature plant parts still influence its own architecture by long-distance responses within the plant. Future studies should focus on distinguishing which part of the mature plant part is responsible for this and if the diminishing effects are due to ageing or distance. Also, I applied far-red light, while other wavelengths such as blue light are also known to have a strong influence on plant growth and development. Studies that focus on responses related to signalling as a result of hormones can determine dose response curves, i.e. a range of auxin concentrations can be applied to determine the magnitude of inducing changes in leaflet angle (Pantazopoulou et al., 2017). This would then aid in simulating the auxin balance of a plant, which is complex but plays a vital role in growth and development of plants.

In Chapter 4 I studied variability of the light distribution in the canopy. In this research there is one obvious aspect that requires future studying, namely the impact of variability in light absorption on net photosynthesis. Another aspect is that there was no focus on light spectrum, although it was shown in (Chapter 3) to have an influence on plant architecture even when placed down in the canopy. Even though the variability in light absorption was modelled under different scenarios, it was not possible to make a clear protocol on how to make a fair experimental comparison between intra-canopy and top lighting. In the absence of sunlight a rough idea can be given on how to make a fair comparison between intra-canopy and top lighting. For top lighting the light intensity could be measured just above the top of the canopy. By comparing this to calculations on how much light there would be without any light loss to structural components of the greenhouse, an estimation of light loss can be acquired. Lamps in the intra-canopy lighting can then be adjusted in intensity based on this. This does require further research as the efficiency of intra-canopy lighting could be largely underestimated if the incident light is estimated higher than it would be in reality.

If we want to be able to simulate and predict the effects of intra-canopy lighting on architectural changes, interplant variability and associated plant growth and development in a canopy during a growing season, we need a much better understanding of how light signals affect growth and development at the phytomer level. There are models that can include certain architectural variability such as Greenlab (de Reffye et al., 2021; i.e. variability in axis development, branching, meristem viability) and Ecomeristem (Larue et al., 2019; i.e. variability in tillering dynamics and mortality). These models could be useful in the future where similar studies could be undertaken to determine the importance of architectural changes and trait variability for plant growth. This would require a far more elaborate analysis and interpretation of data. Zhu et al. (2015) investigated this topic in a maize and soybean mixture, and showed that inclusion of interplant variation can result in complementary light capture.

References

Adams, S. R., Cockshull, K. E., & Cave, C. R. J. (2001). Effect of Temperature on the Growth and Development of Tomato Fruits. *Annals of Botany*, *88*(5), 869–877. https://doi.org/10.1006/anbo.2001.1524

Adams, S. R., & Valdeés, V. M. (2002). The effect of periods of high temperature and manipulating fruit load on the pattern of tomato yields. *The Journal of Horticultural Science and Biotechnology*, *77*(4), 461–466. https://doi.org/10.1080/14620316.2002.11511522

Alban, V., Didier, C., & Escobar-Gutiérrez, J. A. (2008). A study of ryegrass architecture as a self-regulated system, using functional-structural plant modelling. *Functional Plant Biology*, *35*(10), 911–924. https://doi.org/10.1071/FP08050

Anten, N. P. R., & Vermeulen, P. J. (2016). Tragedies and crops: Understanding natural selection to improve cropping systems. *Trends in Ecology & Evolution*, *31*(6), 429–439. https://doi.org/10.1016/j.tree.2016.02.010

Ballaré, C. L., & Pierik, R. (2017). The shade-avoidance syndrome: Multiple signals and ecological consequences. *Plant, Cell & Environment*, *40*(11), 2530–2543. https://doi.org/10.1111/pce.12914

Ballaré, C. L., Scopel, A. L., & Sánchez, R. A. (1991). Photocontrol of stem elongation in plant neighbourhoods: Effects of photon fluence rate under natural conditions of radiation. *Plant, Cell & Environment*, *14*(1), 57–65. https://doi.org/10.1111/j.1365-3040.1991.tb01371.x

Barczi, J.-F., Rey, H., Caraglio, Y., De Reffye, P., Barthélémy, D., Dong, Q. X., & Fourcaud, T. (2008). Amapsim: A structural whole-plant simulator based on botanical knowledge and designed to host external functional models. *Annals of Botany*, *101*(8), 1125–1138. https://doi.org/10.1093/aob/mcm194

Black, M., & Shuttleworth, J. E. (1974). The role of the cotyledons in the photocontrol of hypocotyl extension in cucumis sativus l. *Planta*, *117*, 57–66. https://doi.org/10.1007/BF00388678

Boonen, C., Samson, R., Janssens, K., Pien, H., Lemeur, R., & Berckmans, D. (2002). Scaling the spatial distribution of photosynthesis from leaf to canopy in a plant growth chamber. *Ecological Modelling*, *156*(2-3), 201–212. https://doi.org/10.1016/S0304-3800(02)00171-0

Borger, C. P. D., Hashem, A., & Powles, S. B. (2016). Manipulating crop row orientation and crop density to suppress lolium rigidum. *Weed Research*, *56*(1), 22–30. https://doi.org/10.1111/wre.12180

Borger, C. P. D., Hashem, A., & Pathan, S. (2010). Manipulating crop row orientation to suppress weeds and increase crop yield. *Weed Science - WEED SCI*, *58*(2), 174–178. https://doi.org/10.1614/WS-09-094.1

Buck-Sorlin, G., de Visser, P. H. B., Henke, M., Sarlikioti, V., van der Heijden, G. W. A. M., Marcelis, L. F. M., & Vos, J. (2011). Towards a functional–structural plant model of cut-rose: simulation of light environment, light absorption, photosynthesis and interference with the plant structure. *Annals of Botany*, *108*(6), 1121–1134. https://doi.org/10.1093/aob/mcr190

Camelo, A. F. L., & Gómez, P. A. (2004). Comparison of color indexes for tomato ripening. *Horticultura Brasileira*, *22*(3), 534–537. https://doi.org/10.1590/S0102-05362004000300006

Campos, I., Neale, C., & Calera, A. (2017). Is row orientation a determinant factor for radiation interception in row vineyards? *Australian Journal of Grape and Wine Research*, *23*(1), 77–86. https://doi.org/10.1111/ajgw.12246

Casal, J. J. (2013). Photoreceptor signaling networks in plant responses to shade [PMID: 23373700]. *Annual Review of Plant Biology*, *64*(1), 403–427. https://doi.org/10.1146/annurev-arplant-050312-120221

Casal, J. J., & Smith, H. (1988). Persistent effects of changes in phytochrome status on internode growth in light-grown mustard: Occurrence, kinetics and locus of perception. *Planta*, *175*(2), 214–220. https://doi.org/10.1007/BF00392430

Casal, J. J., & Smith, H. (1989). The 'end-of-day' phytochrome control of internode elongation in mustard: Kinetics, interaction with the previous fluence rate, and ecological implications. *Plant, Cell & Environment*, *12*(5), 511–520. https://doi.org/10.1111/j.1365-3040.1989.tb02124.x

Chelle, M. (2005). Phylloclimate or the climate perceived by individual plant organs: What is it? how to model it? what for? *New Phytologist*, *166*(3), 781–790. https://doi.org/10.1111/j.1469-8137.2005.01350.x

Chelle, M., & Andrieu, B. (1998). The nested radiosity model for the distribution of light within plant canopies. *Ecological Modelling*, *111*(1), 75–91. https://doi.org/10.1016/S0304-3800(98)00100-8

Chelle, M., & Andrieu, B. [Bruno]. (2007). Modelling the light environment of virtual crop canopies. https://doi.org/10.1007/1-4020-6034-3_7

Chen, T.-W., Nguyen, T. M. N., Kahlen, K., & Stützel, H. (2014). Quantification of the effects of architectural traits on dry mass production and light interception of tomato canopy under different temperature regimes using a dynamic functional–structural plant model. *Journal of Experimental Botany*, *65*(22), 6399–6410. https://doi.org/10.1093/jxb/eru356

Chen, X., Yao, Q., Gao, X., Jiang, C., Harberd, N. P., & Fu, X. (2016). Shoot-to-root mobile transcription factor hy5 coordinates plant carbon and nitrogen acquisition. *Current Biology*, *26*(5), 640–646. https://doi.org/10.1016/j.cub.2015.12.066

Chenu, K., Rey, H., Dauzat, J., Lydie, G., & Lecœur, J. (2008). Estimation of light interception in research environments: A joint approach using directional light sensors and 3d virtual plants applied to sunflower (helianthus annuus) and arabidopsis thaliana in natural and artificial conditions. *Functional Plant Biology*, *35*(10), 850–866. https://doi.org/10.1071/FP08057

Cieslak, M., Seleznyova, A. N., & Hanan, J. (2010). A functional–structural kiwifruit vine model integrating architecture, carbon dynamics and effects of the environment. *Annals of Botany*, *107*(5), 747–764. https://doi.org/10.1093/aob/mcq180

Cole, B., Kay, S. A., & Chory, J. (2011). Automated analysis of hypocotyl growth dynamics during shade avoidance in arabidopsis. *The Plant Journal*, *65*(6), 991–1000. https://doi.org/10.1111/j.1365-313X.2010.04476.x

Connor, D., Centeno, A., & Gomez-del-Campo, M. (2009). Yield determination in olive hedgerow orchards. ii. analysis of radiation and fruiting profiles. *Crop and Pasture Science*, *60*, 443–452. https://doi.org/10.1071/CP08253

Courbier, S., Grevink, S., Sluijs, E., Bonhomme, P.-O., Kajala, K., van Wees, S. C. M., & Pierik, R. (2020). Far-red light promotes botrytis cinerea disease development in tomato leaves via jasmonate-dependent modulation of soluble sugars. *Plant, Cell & Environment*, *43*(11), 2769–2781. https://doi.org/10.1111/pce.13870

Da Silva, D., Han, L., Faivre, R., & Costes, E. (2014). Influence of the variation of geometrical and topological traits on light interception efficiency of apple trees: sensitivity analysis and metamodelling for ideotype definition. *Annals of Botany*, *114*(4), 739–752. https://doi.org/10.1093/aob/mcu034

Davis, P. A., & Burns, C. (2016). Photobiology in protected horticulture. *Food and Energy Security*, *5*(4), 223–238. https://doi.org/10.1002/fes3.97

De Pury, D. G. G., & Farquhar, G. D. (1997). Simple scaling of photosynthesis from leaves to canopies without the errors of big-leaf models. *Plant, Cell & Environment*, *20*(5), 537–557. https://doi.org/10.1111/j.1365-3040.1997.00094.x

de Reffye, P., Hu, B., Kang, M., Letort, V., & Jaeger, M. (2021). Two decades of research with the GreenLab model in agronomy. *Annals of Botany*, *127*(3), 281–295. https://doi.org/10.1093/aob/mcaa172

de Visser, P. H. B., Sarlikioti, V., & Buck-Sorlin, G. H. (2010). A 3d greenhouse model to determine the optimal lighting strategy and crop structure for light capture and photosynthesis in tomato.

de Visser, P. H. B., van der Heijden, G., & Buck-Sorlin, G. H. (2014). Optimizing illumination in the greenhouse using a 3d model of tomato and a ray tracer. *Frontiers in Plant Science*, *5*, 48. https://doi.org/10.3389/fpls.2014.00048

de Wit, M., George, G. M., Ince, Y. Ç., Dankwa-Egli, B., Hersch, M., Zeeman, S. C., & Fankhauser, C. (2018). Changes in resource partitioning between and within organs support growth adjustment to neighbor proximity in brassicaceae seedlings. *Proceedings of the National Academy of Sciences*, *115*(42), E9953–E9961. https://doi.org/10.1073/pnas.1806084115

de Wit, M., Keuskamp, D. H., Bongers, F. J., Hornitschek, P., Gommers, C. M., Reinen, E., Martínez-Cerón, C., Fankhauser, C., & Pierik, R. (2016). Integration of phytochrome and cryptochrome signals determines plant growth during competition for light. *Current Biology*, *26*(24), 3320–3326. https://doi.org/10.1016/j.cub.2016.10.031

de Wit, M., Ljung, K., & Fankhauser, C. (2015). Contrasting growth responses in lamina and petiole during neighbor detection depend on differential auxin responsiveness rather than different auxin levels. *New Phytologist*, *208*(1), 198–209. https://doi.org/10.1111/nph.13449

Dourado-Neto, D., Teruel, D. A., Reichardt, K., Nielsen, D. R., Frizzone, J. A., & Bacchi, O. O. S. (1998). Principles of crop modeling and simulation: I. uses of mathematical models in agricultural science. *Scientia Agricola*, *55*, 46–50. https://doi.org/10.1590/S0103-90161998000500008

Dueck, T. A., Janse, J., Eveleens, B. A., Kempkes, F. L. K., & Marcelis, L. F. M. (2011). Growth of tomatoes under hybrid led and hps lighting. *International Symposium on Advanced Technologies and Management Towards Sustainable Greenhouse Ecosystems: Greensys2011 952*, 335–342.

Endo, M., Araki, T., & Nagatani, A. (2016). Tissue-specific regulation of flowering by photoreceptors. *Cellular and Molecular Life Sciences*, *73*(4), 829–839. https://doi.org/10.1007/s00018-015-2095-8

Evers, J. B., van der Krol, A. R., Vos, J., & Struik, P. C. (2011). Understanding shoot branching by modelling form and function. *Trends in Plant Science*, *16*(9), 464–467. https://doi.org/10.1016/j.tplants.2011.05.004

Falster, D. S., Duursma, R. A., & FitzJohn, R. G. (2018). How functional traits influence plant growth and shade tolerance across the life cycle. *Proceedings of the National Academy of Sciences*, *115*(29), E6789–E6798. https://doi.org/10.1073/pnas.1714044115

Farquhar, G. D., von Caemmerer, S., & Berry, J. A. (1980). A biochemical model of photosynthetic co2 assimilation in leaves of c3 species. *Planta*, *149*, 78–90. https://doi.org/10.1007/BF00386231

Fournier, C., Durand, J. L., Ljutovac, S., Schäufele, R., Gastal, F., & Andrieu, B. (2005). A functional-structural model of elongation of the grass leaf and its relationships with the phyllochron. *The New Phytologist*, *166*(3), 881–894. https://doi.org/10.1111/j.1469-8137.2005.01371.x

Fraser, D. P., Hayes, S., & Franklin, K. A. (2016). Photoreceptor crosstalk in shade avoidance. *Current Opinion in Plant Biology*, *33*, 1–7. https://doi.org/10.1016/j.pbi.2016.03.008

Gijzen, H., & Goudriaan, J. (1989). A flexible and explanatory model of light distribution and photosynthesis in row crops. *Agricultural and Forest Meteorology*, *48*(1), 1–20. https://doi.org/10.1016/0168-1923(89)90004-X

Goldsmith, M. H. M., Cataldo, D. A., Karn, J., Brenneman, T., & Trip, P. (1974). The rapid non-polar transport of auxin in the phloem of intact coleus plants. *Planta*, *116*(1), 301–317. https://doi.org/10.1007/BF00390855

Gómez, C., & Mitchell, C. A. (2016). Physiological and productivity responses of high-wire tomato as affected by supplemental light source and distribution within the canopy. *Journal of the American Society for Horticultural Science J. Amer. Soc. Hort. Sci.*, *141*(2), 196–208. https://doi.org/10.21273/JASHS.141.2.196

Goudriaan, J., & van Laar, H. H. (1994). *Modelling potential crop growth processes*. Dordrecht: Springer-Science+Business Media.

Grimm, V., & Railsback, S. F. (2005). Individual-based modeling and ecology. In *Individual-based modeling and ecology*. Princeton university press.

Henke, M., & Buck-Sorlin, G. H. (2017). Using a full spectral raytracer for calculating light microclimate in functional-structural plant modelling. *Computing and Informatics*, *36*(6), 1492–1522. https://doi.org/10.4149/cai_2017.6.1492

Heuvelink, E. (1996). Dry Matter Partitioning in Tomato: Validation of a Dynamic Simulation Model. *Annals of Botany*, *77*(1), 71–80. https://doi.org/10.1006/anbo.1996.0009

Hogewoning, S., Trouwborst, G., Engbers, G. H. M., Harbinson, J., Ieperen, W., Schapendonk, A., Pot, C. S., & Kooten, O. (2006). Plant physiological acclimation to irradiation by light-emitting diodes (leds). *Acta Horticulturae 761 (2007)*, *761*. https://doi.org/10.17660/ActaHortic.2007.761.23

Holmes, M., & Smith, H. (1975). The function of phytochrome in the natural environment. *Nature*, *254*, 512–514. https://doi.org/10.1038/254512a0

Hovi-Pekkanen, T., Näkkilä, J., & Tahvonen, R. (2006). Increasing productivity of sweet pepper with interlighting. *Acta Horticulturae*, 165–170. https://doi.org/10.17660/ActaHortic.2006.711.19

Hovi-Pekkanen, T., Näkkilä, J., & Tahvonen, R. (2004). Interlighting improves production of year-round cucumber. *Scientia Horticulturae*, *102*(3), 283–294. https://doi.org/10.1016/j.scienta.2004.04.003

Hovi-Pekkanen, T., & Tahvonen, R. (2008). Effects of interlighting on yield and external fruit quality in year-round cultivated cucumber. *Scientia Horticulturae*, *116*(2), 152–161. https://doi.org/10.1016/j.scienta.2007.11.010

Iglesias, M. J., Sellaro, R., Zurbriggen, M. D., & Casal, J. J. (2018). Multiple links between shade avoidance and auxin networks. *Journal of Experimental Botany*, *69*(2), 213–228. https://doi.org/10.1093/jxb/erx295

Ji, Y., Ouzounis, T., Courbier, S., Kaiser, E., Nguyen, P. T., Schouten, H. J., Visser, R. G. F., Pierik, R., Marcelis, L. F. M., & Heuvelink, E. (2019). Far-red radiation increases dry mass partitioning to fruits but reduces botrytis cinerea resistance in tomato. *Environmental and Experimental Botany*, *168*, 103889. https://doi.org/10.1016/j.envexpbot.2019.103889

Johnson, W. C., & Davis, J. W. (2015). Perpendicular cultivation for improved in-row weed control in organic peanut production. *Weed Technology*, *29*(1), 128–134. https://doi.org/10.1614/WT-D-14-00083.1

Joshi, N. C., Ratner, K., Eidelman, O., Bednarczyk, D., Zur, N., Many, Y., Shahak, Y., Aviv-Sharon, E., Achiam, M., Gilad, Z., & Charuvi, D. (2019). Effects of daytime intra-canopy led illumination on photosynthesis and productivity of bell pepper grown in protected cultivation. *Scientia Horticulturae*, *250*, 81–88. https://doi.org/10.1016/j.scienta.2019.02.039

Kaiser, E., Ouzounis, T., Giday, H., Schipper, R., Heuvelink, E., & Marcelis, L. F. M. (2019). Adding Blue to Red Supplemental Light Increases Biomass and Yield of Greenhouse-Grown Tomatoes , but Only to an Optimum. *9*(January), 1–11. https://doi.org/10.3389/fpls.2018.02002

Kalaitzoglou, P., van Ieperen, W., Harbinson, J., van der Meer, M., Martinakos, S., Weerheim, K., Nicole, C. C. S., & Marcelis, L. F. M. (2019). Effects of continuous or end-of-day far-red light on tomato plant growth, morphology, light absorption, and fruit production. *Frontiers in Plant Science*, *10*, 322. https://doi.org/10.3389/fpls.2019.00322

Kang, M., Yang, L., Zhang, B., & de Reffye, P. (2011). Correlation between dynamic tomato fruit-set and source–sink ratio: a common relationship for different plant densities and seasons? *Annals of Botany*, *107*(5), 805–815. https://doi.org/10.1093/aob/mcq244

Kergoat, L., Lafont, S., Arneth, A., Le Dantec, V., & Saugier, B. (2008). Nitrogen controls plant canopy light-use efficiency in temperate and boreal ecosystems. *Journal of Geophysical Research: Biogeosciences*, *113*(G4). https://doi.org/10.1029/2007JG000676

Keuskamp, D. H., Pollmann, S., Voesenek, L. A. C. J., Peeters, A. J. M., & Pierik, R. (2010). Auxin transport through pin-formed 3 (pin3) controls shade avoidance and fitness during competition. *Proceedings of the National Academy of Sciences*, *107*(52), 22740–22744. https://doi.org/10.1073/pnas.1013457108

Keuskamp, D. H., Sasidharan, R., Vos, I., Peeters, A. J. M., Voesenek, L. A. C. J., & Pierik, R. (2011). Blue-light-mediated shade avoidance requires combined auxin and brassinosteroid action in arabidopsis seedlings. *The Plant Journal*, *67*(2), 208–217. https://doi.org/10.1111/j.1365-313X.2011.04597.x

Khemira, H., Lombard, P., Sugar, D., & Azarenko, A. (1993). Hedgerow orientation affects canopy exposure, flowering, and fruiting of 'anjou' pear trees. *HortScience*, *28*(10), 984–987. https://doi.org/10.21273/HORTSCI.28.10.984

Kim, D., Kang, W. H., Hwang, I., Kim, J., Kim, J. H., Park, K. S., & Son, J. E. (2020). Use of structurally-accurate 3d plant models for estimating light interception and photosynthesis of sweet pepper (capsicum annuum) plants. *Computers and Electronics in Agriculture*, *177*, 105689. https://doi.org/10.1016/j.compag.2020.105689

Kimura, S., & Sinha, N. (2008). Tomato (solanum lycopersicum): A model fruit-bearing crop. *CSH protocols*, *2008*, 105. https://doi.org/10.1101/pdb.emo105

Kniemeyer, O. (2008). *Design and implementation of a graph grammar based language for functional–structural plant modelling* (Doctoral dissertation). Cottbus: BTU.

Kniemeyer, O., Buck-Sorlin, G., & Kurth, W. (2007). Groimp as a platform for functional-structural modelling of plants. *Frontis*, 43–52. https://doi.org/10.1007/1-4020-6034-3_4

Kohnen, M. V., Schmid-Siegert, E., Trevisan, M., Petrolati, L. A., Sénéchal, F., Müller-Moulé, P., Maloof, J., Xenarios, I., & Fankhauser, C. (2016). Neighbor detection induces organ-specific transcriptomes, revealing patterns underlying hypocotyl-specific growth. *The Plant Cell*, *28*(12), 2889–2904. https://doi.org/10.1105/tpc.16.00463

Kozuka, T., Kobayashi, J., Horiguchi, G., Demura, T., Sakakibara, H., Tsukaya, H., & Nagatani, A. (2010). Involvement of auxin and brassinosteroid in the regulation of petiole elongation under the shade. *Plant Physiology*, *153*(4), 1608–1618. https://doi.org/10.1104/pp.110.156802

Kroon, H., Huber, H., Stuefer, J., & van Groenendael, J. (2005). A modular concept of phenotypic plasticity in plants. *The New phytologist*, *166*(1), 73–82. https://doi.org/10.1111/j.1469-8137.2004.01310.x

Küpers, J. J., van Gelderen, K., & Pierik, R. (2018). Location matters: Canopy light responses over spatial scales. *Trends in Plant Science*, *23*(10), 865–873. https://doi.org/10.1016/j.tplants.2018.06.011

Larue, F., Fumey, D., Rouan, L., Soulié, J.-C., Roques, S., Beurier, G., & Luquet, D. (2019). Modelling tiller growth and mortality as a sink-driven process using Ecomeristem: implications for biomass sorghum ideotyping. *Annals of Botany*, *124*(4), 675–690. https://doi.org/10.1093/aob/mcz038

Leivar, P., & Quail, P. H. (2011). Pifs: Pivotal components in a cellular signaling hub. *Trends in Plant Science*, *16*(1), 19–28. https://doi.org/10.1016/j.tplants.2010.08.003

Li, T., Heuvelink, E., Dueck, T. A., Janse, J., Gort, G., & Marcelis, L. F. M. (2014). Enhancement of crop photosynthesis by diffuse light: quantifying the contributing factors. *Annals of Botany*, *114*(1), 145–156. https://doi.org/10.1093/aob/mcu071

Li, Z., Guo, R., Li, M., Chen, Y., & Li, G. (2020). A review of computer vision technologies for plant phenotyping. *Computers and Electronics in Agriculture*, *176*, 105672. https://doi.org/10.1016/j.compag.2020.105672

Lindenmayer, A. (1968a). Mathematical models for cellular interactions in development i. filaments with one-sided inputs. *Journal of Theoretical Biology*, *18*(3), 280–299. https://doi.org/10.1016/0022-5193(68)90079-9

Lindenmayer, A. (1968b). Mathematical models for cellular interactions in development ii. simple and branching filaments with two-sided inputs. *Journal of Theoretical Biology*, *18*(3), 300–315. https://doi.org/10.1016/0022-5193(68)90080-5

Lloyd, J., & Farquhar, G. D. (1996). The co2 dependence of photosynthesis, plant growth responses to elevated atmospheric co2 concentrations and their interaction with soil nutrient status. i. general principles and forest ecosystems. *Functional Ecology*, *10*(1), 4–32.

Lombard, P. B., & Westwood, M. N. (1977). Effect of hedgerow orientation on pear fruiting. *HortScience*, *69*, 175–182. https://doi.org/10.17660/ActaHortic.1977.69.23

Louarn, G., & Song, Y. (2020). Two decades of functional–structural plant modelling: Now addressing fundamental questions in systems biology and predictive ecology. *Annals of Botany*, *126*, 501–509. https://doi.org/10.1093/aob/mcaa143

Luquet, D., Dingkuhn, M., Kim, H., Tambour, L., & Clement-Vidal, A. (2006). EcoMeristem, a model of morphogenesis and competition among sinks in rice. 1. Concept, validation and sensitivity analysis. *Functional Plant Biology*, *33*(4), 309–323. https://doi.org/10.1071/FP05266

Maddonni, G. A., Chelle, M., Drouet, J. L., & Andrieu, B. (2001). Light interception of contrasting azimuth canopies under square and rectangular plant spatial distributions: Simulations and crop measurements. *Field Crops Research*, *70*(1), 1–13. https://doi.org/10.1016/S0378-4290(00)00144-1

Mailhol, J. C., Olufayo, A. A., & Ruelle, P. (1997). Sorghum and sunflower evapotranspiration and yield from simulated leaf area index. *Agricultural Water Management*, *35*(1), 167–182. https://doi.org/10.1016/S0378-3774(97)00029-2

Marcelis, L. F. M. (1992). The Dynamics of Growth and Dry Matter Distribution in Cucumber. *Annals of Botany*, *69*(6), 487–492. https://doi.org/10.1093/oxfordjournals.aob.a088376

Marcelis, L. F. M. (1993). Fruit growth and biomass allocation to the fruits in cucumber. 1. effect of fruit load and temperature. *Scientia Horticulturae*, *54*(2), 107–121. https://doi.org/10.1016/0304-4238(93)90059-Y

Marcelis, L. F. M., Heuvelink, E., & Goudriaan, J. (1998). Modelling biomass production and yield of horticultural crops: A review. *Scientia Horticulturae*, *74*(1), 83–111. https://doi.org/10.1016/S0304-4238(98)00083-1

Marshall-Colon, A., Long, S. P., Allen, D. K., Allen, G., Beard, D. A., Benes, B., Von Caemmerer, S., Christensen, A., Cox, D. J., Hart, J. C., et al. (2017). Crops in silico: Generating virtual crops using an integrative and multi-scale modeling platform. *Frontiers in plant science*, *8*, 786. https://doi.org/10.3389/fpls.2017.00786

Michaud, O., Fiorucci, A.-S., Xenarios, I., & Fankhauser, C. (2017). Local auxin production underlies a spatially restricted neighbor-detection response in arabidopsis. *Proceedings of the National Academy of Sciences of the United States of America*, *114*(28), 7444–7449. https://doi.org/10.1073/pnas.1702276114/-/DCSupplemental

Monsi, M., & Saeki, T. (2005). On the Factor Light in Plant Communities and its Importance for Matter Production. *Annals of Botany*, *95*(3), 549–567. https://doi.org/10.1093/aob/mci052

Mutsaers, H. J. W. (1980). The effect of row orientation, date and latitude on light absorption by row crops. *The Journal of Agricultural Science*, *95*(2), 381–386. https://doi.org/10.1017/S0021859600039411

Ni, W., Xu, S.-L., Tepperman, J. M., Stanley, D. J., Maltby, D. A., Gross, J. D., Burlingame, A. L., Wang, Z.-Y., & Quail, P. H. (2014). A mutually assured destruction mechanism attenuates light signaling in arabidopsis. *Science*, *344*(6188), 1160–1164. https://doi.org/10.1126/science.1250778

Nicole, C. C. S., Charalambous, F., Martinakos, S., van de Voort, S., Li, Z., Verhoog, M., & Krijn, M. (2016). Lettuce growth and quality optimization in a plant factory. *Acta Horticulturae*, *1134*, 231–238. https://doi.org/10.17660/ActaHortic.2016.1134.31

Oguchi, R., Hikosaka, K., & Hirose, T. (2003). Does the photosynthetic light-acclimation need change in leaf anatomy? *Plant, Cell & Environment*, *26*(4), 505–512. https://doi.org/10.1046/j.1365-3040.2003.00981.x

Ott, L., & Longnecker, M. (2006). *An introduction to statistical methods and data analysis*. Cengage Learning, Inc.

Pantazopoulou, C. K., Bongers, F. J., Küpers, J. J., Reinen, E., Das, D., Evers, J. B., Anten, N. P., & Pierik, R. (2017). Neighbor detection at the leaf tip adaptively regulates upward leaf movement through spatial auxin dynamics. *Proceedings of the National Academy of Sciences of the United States of America*, *114*(28), 7450–7455. https://doi.org/10.1073/pnas.1702275114

Paponov, M., Kechasov, D., Lacek, J., Verheul, M. J., & Paponov, I. A. (2020). Supplemental light-emitting diode inter-lighting increases tomato fruit growth through enhanced photosynthetic light use efficiency and modulated root activity. *Frontiers in Plant Science*, *10*(1656). https://doi.org/10.3389/fpls.2019.01656

Pepin, S., Fortier, E., Béchard-Dubé, S. A., Dorais, M., Ménard, C., & Bacon, R. (2014). Beneficial effects of using a 3-d led interlighting system for organic greenhouse tomato grown in canada under low natural light conditions. *Acta Horticulturae*, 239–246. https://doi.org/10.17660/ActaHortic.2014.1041.28

Perez, R. P. A., Dauzat, J., Pallas, B., Lamour, J., Verley, P., Caliman, J.-P., Costes, E., & Faivre, R. (2017). Designing oil palm architectural ideotypes for optimal light interception and carbon assimilation through a sensitivity analysis of leaf traits. *Annals of Botany*, *121*(5), 909–926. https://doi.org/10.1093/aob/mcx161

Pettersen, R. I., Torre, S., & Gislerød, H. R. (2010). Effects of intracanopy lighting on photosynthetic characteristics in cucumber. *Scientia horticulturae*, *125*(2), 77–81. https://doi.org/10.1016/j.scienta.2010.02.006

Pradal, C., Dufour-Kowalski, S., Boudon, F., Fournier, C., & Godin, C. (2008). Openalea: A visual programming and component-based software platform for plant modelling. *Functional plant biology*, *35*(10), 751–760. https://doi.org/10.1071/FP08084

Prieto, J. A., Louarn, G., Perez, P. J., Ojeda, H., Simonneau, T., & Lebon, E. (2019). A functional–structural plant model that simulates whole- canopy gas exchange of grapevine plants (vitis vinifera l.) under different training systems. *Annals of Botany*. https://doi.org/10.1093/aob/mcz203

Procko, C., Crenshaw, C. M., Ljung, K., Noel, J. P., & Chory, J. (2014). Cotyledon-generated auxin is required for shade-induced hypocotyl growth in brassica rapa. *Plant Physiology*, *165*(3), 1285–1301. https://doi.org/10.1104/pp.114.241844

Prusinkiewicz, P., & Hanan, J. (1990). Visualization of botanical structures and processes using parametric l-systems.

Qian, T., Dieleman, J. A., Elings, A., Gelder, A. D., & Marcelis, L. F. M. (2015). Response of tomato crop growth and development to a vertical temperature gradient in a semi-closed greenhouse. *The Journal of Horticultural Science and Biotechnology*, *90*(5), 578–584. https://doi.org/10.1080/14620316.2015.11668717

Qian, T., Elings, A., Dieleman, J. A., Gort, G., & Marcelis, L. F. M. (2012). Estimation of photosynthesis parameters for a modified farquhar–von caemmerer–berry model using simultaneous estimation method and nonlinear mixed effects model. *Environmental and Experimental Botany*, *82*, 66–73. https://doi.org/10.1016/j.envexpbot.2012.03.014

Ranjan, A., Ichihashi, Y., & Sinha, N. R. (2012). The tomato genome: Implications for plant breeding, genomics and evolution. *Genome Biology*, *13*(8), 1–8.

Richter, G. M., Acutis, M., Trevisiol, P., Latiri, K., & Confalonieri, R. (2010). Sensitivity analysis for a complex crop model applied to durum wheat in the mediterranean. *European Journal of Agronomy*, *32*(2), 127–136. https://doi.org/10.1016/j.eja.2009.09.002

Runyon, J., Waring, R. H., Goward, S. N., & Welles, J. M. (1994). Environmental limits on net primary production and light-use efficiency across the oregon transect. *Ecological Applications*, *4*(2), 226–237. https://doi.org/10.2307/1941929

Samson, R., Follens, S., & Lemeur, R. (1997). Scaling leaf photosynthesis to canopy in a mixed deciduous forest. ii. a simulation study for two growing seasons. *Silva Gandavensis*, *62*. https://doi.org/10.21825/sg.v62i0.843

Särkkä, L. E., Jokinen, K., Ottosen, C.-O., & Kaukoranta, T. (2017). Effects of hps and led lighting on cucumber leaf photosynthesis, light quality penetration and temperature in the canopy, plant morphology and yield. *Agricultural and Food Science*, *26*(2), 102–110-102–110. https://doi.org/10.23986/afsci.60293

Sarlikioti, V., de Visser, P. H. B., Buck-Sorlin, G. H., & Marcelis, L. F. M. (2011a). How plant architecture affects light absorption and photosynthesis in tomato: towards an ideotype for plant architecture using a functional–structural plant model. *Annals of Botany*, *108*(6), 1065–1073. https://doi.org/10.1093/aob/mcr221

Sarlikioti, V., de Visser, P. H. B., & Marcelis, L. F. M. (2011b). Exploring the spatial distribution of light interception and photosynthesis of canopies by means of a functional–structural plant model. *Annals of Botany*, *107*(5), 875–883. https://doi.org/10.1093/aob/mcr006

Sarlikioti, V., Marcelis, L. F. M., & de Visser, P. H. B. (2009). Towards a 3d structural tomato model for calculating light interception. *International Symposium on High Technology for Greenhouse Systems: GreenSys2009 893*, 721–728.

Sasidharan, R., Chinnappa, C. C., Staal, M., Elzenga, J. T. M., Yokoyama, R., Nishitani, K., Voesenek, L. A. C. J., & Pierik, R. (2010). Light quality-mediated petiole elongation in arabidopsis during shade avoidance involves cell wall modification by xyloglucan endotransglucosylase/hydrolases. *Plant Physiology*, *154*(2), 978–990. https://doi.org/10.1104/pp.110.162057

Schmidt, D., & Kahlen, K. (2018). Towards more realistic leaf shapes in functional-structural plant models. *Symmetry*, *10*(7). https://doi.org/10.3390/sym10070278

Schwarz, D., & Kläring, H.-P. (2001). Allometry to estimate leaf area of tomato. *Journal of Plant Nutrition*, *24*(8), 1291–1309. https://doi.org/10.1081/PLN-100106982

Shin, A.-Y., Han, Y.-J., Baek, A., Ahn, T., Kim, S. Y., Nguyen, T. S., Son, M., Lee, K. W., Shen, Y., Song, P.-S., & Kim, J.-I. (2016). Evidence that phytochrome functions as a protein kinase in plant light signalling. *Nature Communications*, *7*, 11545. https://doi.org/10.1038/ncomms11545

Shin, J., Hwang, I., Kim, D., Moon, T., Kim, J., Kang, W. H., & Son, J. E. (2021). Evaluation of the light profile and carbon assimilation of tomato plants in greenhouses with respect to film diffuseness and regional solar radiation using ray-tracing simulation. *Agricultural and Forest Meteorology*, *296*, 108219. https://doi.org/10.1016/j.agrformet.2020.108219

Sinclair, T. R., Tanner, C. B., & Bennett, J. M. (1984). Water-Use Efficiency in Crop Production. *BioScience*, *34*(1), 36–40. https://doi.org/10.2307/1309424

Smith, H., & Whitelam, G. C. (1997). The shade avoidance syndrome: Multiple responses mediated by multiple phytochromes. *Plant, Cell & Environment*, *20*(6), 840–844. https://doi.org/10.1046/j.1365-3040.1997.d01-104.x

Song, Q., Zhang, G., & Zhu, X.-G. (2013). Optimal crop canopy architecture to maximise canopy photosynthetic CO2 uptake under elevated CO2 – a theoretical study using a mechanistic model of canopy photosynthesis. *Functional Plant Biology*, *40*, 108–124. https://doi.org/10.1071/FP12056

Spitters, C. J. T., Toussaint, H. A. J. M., & Goudriaan, J. (1986). Separating the diffuse and direct component of global radiation and its implications for modeling canopy photosynthesis part i. components of incoming radiation. *Agricultural and Forest Meteorology*, *38*(1), 217–229. https://doi.org/10.1016/0168-1923(86)90060-2

Strauss, S., Lempe, J., Prusinkiewicz, P., Tsiantis, M., & Smith, R. S. (2020). Phyllotaxis: Is the golden angle optimal for light capture? *New Phytologist*, *225*(1), 499–510. https://doi.org/10.1111/nph.16040

Tao, Y., Ferrer, J.-L., Ljung, K., Pojer, F., Hong, F., Long, J. A., Li, L., Moreno, J. E., Bowman, M. E., Ivans, L. J., Cheng, Y., Lim, J., Zhao, Y., Ballaré, C. L., Sandberg, G., Noel, J. P., & Chory, J. (2008). Rapid synthesis of auxin via a new tryptophan-dependent pathway is required for shade avoidance in plants. *Cell*, *133*(1), 164–176. https://doi.org/10.1016/j.cell.2008.01.049

Thornley, J. H. M., Hand, D. W., & Wilson, J. W. (1992). Modelling light absorption and canopy net photosynthesis of glasshouse row crops and application to cucumber. *Journal of Experimental Botany*, *43*(3), 383–391.

Trentacoste, E. R., Connor, D. J., & Gómez-del-Campo, M. (2015). Row orientation: Applications to productivity and design of hedgerows in horticultural and olive orchards. *Scientia Horticulturae*, *187*, 15–29. https://doi.org/10.1016/j.scienta.2015.02.032

Trentacoste, E. R., Gómez-del-Campo, M., & Rapoport, H. F. (2016). Olive fruit growth, tissue development and composition as affected by irradiance received in different hedgerow positions and orientations. *Scientia Horticulturae*, *198*, 284–293. https://doi.org/10.1016/j.scienta.2015.11.040

Trouwborst, G., Hogewoning, S. W., Harbinson, J., & van Ieperen, W. (2011). The influence of light intensity and leaf age on the photosynthetic capacity of leaves within a tomato canopy [028/2011]. *Journal of Horticultural Science and Biotechnology*, *86*(4), 403–407. https://doi.org/10.1080/14620316.2011.11512781

Trouwborst, G., Oosterkamp, J., Hogewoning, S. W., Harbinson, J., & van Ieperen, W. (2010). The responses of light interception, photosynthesis and fruit yield of cucumber to LED-lighting within the canopy. *Physiologia Plantarum*, *138*(3), 289–300. https://doi.org/10.1111/j.1399-3054.2009.01333.x van der Meer, M., de Visser, P. H. B., Heuvelink, E., & Marcelis, L. F. M. (2021). Row orientation affects the uniformity of light absorption, but hardly affects crop photosynthesis in hedgerow tomato crops. *in silico Plants*, *3*(2). https://doi.org/10.1093/insilicoplants/diab025

van Ittersum, M. K., Leffelaar, P. A., van Keulen, H., Kropff, M. J., Bastiaans, L., & Goudriaan, J. (2003). On approaches and applications of the wageningen crop models [Modelling Cropping Systems: Science, Software and Applications]. *European Journal of Agronomy*, *18*(3), 201–234. https://doi.org/10.1016/S1161-0301(02)00106-5

van Gelderen, K., Kang, C., Paalman, R., Keuskamp, D., Hayes, S., & Pierik, R. (2018). Far-red light detection in the shoot regulates lateral root development through the hy5 transcription factor. *The Plant Cell*, *30*(1), 101–116. https://doi.org/10.1105/tpc.17.00771

van Ieperen, W., & Trouwborst, G. (2008). The application of leds as assimilation light source in greenhouse horticulture: A simulation study. *Acta Horticulturae*, *801*, 1407–1414. https://doi.org/10.17660/ActaHortic.2008.801.173

Veach, E. (1997). *Robust monte carlo methods for light transport simulation* (Doctoral dissertation). Stanford University.

Vermeiren, J., Villers, S. L. Y., Wittemans, L., Vanlommel, W., van Roy, J., Marien, H., Coussement, J. R., & Steppe, K. (2020). Quantifying the importance of a realistic tomato (Solanum lycopersicum) leaflet shape for 3-D light modelling. *Annals of Botany*, *126*(4), 661–670. https://doi.org/10.1093/aob/mcz205

Viczián, A., Klose, C., Ádám, É., & Nagy, F. (2017). New insights of red light-induced development. *Plant, Cell & Environment*, *40*(11), 2457–2468. https://doi.org/10.1111/pce.12880

Von Caemmerer, S. (2013). Steady-state models of photosynthesis. *Plant, Cell & Environment*, *36*(9), 1617–1630. https://doi.org/10.1111/pce.12098

Vos, J., Evers, J. B., Buck-Sorlin, G. H., Andrieu, B., Chelle, M., & de Visser, P. H. B. (2010). Functional–structural plant modelling: a new versatile tool in crop science. *Journal of Experimental Botany*, *61*(8), 2101–2115. https://doi.org/10.1093/jxb/erp345

Vos, J., Marcelis, L. F. M., & Evers, J. B. (2007). Functional-structural plant modelling in crop production: Adding a dimension. In J. Vos, L. Marcelis, P. de Visser, P. Struik, & J. Evers (Eds.), *Functional-structural plant modelling in crop production* (pp. 1–12). Springer.

Westerband, A. C., Funk, J. L., & Barton, K. E. (2021). Intraspecific trait variation in plants: a renewed focus on its role in ecological processes. *Annals of Botany*, *127*(4), 397–410. https://doi.org/10.1093/aob/mcab011

Whitelam, G. C., & Johnson, C. B. (1982). Photomorphogenesis in impatiens parviflora and other plant species under simulated natural canopy radiations. *New Phytologist*, *90*(4), 611–618. https://doi.org/10.1111/j.1469-8137.1982.tb03270.x

Wiechers, D., Kahlen, K., & Stützel, H. (2011). Evaluation of a radiosity based light model for greenhouse cucumber canopies. *Agricultural and Forest Meteorology*, *151*(7), 906–915. https://doi.org/10.1016/j.agrformet.2011.02.016

Wilson, J. W., Hand, D. W., & Hannah, M. A. (1992). Light Interception and Photosynthetic Efficiency in Some Glasshouse Crops. *Journal of Experimental Botany*, *43*(3), 363–373. https://doi.org/10.1093/jxb/43.3.363

Wubs, A. M., Heuvelink, E., & Marcelis, L. F. M. (2009a). Abortion of reproductive organs in sweet pepper (capsicum annuum l.): A review. *The Journal of Horticultural Science and Biotechnology*, *84*(5), 467–475. https://doi.org/10.1080/14620316.2009.11512550

Wubs, A. M., Ma, Y., Heuvelink, E., & Marcelis, L. F. M. (2009b). Genetic differences in fruit-set patterns are determined by differences in fruit sink strength and a source : sink threshold for fruit set. *Annals of Botany*, *104*(5), 957–964. https://doi.org/10.1093/aob/mcp181

Yan, W., Zhang, Y., Zhang, Y., Cheng, R., Zhang, Y., Yang, Q., & Li, T. (2018). Effects of supplementary artificial light on growth of the tomato (¡i¿solanum lycopersicum¡/i¿) in a chinese solar greenhouse. *The Horticulture Journal*, *87*(4), 516–523. https://doi.org/10.2503/hortj.okd-165

Yuan, W., Liu, S., Zhou, G., Zhou, G., Tieszen, L. L., Baldocchi, D., Bernhofer, C., Gholz, H., Goldstein, A. H., Goulden, M. L., Hollinger, D. Y., Hu, Y., Law, B. E., Stoy, P. C., Vesala, T., & Wofsy, S. C. (2007). Deriving a light use efficiency model from eddy covariance flux data for predicting daily gross primary production across biomes. *Agricultural and Forest Meteorology*, *143*(3), 189–207. https://doi.org/10.1016/j.agrformet.2006.12.001

Zhang, N., van Westreenen, A., He, L., Evers, J. B., Anten, N. P. R., & Marcelis, L. F. M. (2021). Light from below matters: Quantifying the consequences of responses to far-red light reflected upwards for plant performance in heterogeneous canopies. *Plant, Cell & Environment*, *44*(1), 102–113. https://doi.org/10.1111/pce.13812

Zhao, Y. (2018). Essential roles of local auxin biosynthesis in plant development and in adaptation to environmental changes [PMID: 29489397]. *Annual Review of Plant Biology*, *69*(1), 417–435. https://doi.org/10.1146/annurev-arplant-042817-040226

Zhu, B., Liu, F., Xie, Z., Guo, Y., Li, B., & Ma, Y. (2020). Quantification of light interception within image-based 3-D reconstruction of sole and intercropped canopies over the entire growth season. *Annals of Botany*, *126*(4), 701–712. https://doi.org/10.1093/aob/mcaa046

Zhu, J., van der Werf, W., Anten, N. P. R., Vos, J., & Evers, J. B. (2015). The contribution of phenotypic plasticity to complementary light capture in plant mixtures. *New Phytologist*, *207*(4), 1213–1222. https://doi.org/10.1111/nph.13416

Zhu, X.-G., Song, Q., & Ort, D. R. (2012). Elements of a dynamic systems model of canopy photosynthesis. *Current opinion in plant biology*, *15*(3), 237–244. https://doi.org/10.1016/j.pbi.2012.01.010

Summary

The aim of this thesis was to study the variability in light absorption and photosynthesis within tomato canopies, where a combination of experimentation and 3D modelling was used. The main hypothesis in this thesis was that including this variation gives a much more realistic simulation of the crop canopy.

A first source of variability in light absorption and photosynthesis is the positioning of plant and leaves in a 3D space. Plant positioning in rows causes inter- and intra-row shading, which affects the light distribution and pattern throughout the whole day. For hedgerow productivity and product quality, a north–south row orientation is often favourable. This is thought to be the result of a more equal distribution of light to the most important leaves and fruits between both east- and west-facing parts of the rows during a day in a north–south row orientation. A south-facing side can be light-saturated, while the north-facing side of a tree is still limited by light, resulting in unequal fruit set, fruit abortion or fruit rot.

A second source of variability in light absorption and photosynthesis is the introduction of intra-canopy lighting with LEDs. Placing intra-canopy lighting has a major influence on light distribution within the canopy, affecting the uniformity as well as light spectrum gradient in the crop. This affects a third topic of interest in this thesis, namely the effect of spatial differences in light spectrum on plant growth. Changes in morphology resulting from an individual organ's (i.e. leaf, stem or fruit) perceived light microclimate can be at the level of the organ itself (local) and at the plant level where it also affects other plant organs (long-distance). Local versus long-distance responses to light spectrum are commonly studied in (de-etiolated) seedlings, allowing for fast research. Extrapolating studies on local lighting on de-etiolated seedlings, rosette plants or very young plants to tall plants (e.g. longer than 1 m) is difficult if not impossible. Whether and to which extent local supplementation of FR resulted in local or long-distance architectural and growth responses in full-grown tomato plants was unclear. Yet an understanding of how this works is relevant for accurately predicting plant growth under intra-canopy lighting conditions.

The potential of intra-canopy light-emitting diode (LED) lighting to enhance or modify crop growth and yield has been explored in the past decade in greenhouse cultivation. The changes in spatial heterogeneity of light absorption that come with the introduction of intra-

canopy lighting have not been thoroughly explored. By providing supplementary light within the crop reflective loss of the upper canopy is reduced. Furthermore, a more homogeneous vertical light distribution and therefore a higher photosynthetic use efficiency of the absorbed light could be achieved. Due to the curvilinear shape of the light response curve of leaf photosynthesis the crop photosynthesis is higher when all leaves have the same intensity, compared to a situation with the same average light intensity but with variation among individual leaves. Despite the knowledge, measuring spatial heterogeneity of incident and absorbed light in detail is hard. The spatial variability of absorbed light is important when physiological processes such as photosynthesis are compared between light treatments. An FSPM is an excellent tool for studying the spatial variability.

A last source of variation addressed in this thesis is plant to plant variation (interplant variation). Interplant variation may play an important role in determining individual plant and whole canopy performance, where interplant variation in architecture and photosynthesis traits have direct effects on light absorption and photosynthesis. Interplant variation has been studied for a longer time in ecology, greenhouse horticulture and field crops, where in greenhouse horticulture and field crops uniformity is of importance. Differences in whole plant fruit growth have been linked to environmental factors such as light intensity, photoperiod, CO_2 concentration, temperature, relative air humidity, water and nutrient supply and canopy architecture.

As mentioned in the above paragraphs, in canopies a large variation exists between and within plants with respect to architecture and the distribution of light (both intensity and spectrum).

In this thesis tomato *(Solanum lycopersicum)* was used as a model plant for fruit-bearing crops. Tomato is easy to use for research due to the fact that it has simple diploid genetics, a short generation time, routine transformation technology and is easy to maintain. Research studies on tomato brings knowledge that can be applied to other plants in the Solanaceae family, such as eggplant and peppers. Tomato plants are generally cultivated in high-wire double row systems when grown in high-tech greenhouses. For greenhouses the cultivars chosen have an indeterminate growth habit allowing almost year-round cultivation in the Netherlands. When the plants reach several meters high, they are lowered weekly along the path.

In **Chapter 1** a broad background is given on different types of crop models used to predict plant growth and yield, the introduction of LED light sources and challenges of measuring light within a canopy, architectural variation that exists inside canopies and tomato plant used in this research. At the end Chapter 1 the knowledge gaps and hypotheses that were investigated in this thesis as well as the outline of each chapter were described.

In **Chapter 2** a combination of experimentation and functional-structural plant modelling (FSPM) was presented where row orientation effects were studied on the inter-and within-row variation of light absorption and photosynthesis in tomato. The FSPM was used to analyse light absorption and photosynthesis for each of the row facing directions in a double-row trellis system (e.g. north- and south-facing rows for the east–west row orientation). It was concluded that although south-facing rows were expected to have a higher photosynthesis than north-facing rows, plant morphology was acclimated such that differences in light absorption and photosynthesis between north- and south-facing rows were minimal. Rows oriented north–south were more uniform in light absorption and photosynthesis than east–west rows, but the overall crop light absorption and photosynthesis were minimally affected (both 3 % lower compared to east–west orientation). Despite an overall equal canopy light absorption and photosynthesis there were still significant differences in fruit production at the row level between the north- and south-facing rows due to a higher partitioning to fruits in the south-facing rows. As such, variability in economic product was higher in the east-west row orientation.

In **Chapter 3** local and long-distance plant responses to localized light spectrum were studied in large plants. It was investigated whether local supplementation of FR resulted in local or long-distance architectural and growth responses in full-grown tomato plants. Tomato plants were grown in a climate chamber and separated horizontally with white plastic. It was found that locally supplied FR has long-distance effects on length and dry weight of the stem and on SLA, while some other parameters (petiole elongation, petiole angle, leaf weight) are only locally affected. When FR was supplied to the lower half of the plant SLA, stem length, and stem dry weight of the upper half also increased, but to a lesser extent than when FR was supplied to the upper half.

In **Chapter 4** changes in spatial heterogeneity of light absorption that come with the introduction of intra-canopy lighting were explored by use of FSPM. An FSPM was calibrated and validated, which combined plant morphology with a ray tracing model to estimate light absorption on a leaflet level. Canopy light distribution was then quantified and visualized in three voxel directions by means of average absorbed photosynthetic photon flux density (PPFD) and coefficient of variation (CV) within that voxel. Combined intra-canopy and top lighting had in all directions a more uniform light absorption than intra-canopy or top lighting alone. Intra-canopy lighting resulted in 8% higher total light absorption than top lighting, while combining 50% intra-canopy lighting with 50% top lighting, increased light absorption by 4%.

In **Chapter 5** plant to plant variation (interplant variation) was studied to determine the effect on individual plant and whole canopy performance, where interplant variation in architecture and photosynthesis traits had direct effects on light absorption and photosynthesis. It is discussed that introducing interplant variation in architecture and photosynthesis traits in a FSPM did -depending on the trait- not or negatively affect canopy light absorption and net photosynthesis compared to the reference model without interplant variation. This leads to the conclusion that a uniform average crop would have been better than having a crop with variability included for total crop productivity. Despite being capable of improving the accuracy of simulation of canopy light interception and photosynthesis the effects at canopy level were relatively small (<4% for light absorption and <7% for net photosynthesis).

In **Chapter 6** the results of this thesis are summarized and put into a more general context with relevancy outside of this thesis. The advantages and the shortcomings of the 3D model assisted approach as well as further steps for research are discussed. Further steps for research should focus on distinguishing which plant tissue is responsible for inducing long-distance far-red light responses. Besides this, the effects were found smaller when the mature lower plant part was lighted with far-red light. Further research should therefore also focus on determining if the diminishing effects are due to ageing or distance. The 3D model showed to be a powerful tool to quantify the spatial distribution of light, yet the ability of the model to predict effects on photosynthesis have only been used sparsely, mainly due to lack of knowledge on local acclimation to light. Thus, the impact of spatial variability in light absorption on net photosynthesis should be further explored in future studies. This would give an idea on the impact of variability on crop growth resulting from intra-canopy lighting. Another aspect with respect to intra-canopy lighting is that there was no focus on light spectrum, although it was shown to have an influence on plant architecture even when placed down in the canopy. If we want to be able to simulate and predict the effects of intra-canopy lighting on architectural changes, interplant variability and associated plant growth and development in a canopy during a growing season, we need a much better understanding of how light signals affect growth and development at the phytomer level.

Acknowledgements

During the stretch of this PhD I got to share my time with so many kind spirits.

I would like to start off by thanking my supervising team Leo, Ep and Pieter for year-after-year meetings and having the confidence to put a PhD position into my hands. We got to spend a lot of time together working out ideas and possible explanations for findings. Leo, you always manage to find key points to focus on, what to discuss and sort-of-speak to filter the gold from the rubbish. Whenever stuck, a meeting on the particular topic in question would be a step forward, even when we occasionally did not agree with each other. Pieter, your insights in modelling and view on the bigger picture were very helpful. Also, formulating criticism in such a positive way that I would wonder if I needed to improve anything, but then when reading again I realize I did. Ep, your particular expertise on statistics and visions of expressing graphs in different ways was very helpful.

Rachel, your enthusiasm and limitless supply of new ideas and ways to look at our work together were amazing. I was looking forward to our weekly discussions and enjoyed the collaboration a lot. Many thanks for the wonderful moments.

I would like to thank my two friends and paranymphs Ferran and Henry, who will help defend my thesis on the day itself, and who helped me with logistics for the after-chill and after-party in the same week, besides never-ending moral support.

A big shout-out to all my colleagues in the department, and in particular my direct colleagues with whom I spent by far the most time in the office and occasionally outside office hours; Priscilla, Ana, Cristina, Ningyi, Alejandro, Arian, Faline, Rachel, Dorthe, Evelien, Yongran, Fahrizal, Yutaka, Ying, Sharath, Kim, Hua, Sara, Elias. It was a great experience getting to know all of you in our small but cosy working space!

It was a challenging but exciting learning experience to have supervised MSc students. Petra, Csongor, Hyeran and Gyeole, thanks for the time and effort you all have put into your thesis and discussions, which in the end helped this PhD thesis a lot. Petra, thank you for going through model development with me in the early phase of my PhD. Csongor, I really enjoyed the many critical questions that I did not even understood at times! Gyeole, your undying passion for tomato plants still amazes me. The experiment we were performing and your daily enthusiasm in anything you were doing and being a friend, it was a really great experience. Hyeran, thank you for your efforts on the parameter variability study and the great amount of questions and ideas that you continuously wanted to discuss. This was a very good base to write the final chapter for.

Special thanks to the technicians and in particular to Maarten whom helped me with setting up the sensors software in evening hours in times of desperate need. Also very happy to have had the support of the Klima team, Gerrit, Taede, David and Rinie who guided me with the far-red light experiment in every way possible. A special thanks to the whole unifarm greenhouse team who managed to modify the row orientation last minute, despite this request coming in rather late (massive apologies for this again). Thanks to you all Maarten, Sean and Geurt for looking after the greenhouse plants with great care and Erik and Ferdinand for helping with technical installations. Thank you Wim for helping me organize my harvests in the dry lab and your never ending sense of dry humor.

During the thesis I was part of the Plant Form and Function discussion group which really helped a lot in the process of model development and putting models in a broader perspective. I would like to thank all the active participants in this group; Arian, Ambra, Rachel, Franca, Jorad, Gu, Ioannis, Alejandro, Martin, Ningyi, Jochem, Bob and every other MSc and PhD that was there during my time that made this a success. Arian, besides our time in the it was a great learning experience to discuss and implement code in- and outside GroIMP, I learnt a lot from you.

I really enjoyed the short times I got to spend at the lightlab. Bram, who was always enthusiastic, helpful and would share his expertise on lighting materials and the research going on in the field with joy. As well as Vida, with whom I did not spend much time but was always kind to offer help and expertise when needed.

Many thanks to my family for moral support and actual contributions to this thesis. My brother Reinier, thanks for the advice on what to and what not to do during a PhD in early stages. My sister Anna for making the illustration of the experimental setup in the third chapter, and my mother Wil and sister Anna for their joint effort on making the thesis cover!

About the author

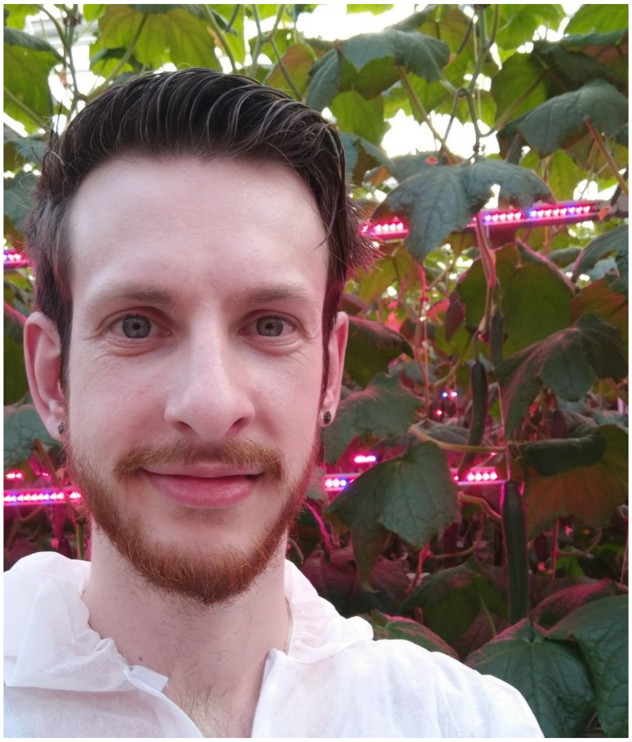

Maarten van der Meer landed on earth in Alphen aan den Rijn on 3 July 1991 in a farm next to the Rhine river. After finishing high school and acquiring the HAVO certificate, he started the studies animal care and management. Realizing the prospects of this were very poor and animal management felt more like animal exploitation he decided to quit this study after 5 weeks. During this year he picked up different jobs, such as gardening, cleaning houses and call center work. After this year, he started doing VWO 2-years-in-one and graduated with a certificate in a year. Maarten then started studying Civil Engineering at the Technical University of Delft and quit this within a week, realizing he felt no connection to the people and the city. A week later he started the BSc Plant Sciences at WUR and graduated there within 3 years with a major in Crop Production and Ecology and a minor in Organic Plant Production and Society. Following this Maarten continued with a MSc Plant Sciences at WUR and graduated 2 years later with a major in Greenhouse Horticulture. These were also the years where he got introduced with functional-structural plant modelling and spent time developing a lettuce model during his master thesis and internship. After graduating from the master Maarten started a PhD in the Horticulture and Product Physiology department. After several years into the PhD and no longer officially employed, he felt the need to focus on other jobs and worked several months as Test Automation Engineer, and afterwards for the remainder of the year installing solar panels. Then Maarten came back to his PhD during the winter months to write up the remaining parts. Now he will move to Berlin and find his following career path there. When not at work, Maarten likes to spend time playing squash, reading science fiction, playing board games, DnD and similar roleplay story games, going for bouldering, parties, studying marine life, doing pottery and listening to podcasts and audiobooks. One of his current favorites is the Deep Sea Podcast, and he recommends this to everyone.

PE&RC Training and Education Statement

With the training and education activities listed below the PhD candidate has complied with the requirements set by the C.T. de Wit Graduate School for Production Ecology and Resource Conservation (PE&RC) which comprises of a minimum total of 32 ECTS (= 22 weeks of activities)

Review of literature (4.5 ECTS)

- Developing a functional-structural plant model for tomato to simulate heterogeneity in light absorption and photosynthesis

Writing of project proposal (4.5 ECTS)

- An integrated approach for dynamically simulating photosynthesis, morphogenesis, assimilate partitioning and transpiration of 3D plant canopies

Post-graduate courses (3 ECTS)

- Modelling plant form and function using GroIMP; WUR (2016)
- Statistical uncertainty analysis of dynamic models; PERC (2017)

Invited review of (unpublished) journal manuscript (1 ECTS)

- Frontiers in Plant Science: morphological plant modelling: Unleashing geometric and topologic potential within the plant sciences (2017)

Competence strengthening / skills courses (2.2 ECTS)

- Brain training; WGS (2015)
- Scientific writing; WGS (2016)
- Reviewing a scientific paper (RCP) (2017)

Scientific integrity/ethics in science activities (1.1 ECTS)

- Research integrity; WUR (2015)
- Research ethics seminar (ResEth); WGS (2017)

PERC Annual meetings, seminars and the PERC weekend (2.1 ECTS)

- PERC Days (2015, 2016)
- PERC Weekends (2015, 2018)

Discussion groups / local seminars or scientific meetings (7.5 ECTS)

- FLOP: Frontier Literature in Plant Physiology (2016-2020)
- PFF: Plant Form and Function (2015-2021)

International symposia, workshops and conferences (4.4 ECTS)

- Model-IT symposium; Wageningen, the Netherlands (2015)
- FSPMA; Qingdao, China (2016)

Lecturing / supervision of practicals / tutorials (2.1 ECTS)

- Physiology and development of plants in horticulture (2015-2017)
- Concepts in environmental plant physiology (2016)

BSc/MSc thesis supervision (11 ETS)

- Development of a functional-structural plant model to simulate the distribution of transpiration within a greenhouse-grown tomato plant
- In search of the optimal greenhouse tomato row orientation using functional-structural plant modelling, with focus on stomatal conductance
- Effects of local supplementation of far-red light to either full-grown or young plant parts on tomato morphology
- Sensitivity of canopy light absorption and photosynthesis to plant to plant variation of architecture parameters in functional-structural plant model of tomato

The research described in this thesis was financially supported by the Wellensiek Fund. Financial support from Wageningen University for printing this thesis is gratefully acknowledged.

Special thanks to my mother Wil van der Meer and my sister Anna Verhoog for the design of the thesis cover.